Charles University
Faculty of Science

Study programme:
Branch of study:

Mgr. Karel Marschner

Development of Instrumentation and Methodology for Elemental and Speciation Analysis of Arsenic Based on Hydride Generation and on Atomic Fluorescence Spectrometric Detection

Vývoj instrumentace a metodologie pro prvkovou a speciační analýzu arsenu založenou na generování hydridů a na detekci atomovou fluorescenční spektrometrií

Doctoral thesis

Supervisor: prof. RNDr. Jiří Dědina, CSc., DSc.

Supervisor-consultant: RNDr. Stanislav Musil, Ph.D.
Doc. RNDr. Petr Rychlovský, CSc.

Praha 2017

Prohlášení

Prohlašuji, že jsem tuto závěrečnou práci zpracoval samostatně a že jsem uvedl všechny použité informační zdroje a literaturu. Tato práce ani její podstatná část nebyla předložena k získání jiného nebo stejného akademického titulu.

Jsem si vědom toho, že případné využití výsledků, získaných v této práci, mimo Univerzitu Karlovu je možné pouze po písemném souhlasu této univerzity.

V Praze dne 10. července 2017. Mgr. Karel Marschner

The presented work was financially supported by the Czech Science Foundation (grant no. 14-23532S and 17-04329S), by the Institute of the Analytical Chemistry of the Czech Academy of Sciences, v. v. i. (project no. RVO: 68081715), by the Ministry of education and sports of the Czech Republic (program Kontakt II, project no. LH12040 and LH15174), and by the Charles University (project SVV).

This dissertation thesis was elaborated at the Institute of Analytical Chemistry of the Czech Academy of Sciences, v. v. i., Detached workplace – Department of Trace Element Analysis, Vídeňská 1083, 142 20 Prague 4, Czech Republic.

The presented thesis is based on the following papers that are included as appendices:

Paper I

Marschner K., Musil S., Dědina J.: Achieving 100% Efficient Postcolumn Hydride Generation for As Speciation Analysis by Atomic Fluorescence Spectrometry. *Analytical Chemistry*, **88**, 4041−4047 (2016).

Paper II

Marschner K., Musil S., Dědina J.: Demethylation of Methylated Arsenic Species during Generation of Arsanes with Tetrahydridoborate(1−) in Acidic Media. *Analytical Chemistry*, **88**, 6366−6373 (2016).

Paper III

Marschner K., Musil S., Mikšík I., Dědina J.: Hydride generation from arsenosugars submitted to *Journal of Analytical Atomic Spectrometry*.

Declaration of co-authors

On behalf of the other co-authors I declare that Mgr. Karel Marschner contributed substantially to Paper I (his contribution 80%) and his participation in Paper I was as follows: development of the instrumental setup, all the experimental work, data evaluation, manuscript preparation, and corresponding author.

On behalf of the other co-authors I declare that Mgr. Karel Marschner contributed substantially to Paper II (his contribution 80%) and his participation in Paper II was as follows: development of the instrumental setup, all the experimental work, data evaluation, manuscript preparation, and corresponding author.

On behalf of the other co-authors I declare that Mgr. Karel Marschner contributed substantially to Paper III (his contribution 70%) and his participation in Paper III was as follows: development of the instrumental setup, most of the experimental work, data evaluation, manuscript preparation, and corresponding author.

Prague, July 2017 prof. RNDr. Jiří Dědina, CSc., DSc.

Abstract (EN)

The presented dissertation is devoted to hydride generation from arsenic species and its application for speciation analysis based on atomic fluorescence detection.

Hydride generation from toxicologically relevant arsenic species was optimized in order to achieve a 100% efficiency. The resulted experimental setup was subsequently used for speciation analysis of arsenic in human urine by high performance liquid chromatography with detection by atomic fluorescence spectrometry. The accuracy of the developed method was verified by comparative analyses of human urine samples collected from five individuals with an independent reference method.

The cleavage of As–C bond during the reaction of methylated arsenic species with tetrahydridoborate(1–) (THB) in acidic media was studied in detail. Pronounced demethylation of methylated arsenic species was found during the reaction of THB with HCl, H_2SO_4, and $HClO_4$ while hydride generation from CH_3COOH or TRIS buffer after prereduction with L-cysteine resulted in the exclusive formation of the corresponding hydrides. Firstly, this phenomenon can endanger the accuracy of arsenic speciation which is based on hydride generation of substituted arsanes. Secondly, the more complex arsenic species can be converted to the hydride. That was demonstrated on hydride generation of arsenosugars.

Keywords: Arsenic, arsenic species, atomic fluorescence spectrometry, hydride generation.

Abstrakt (CZ)

Předkládaná disertační práce je zaměřena na speciační analýzu arsenu pomocí generování hydridů s detekcí atomovou fluorescenční spektrometrií.

Generování hydridů z toxikologicky závažných sloučenin arsenu bylo optimalizováno tak, aby bylo dosaženo 100% účinnosti. Toto experimentální uspořádání bylo následně využito pro speciační analýzu arsenu v lidské moči pomocí vysokoúčinné kapalinové chromatografie s detekcí atomovou fluorescenční spektrometrií. Přesnost vyvinuté metody byla ověřena pomocí analýz vzorků lidské moči, shromážděných od pěti jedinců, srovnáním s nezávislou referenční metodou.

Detailně byl studován vliv reakce tetrahydridoboritanu v kyselém prostředí na přerušení As–C vazby u methylovaných sloučenin arsenu. Výrazná demethylace byla pozorována v prostředí HCl, H_2SO_4 a $HClO_4$, zatímco během generování hydridů z prostředí CH_3COOH nebo TRIS pufru po předredukci L-cysteinem žádná demethylace pozorována nebyla. Tento jev ohrožuje přesnost speciační analýzy arsenu, která je založena na generování substituovaných arsanů. Na druhou stranu ale umožňuje generovat arsany z mnohem složitějších sloučenin arsenu, což bylo demonstrováno generováním těkavých arsanů z arsenocukrů.

Klíčová slova: Arsen, specie arsenu, atomová fluorescenční spektrometrie, generování hydridů.

Table of Content

List of Symbols and Abbreviations

AFS	atomic fluorescence spectrometry
As-sugar-gly	3-[5'-deoxy-5'-(dimethylarsinoyl)-β-ribofuranosyloxy]-2-hydroxypropylene glycol
As-sugar-PO_4	3-[5'-deoxy-5'-(dimethylarsinoyl)-β-ribofuranosyloxy]-2-hydroxypropyl 2,3-hydroxypropyl phosphate
As-sugar-SO_3	3-[5'-deoxy-5'-(dimethylarsinoyl)-β-ribofuranosyloxy]-2-hydroxypropanesulfonic acid
As-sugar-SO_4	3-[5'-deoxy-5'-(dimethylarsinoyl)-β-ribofuranosyloxy]-2-hydroxypropyl hydrogen sulfate
CD	capillary distance
CT	cryogenic trap
DBD	dielectric barrier discharge
DIW	deionized water
$DMAs^V$	dimethylarsinate
E^0	standard reduction potential [V]
EDL	electrodeless discharge lamp
ESI	electrospray ionization
FIGS	flame-in-gas shield
GLS	gas-liquid separator
HC	hydrolysis coil
HPLC	high performance liquid chromatography
HG	hydride generation
i.d.	inner diameter
iAs^{III}	arsenite
iAs^V	arsenate
ICP-MS	inductively coupled plasma mass spectrometer
LD50	median lethal dose
L-cys	L-cysteine
MAs^V	methylarsonate
MDF	miniature diffusion flame
OH	observation height
PP1/PP2	peristaltic pumps

RC	reaction coil
SRM	standard reference material
THB	tetrahydridoborate(1–)
$TMAs^{V}O$	trimethylarsine oxide
VSG	volatile species generation

1 Introduction and Objectives

The presented dissertation summarizes the results contained in three original research papers (two were published and one has been submitted) in prestigious international scientific journals in the field of analytical atomic spectrometry and analytical chemistry. The dissertation is focused on speciation analysis of arsenic based on hydride generation. It presents an important progress in this field.

The theoretical part briefly describes arsenic species and their toxicities and all volatile species useful for analytical atomic spectrometry. A special focus is taken on chemical hydride generation by means of the reaction between hydride forming elements (especially of arsenic) with tetrahydridoborate(1−) in acidic media and on detection by atomic fluorescence spectrometry with flame atomization.

The general objectives of this thesis were following:

1) to develop a simple hydride generator which converts four arsenic species (inorganic and methylated) quantitatively to arsanes without any pre-reduction step (Paper I),
2) to connect the developed hydride generator to high performance liquid chromatography and use it to speciation analysis of arsenic in real samples (Paper I),
3) to study the mechanism of cleavage of As–C bond during hydride generation from methylated arsenic species by the reaction with tetrahydridoborate(1−) in acidic media. (Paper II),
4) to study the possibility of forming volatile arsanes from more complex arsenic species (arsenosugars) (Paper III).

2 Theoretical Part

2.1 Arsenic Species and Their Toxicity

Determination of arsenic species is an important task due to their abundances in the environment and impact on human health. The most toxic and abundant arsenic species are inorganic ones, with median lethal dose (LD50) for intramuscular injection to mouse 8 and 22 mg kg^{-1} (expressed as As mass) for arsenite (iAs^{III}) and arsenate (iAs^{V}), respectively.[1] In some world regions (especially in Bangladesh) the inorganic arsenic contamination of groundwater is a serious problem.[2] The long-term exposure to inorganic arsenic is associated with skin lesions, skin cancer, internal cancers (bladder, kidney and lungs), neurological effects, hypertension and cardiovascular disease, pulmonary disease, peripheral vascular disease and diabetes mellitus.[2,3,4]

Methylated arsenic species are also toxicologically important because many (but not all) mammalians methylate inorganic arsenic. Chalanger[5] proposed a mechanism in which inorganic arsenic is metabolized by a sequential process involving a two electron reduction of pentavalent arsenic to trivalent, followed by an oxidative methylation to pentavalent methylated arsenic species. Methylation continues until trimethylarsine oxide ($TMAs^{V}O$) is reached and it can be summarized as follows:[1]

$$\begin{aligned} As^{V}O_4^{3-} + 2e^{-} \rightarrow As^{III}O_3^{3-} + CH_3^{+} \rightarrow CH_3As^{V}O_3^{2-} + 2e^{-} \rightarrow CH_3As^{III}O_2^{2-} + CH_3^{+} \rightarrow \\ \rightarrow (CH_3)_2As^{V}O_2^{-} + 2e^{-} \rightarrow (CH_3)_2As^{III}O^{-} + CH_3^{+} \rightarrow (CH_3)_3As^{V}O \end{aligned} \quad (1)$$

This “classical” pathway was generally considered as a detoxification reaction of inorganic arsenic. Pentavalent methylated species – methylarsonate (MAs^{V}) and dimethylarsinate ($DMAs^{V}$) are much less toxic, the $LD50_{mouse}$ (oral) are 916 and 648 mg kg^{-1} for MAs^{V}, and $DMAs^{V}$, respectively.[1] However, the methylation of arsenicals has been reported to be a bioactivation process because the toxicity of trivalent methylated species was found to be much higher than iAs^{III}.[1] A different pathway was proposed by Hayakawa et al.[6] who considered the gluthathione to be a mandatory component for promoting arsenic methylation. Yet another pathway was proposed by Rehman and Naranmandura[7] who proposed that inorganic arsenic is bound to proteins in a trivalent form during the successive reductive methylation by arsenic methyltransferase in the presence of glutathione and S-adenosylmethionine.

More than fifty additional arsenic species have been identified in marine organisms.[8,9] Most of them are considered as non-toxic like arsenobetaine or arsenocholine or their toxicity is still studied - like arsenolipids[10,11] or arsenosugars (dimethylarsinoylribosides).[12]

The list of relevant arsenic species which were investigated in this work are shown in table 1.

Table 1 an overview of relevant arsenic species

Abbreviation	Name	Structure
iAs^{III}	arsenite	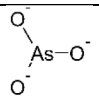
iAs^{V}	arsenate	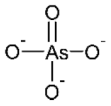
MAs^{V}	methylarsonate	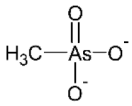
$DMAs^{V}$	dimethylarsinate	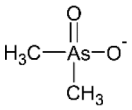
$TMAs^{V}O$	trimethylarsine oxide	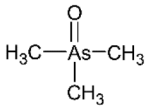
	arsenosugars	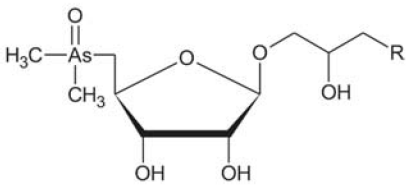
As-sugar-gly	glycerol-ribose[a]	R_1 OH
As-sugar-PO_4	phosphate-ribose[a]	R_2 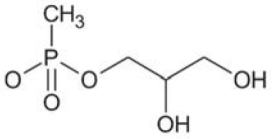
As-sugar-SO_3	sulfate-ribose[a]	R_3 SO_3H
As-sugar-SO_4	sulfonate-ribose[a]	R_4 OSO_3H

[a]The names of arsenosugars specified in this table are simplified according to ref.[13], their complete names are shown in the list of symbols and abbreviations.

2.2 Generation of Volatile Species

Volatile species generation (VSG) is one of the most widely employed derivatization technique for (ultra)trace element determination and speciation analysis in analytical atomic spectrometry.[14] VSG is an alternative to nebulization techniques which are utilized for flames or plasma sources in the analytical atomic spectrometry. In VSG, an analyte is converted to a volatile species and released from a liquid sample into a gaseous phase. VSG offers several advantages: a separation of the analyte from a sample matrix, higher transport efficiency and therefore sensitivity and mild atomization conditions required for efficient atomization.[15]

The procedure of VSG involves two completely independent sequential steps – generation and atomization/detection. Both steps are distinguished in space and can also be distinguished in time. The generation includes conversion of the analyte to the volatile species, their release from the liquid phase into the gaseous one and transport of the released volatile species by a flow of carrier gas into the detector.[16]

The most popular technique of VSG deals with the "classical" hydride forming elements which form binary or substituted hydrides (As, Bi, Ge, In, Pb, Sb, Se, Sn, Te, and Tl) or free atoms (Hg), which are formed during hydride generation (HG) reaction.[16] Volatile species formation from Cd and Zn was also reported. Zn volatile species is most probably a hydride.[17,18] In the case of Cd, conflicting reports on the nature of volatile species exist, either as free atoms[19,20] or as a hydride.[17]

In the last decades, a novel application of HG was introduced for transition metals (excluding II.B subgroup elements). A number of transition metals forming volatile species has been reported: Ag, Au, Co, Cu, Cr, Fe, Mn, Mo, Ni, Rh, Sc, and V.[21] However the nature of generated volatile species has not yet been identified.

A different analytically important volatile species can be formed from As, Bi, Sb, Se, Sn, Pb, Cd, Te, Hg, Ni, Co, Cu, Fe, Ag, Au, Rh, Pd, Pt[22] and even nonmetals I and S [23] via alkylation. Co, Fe, Ni, Se are also known to form analytically useful gaseous carbonyl derivatives.[24,25,26,27]

The generation of other volatile species, such as chelates[28,29,30], oxides[28,29,31] and halides[28,32,33,34] was also described but their impact on the field of analytical chemistry is negligible.

2.2.1 Hydride Generation

HG is the most used technique of VSG. Its original application employed a reduction of inorganic arsenic to arsane by the reaction with metallic Zn in the presence of acid (sulfuric or hydrochloric). This was used for identification of toxic arsenic in Marsh[35] and Gutzeit[36] tests. Almost one century later, this principle was used in Zn/acid apparatus by Holak[37] as sample introduction technique in the modern analytical atomic spectrometry. Later, this reaction was substituted by the reaction with tetrahydridoborate(1–) (THB).[38,39] The reaction of analyte with THB in acidic media is a superior method compared to the metal/acid reaction namely in higher yield, reduction reaction time and blank contamination.[16]

Many research papers dealing with element determination by HG with THB were published. Unfortunately, only a limited number of papers was dedicated to the mechanism of this reaction. The first attempt to clarify the mechanism of the reaction was made by Robbins and Caruso.[40] They postulated that the reaction of THB in acid media leads to a formation of nascent hydrogen which reduces analyte into the hydride:

$$BH_4^- + H_3O^+ + 2H_2O \rightarrow B(OH)_3 + 8H \quad (2)$$

$$A^{m+} + (m+n)\,H \rightarrow AH_n + mH^+ \quad (3)$$

where m and n are the valency of the analyte A in the liquid phase and in the volatile hydride, respectively. Their "nascent hydrogen mechanism" was generally accepted despite the fact it has never been proven.

In 2002 Laborda *et al.*[41] strongly criticized the concept that atomic hydrogen could be formed during the hydrolysis of THB or during the Zn/acid reaction. Considering that the estimated standard reduction potential for the H^+/H couple is $E^0(H^+/H) = -2.106$ V, neither THB [$E^0(H_3BO_3/BH_4^-) = -0.482$ V] nor Zn [$E^0(Zn^{2+}/Zn) = -0.763$ V] would be able to perform the reduction of protons to the atomic hydrogen. Nevertheless, both reagents would be able to perform the hydride generation reactions because their standard potentials are lower than analyte-hydride couple [$E^0(AsO_2^-/AsH_3) = 0.008$ V].

Later D'Ulivo and co-workers[42,43,44] postulated an alternative "hydrogen transfer" theory. In this theory THB is stepwise hydrolyzed in acidic media via hydrolytic intermediates to boric acid and molecular hydrogen:

$$BH_4^- + H_3O^+ \rightarrow BH_3(H_2O) + H_2 \quad (4)$$

$$BH_3(H_2O) + H_2O \rightarrow (H_2O)BH_2OH + H_2 \quad (5)$$

$$(H_2O)BH_2OH + H_2O \rightarrow (H_2O)BH(OH)_2 + H_2 \quad (6)$$

$$(H_2O)BH_2OH + H_3O^+ \rightleftarrows (H_2O)_2BH_2^+ + H_2O \quad (7)$$

$$(H_2O)BH(OH)_2 + H_2O \rightarrow B(OH)_3 + H_2 \quad (8)$$

The equilibrium (7) takes place only in the strong acidic conditions when H_3O^+ concentration is higher than 0.5 mol L^{-1}. Therefore, the THB hydrolysis is then slower when $[H_3O^+] > 0.5$ mol L^{-1} because the $(H_2O)_2BH_2^+$ species is resistant to hydrolysis.[45,46]

Nevertheless, all these equations can be summarized as:

$$BH_4^- + H_3O^+ + 2\ H_2O \rightarrow \text{intermediates} \rightarrow B(OH)_3 + 4H_2 \quad (9)$$

The analyte is then converted to the hydride by reaction with the THB or its hydrolytic intermediates through analyte-borate-complexes:[46]

$$A + BH_4^-/\text{intermediates} \rightarrow \text{hydride} \quad (10)$$

2.2.2 Alternative Volatile Species Generation Techniques

In addition to the chemical VSG, there are other approaches to generate analytical useful volatile species from analyte. Electrochemical HG uses the electric current to reduce the analyte to the hydride.[47] Analogously as for the chemical HG this is not anything new to analytical chemists. In 1861, Bloxam described the electrolytic generation of arsane and stibane.[48,49] Hydrides and Hg^0 vapors are generated in the presence of high purity acids usually in a flow-through electrolytic generator for continuous or flow-injection analysis[50,51,52,53] but also batch analysis was described.[54] Due to use of high purity acid the risk of contamination is minimal compared to chemical HG and the limit of detection (LOD) can be accordingly lower.

The different approach is based on photochemical reaction.[24,55] Photochemical VSG uses low molecular weight organic acids. The structure of generated volatile species depends on the used organic acid, *e.g.* the selenium (IV) species are converted to SeH_2, SeCO, $(CH_3)_2Se$, and $(CH_3CH_2)_2Se$ in the presence of formic, acetic propionic, and malonic acids, respectively.[24] An analogous behavior was observed for iAs^{III}.[56]

The latest technique is based on sonochemical reaction. As for the photochemical technique, the presence of low molecular weight organic acids is necessary. So far this technique is limited to mercury.[57]

2.2.3 Experimental Arrangements of Hydride Generation

There are two basic modes of HG, the direct transfer and collection. In the direct transfer mode, the volatile species is released from liquid sample and directly transported into the detector. The direct transfer mode can be further divided to batch, continuous flow, and flow injection. In the collection mode, the hydride is trapped in a collection device until the evolution is completed and then is transported to an atomizer all at once.[16,32]

In the **batch mode,** an acidified sample solution is placed inside the generator and the THB solution is then introduced either using a pump or manually employing a syringe. The carrier gas flow is introduced either to the dead volume of the generator or below the liquid level. Released hydride is then transported into the detector.[16,32]

The principle of **flow methods** is that the flow of the THB solution is mixed with a flow of the acidified sample solution. The mixture reacts in the reaction coil (RC) and the carrier gas is introduced downstream of the RC. The RC is connected to the gas-liquid separator (GLS) where the gaseous phase is separated from the reacted liquid phase and flows into the detector. Liquid phase is transported into the waste. Nowadays the continuous flow and flow injection are the most popular modes.[16,32]

The important advantage of HG is a possibility of analyte **collection** and therefore its preconcentration.[16,32] The generated hydrides are trapped until the generation step is completed and then they are transported into the atomizer.[37,58,59] Collection methods can be divided according to the location where collection takes place. It can be either in the atomizer (in-atomizer collection) or in a special device. In-atomizer collection can be performed in the graphite furnace (electrothermal atomization),[60,61,62] in quartz tube atomizers,[63,64,65,66,67,68,69] on a tungsten coil which is placed in the inlet arm of a T-shaped quartz tube,[70,71,72,73,74] or on quartz surface followed by atomization in an acetylene–air flame.[75,76]

At present, the collection in special devices is almost exclusively performed in a cryogenic trap (CT), which is usually a U-tube. During the generation step the CT is immersed in the liquid nitrogen through which hydrogen evolved in the reaction vessel

passes freely and is not collected. After the generation step is completed the liquid nitrogen is removed and the cryogenic trap is heated and trapped hydrides are released into the detector.[58,59,77,78,79,80,81,82] This collection procedure allows to achieve LODs typical for ultratrace analysis even with atomic absorption spectrometry *i.e.* with inexpensive instruments.

2.3 Atomization in AFS

In the beginning of analytical applications of AFS, acetylene-oxygen and hydrogen-oxygen flames were used for evaporation and atomization of analyte from aqueous solution.[83] This approach suffered from a high baseline noise caused by scattered radiation.[84] Introduction of analyte into AFS in the gaseous form dramatically lowered LOD.[85] The miniature flame or dielectric barrier discharge (DBD) atomizers are nowadays used in AFS for volatile species atomization.[16] The DBD atomizers are based on a gas discharge in which the plasma is separated from at least one electrode by a dielectric barrier.[86] Due to its simplicity and possible miniaturization, the DBD seems to be a very promising alternative to the flame atomizers.[87,88,89] The miniature flames are currently the most common atomizers for AFS. In general, there are two types of flame atomizers which are used: the miniature diffusion flame (MDF) and the flame-in-gas shield (FIGS) atomizer. The following paragraphs are focused on these two atomizers.

2.3.1 Miniature Diffusion Flame

The elementary optimization of the classical burner design for atomization of volatile species significantly improved the performance of diffusion flames.[16] Such an arrangement, termed MDF, is currently a standard atomizer for AFS in both commercial and laboratory assembled apparatus.[90] The MDF has a very simple design. The core of the atomizer consists of a vertical borosilicate or quartz tube with an inner diameter (i.d.) from 3 to 9 mm. The vertical tube serves as burner of the argon-hydrogen mixture containing volatile species of an analyte.[91]

The spatial temperature distribution in the MDF ranges from 150 to 1300°C. The maximum temperature is in outer zones of the flame where reactions between hydrogen and ambient oxygen take place. The minimal temperature is in the axis of the vertical tube close

to its top. But even the maximum temperature in the MDF is too low to produce a detectable fraction of free atoms in a thermodynamic equilibrium. The mechanism of atomization is based on reaction of volatile species with radicals. These radicals are generated in the outer zones of the MDF by following reactions:[92]

$$H + O_2 \rightleftarrows OH + O \quad (11)$$

$$O + H_2 \rightleftarrows OH + H \quad (12)$$

$$OH + H_2 \rightleftarrows H_2O + H \quad (13)$$

In the presence of excess of hydrogen it is reasonable to assume that only H radicals are formed in quantities corresponding to the total amount of supplied oxygen (*i.e.* two H radicals per oxygen molecule). Since the molecular hydrogen concentration in the flame is much higher than the water concentration, the amount of H radicals is at least by a few orders of magnitude higher than OH radicals.[92]

H radicals which are formed in the outer zones can diffuse to the cooler inner section of the flame. Outside of the hot zone they are terminating by a reaction with molecular oxygen. Therefore, the inner zone of the flame contains a high concentration of H radicals and the actual process of selenium hydride atomization by H radicals in MDF can be described by following reactions:[92]

$$SeH_2 + H \rightleftarrows SeH + H_2 \quad (14)$$

$$SeH + H \rightleftarrows Se + H_2 \quad (15)$$

This H radical atomization process is similar for the other hydrides.[32,93] The analyte is then present exclusively in the free atoms form within the whole flame volume.

The sensitivity in the MDF strongly depends on the total flow rate of the argon-hydrogen mixture, on the hydrogen fraction in the mixture, and on the observation height (OH, the distance from the center of the focused beam to the top of the atomizer – vertical tube). The high flow rate has two contradictory effects: better shielding of free atoms from ambient atmosphere reducing their loss due to the reaction with ambient oxygen which increases the sensitivity. The second effect is free atom dilution which reduces the sensitivity. The observation height has to be chosen with respect to sensitivity and to the atomizer noise.[16]

Nowadays, the MDF is especially applied for atomization of hydrides of

arsenic,[90,94,95,96,97] selenium,[90,94,96,97,98] antimony,[96,98] bismuth,[97,99] and tellurium[97,99]

2.3.2 Flame-in-gas shield

A different type of the atomizer designed for AFS is a FIGS atomizer.[100] It is a hydrogen-oxygen microflame shielded from ambient atmosphere by a flow of argon. The microflame is supported on a capillary which is placed inside the vertical tube (same vertical tube as for MDF). Through this capillary only a small flow of oxygen is introduced. The mixture of argon, hydrogen and volatile species of an analyte is introduced through the vertical tube. The observation volume above the top of the vertical tube is protected from the ambient atmosphere by a laminar flow of argon produced by a shielding unit that is fitted around the vertical tube.[101]

The atomization mechanism of analyte is the same as for the MDF. H radicals formed in the microflame diffuse into the whole observation volume above the vertical tube. Similar to the MDF, the sensitivity is influenced by the hydrogen fraction in the mixture. The oxygen flow rate through the capillary is another parameter which influences strongly the sensitivity: a very low flow rate can be insufficient for a complete atomization of the analyte and a very high flow rate can decrease sensitivity because of temperature expansion.[16,101]

The main benefit of the FIGS compared to the MDF is that the production of H radicals is controlled by the flow of oxygen, isolation of free atoms from ambient atmosphere is controlled by the flow of shielding argon, and dilution of analyte in the observation volume is controlled by the argon-hydrogen total flow rate while in the case of MDF all these parameters are controlled by the flow rate of argon-hydrogen mixture.[16,101]

In summary, the FIGS offers better sensitivity compared to the MDF but on the other hand, the experimental arrangement of FIGS is much more complicated. Also the operation cost are higher due to much higher consumption of argon.[16,100,101]

2.4 Speciation Analysis Based on Hydride Generation

The International Union of Pure and Applied Chemistry defines the speciation analysis as analytical activities of identifying and/or measuring the quantities of one or more individual chemical species in a sample. The chemical species is defined as specific form an element defined as to isotopic composition, electronic or oxidation state and/or complex or

molecular structure.[102]

In principle there are three approaches to speciation analysis based on HG: selective HG, generation of substituted hydrides, and post-column HG.[16] Since arsenic speciation analysis can be performed by all three options they are treated in the following paragraphs using arsenic as an example.

2.4.1 Selective Hydride Generation

The separation of arsenic species can be achieved by selective conversion of arsenic species to hydrides, *e.g.* the distinguishing between trivalent and pentavalent arsenic species is based on the fact that HG efficiency from these species strongly depends on pH. In strong acidic media arsane is generated from both iAs^{III} and iAs^{V} while at higher pH only iAs^{III} is converted to arsane.[103,104,105] However, even in highly concentrated acid there are differences in HG efficiencies from iAs^{III} and iAs^{V}.[103,106,107] Instead of using high acid concentration to determine the sum of iAs^{III} and iAs^{V}, pre-reduction agents are used.

KI with ascorbic acid in HCl was originally used for the pre-reduction of iAs^{V} to iAs^{III}.[108,109,110] Nowadays, pre-reduction by L-cysteine (L-cys)[80,106,107,111] or thioglycolic acid[79] is more popular. The typical procedure is then based on the determination of two aliquots. iAs^{III} is determined in the first aliquot while the sum of iAs^{III} and iAs^{V} is determined in the second (pre-reduced) aliquot.[16]

A different example of pH dependent HG was demonstrated by Musil *et al.* [112] who used high concentration of HCl to suppress generation from methylated species (mainly $DMAs^{V}$) in rice samples for selective determination of inorganic arsenic (iAs^{III} + iAs^{V}).

The main advantage of selective HG is that it does not require any separation step or any modification of the experimental setup.[16]

2.4.2 Generation of Substituted Hydrides

The generation of substituted hydrides is possible when various analyte species can be converted to the corresponding hydrides *e.g.* iAs^{III} and iAs^{V} are converted to AsH_3, MAs^{V} is converted to CH_3AsH_2, $DMAs^{V}$ is converted to $(CH_3)_2AsH$, and $TMAs^{V}O$ is converted to $(CH_3)_3As$. The generated mixture of arsanes is then collected in a CT. After the generation step is completed, the arsanes are subsequently volatilized gradually according to their

different boiling points.[58,59,80,81,82,113] The corresponding boiling points are –55, 2, 36, and 70 °C for arsane, methylarsane, dimethylarsane and trimethylarsane, respectively.[59]

This approach provides three essential advantages. Firstly, minimal sample pretreatment is required. Therefore, the risk of contamination or change of the original analyte distribution (oxidation/reduction or even change in the methylation) is thus minimized. Secondly, the direct analysis in complex biological matrices (homogenized liver tissue and cell lysates).[81,82] which cannot be separated by high performance liquid chromatography (HPLC), can be performed. Thirdly, the procedure LOD are usually much lower than for HPLC based approaches (using the same detector) because the larger sample volume can be used and the peaks are typically sharper than using HPLC.[16]

2.4.3 Post-column Hydride Generation

HPLC connected to an inductively coupled plasma mass spectrometer (ICP-MS) is a powerful and the most common method for determination of arsenic species.[114] HG is applied only to increase the sensitivity and selectivity.[16] These advantages make possible to replace the ICP-MS by AFS to achieve the same or even lower LODs.[98] This post-column HG can be used only for determination of species which are capable to form hydrides. This disadvantage can be eliminated by incorporating an on-line digestion device after the separation step but the corresponding experimental setup become more complicated and also the chromatographic resolution is worse.[115,116,117,118,119]

3 Experimental

Only a basic description of used instruments, hydride generators and atomizers is given in this chapter. The complete description can be found in the Papers I–III.

3.1 Instruments

In the Papers I-III, a laboratory assembled research grade atomic fluorescence spectrometer has been used for all atomic fluorescence measurements. The instrument was equipped with an arsenic electrodeless discharge lamp (EDL, system 2, Perkin-Elmer, USA). The operating current for EDL was 340 mA and the feeding power was square-wave modulated on frequency of 40 Hz. The radiation from the EDL was focused above the vertical axis of the atomizer by a biconvex quartz lens (diameter of 50 mm with focus length of 42 mm at 193 nm). Another two plano-convex lenses (diameter of 17 and 22 mm with focus length of 21 mm at 193nm) were used to focus the fluorescence radiation from the atomizer to the interference filter (193 nm, full width at half maximum 18.7 nm, CVI Melles Griot, USA) and it was collected at an angle 90°. PMT-MH 1922 (solar blind 165–320 nm) from Perkin Elmer Optoelectronics (USA) was used as the detector of fluorescence radiation.

In the Papers I-III, the HPLC–ICP-MS measurements were performed by means of HPLC system Agilent 1200 (USA) connected to Agilent 7700x ICP-MS (USA).

In the Paper III, the MS^2 spectra of arsenic species were performed by HCT-Ultra ETD II Mass Spectrometer (Bruker, USA) with electrospray ionization (ESI, capillary exit voltage was 102.3 V) in positive mode.

3.2 Hydride Generators

In principle, two different types of hydride generators were used for generation of arsanes in this work. Flow injection HG generators was used in Paper I and III. A batch hydride generator was used in Papers II and III.

3.2.1 Flow Injection Hydride Generator

The scheme of the flow injection hydride generator, employing two peristaltic pumps

(PP1 and PP2), is shown in Figure 1. The arsenic standard (in the case of Paper I the arsenic standard was iAs^V pre-reduced by L-cys while in Papers II and IV the arsenic standards were used directly without any pre-reduction) was carried by deionized water (DIW) and mixed with HCl solution (in the case of Paper I with TRIS buffer solution and in the case of Paper IV also with H_2SO_4 solution), followed by mixing with THB solution in the RC. The gaseous phase was separated from the liquid phase in the GLS. The Figure 2 shows schemes of GLS units used in the Papers I, II, and IV (see Paper II for detailed description of GLS units employed). The gaseous phase formed in GLS was transported by a flow of gas consisting of the argon carrier through NaOH dryer[120], then merged with a supplementary argon flow (flame argon) and a hydrogen flow (flame hydrogen) to the atomizer. Liquid waste was removed by the PP2 into the waste.

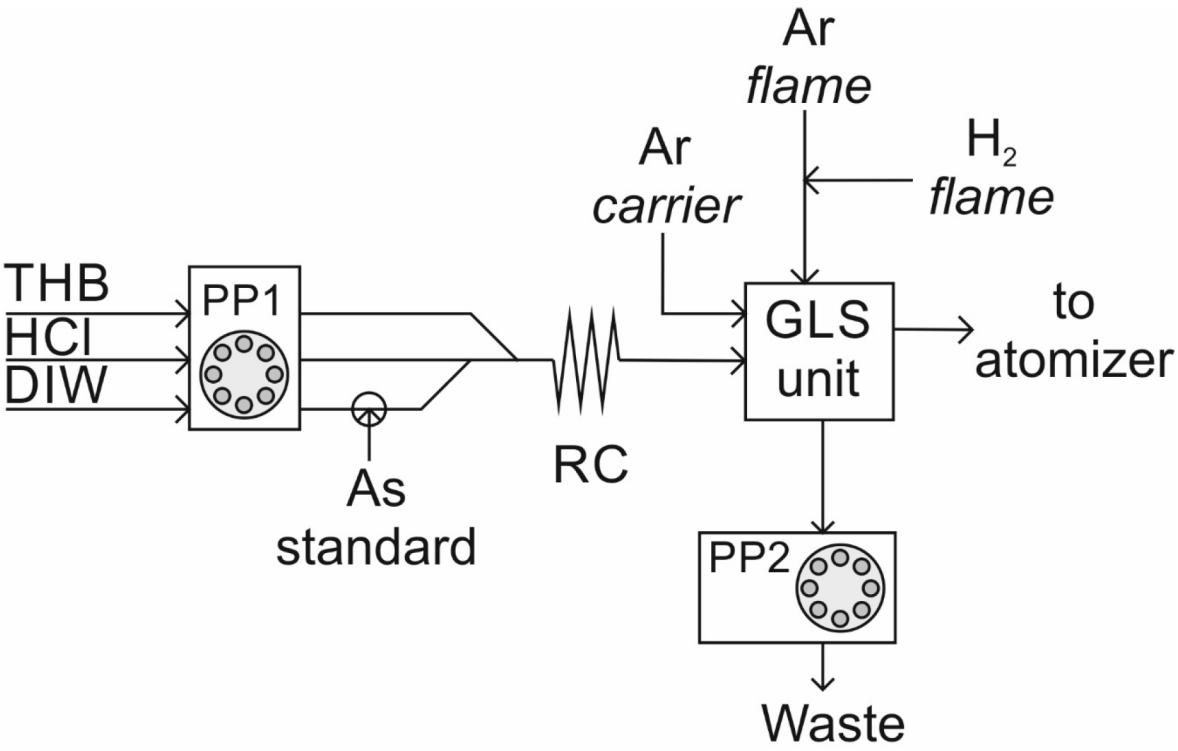

Figure 1 Experimental setup of the flow injection hydride generator: PP1/PP2 – peristaltic pumps, RC – reaction coil; DIW – deionized water; THB – solution of tetrahydridoborate(1–). Adapted with permission from Paper I. Copyright 2016 American Chemical Society.

In the post-column mode of HG (Paper I and III), the injection valve and the channel for DIW was replaced by the outlet from the chromatography column. When explicitly stated (in the Paper III), THB solution was introduced to the generator by two channels (not shown

in the Figure 1). THB introduced by the first channel was mixed in a T-junction with the acidified sample. The reacting mixture flew to the first RC which was connected downstream to another T-junction where the additional THB was introduced. The mixture followed to a second RC connected to the GLS unit.

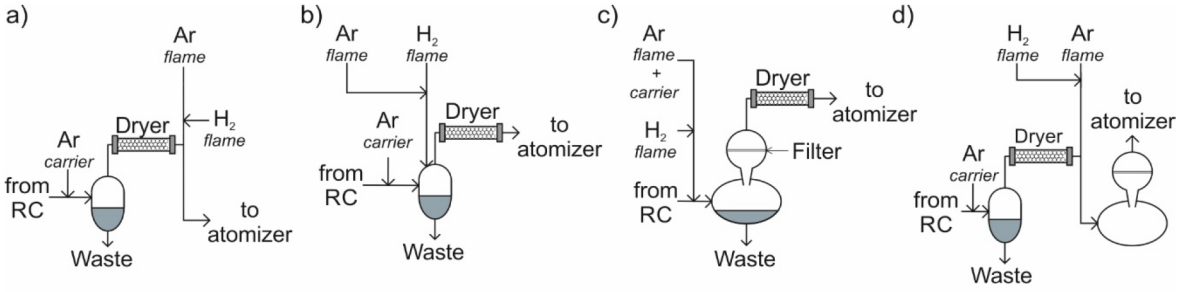

Figure 2 Schemes of used GLS units; a) GLS I, b) GLS unit II, c) GLS unit III, and d) GLS unit IV. Reproduced with permission from Paper I. Copyright 2016 American Chemical Society.

3.2.2 Batch Hydride Generator with Cryogenic Trap

The scheme of the batch hydride generator with CT is shown in Figure 3. Firstly, acid solution together with arsenic standard solution was pumped by the pump PP1. A carrier gas (argon or helium) merged the acid channel downstream the standard introduction point. The mixture was then introduced to the bottom of the GLS so that carrier gas could bubble through the reacting mixture. The acid channel was provided with an additional T-junction upstream the GLS that served for cleaning of the GLS with DIW manually by a syringe. Another channel was used to remove liquid waste from the GLS manually by a syringe. The solution of THB was then pumped by the pump PP2 and it was introduced to the bottom of the GLS below the liquid level (Figure 3a).

If explicitly stated (in the Paper II) the THB flow was mixed with the other acid flow, pumped by the second channel of the pump PP2 (Figure 3b). THB was thus partially decomposed (hydrolysed) in a hydrolysis coil (HC) downstream the point of mixing the THB flow with the other acid flow. The output of the gases from the GLS was connected to the dryer.[120]

The batch generator was operated either in the direct transfer mode or in the collection one. In the direct transfer mode (not shown in Figure 3), the carrier gas was argon

and the gas output from the dryer was merged with flame gases and flew to the atomizer. The set-up of the CT collection mode is shown in Figure 3 – the carrier gas was helium.

The CT device consisted of a glass U-tube filled with a chromatographic packing (Chromosorb WAW-DMCS 45/60, 15% OV-3, Supelco, Bellefonte, USA) and wrapped with a resistance wire for gradual heating. During the collection stage the U-tube was immersed in the liquid nitrogen. The volatilization step started by removing the flask with liquid nitrogen and switching on heating of the U-tube.

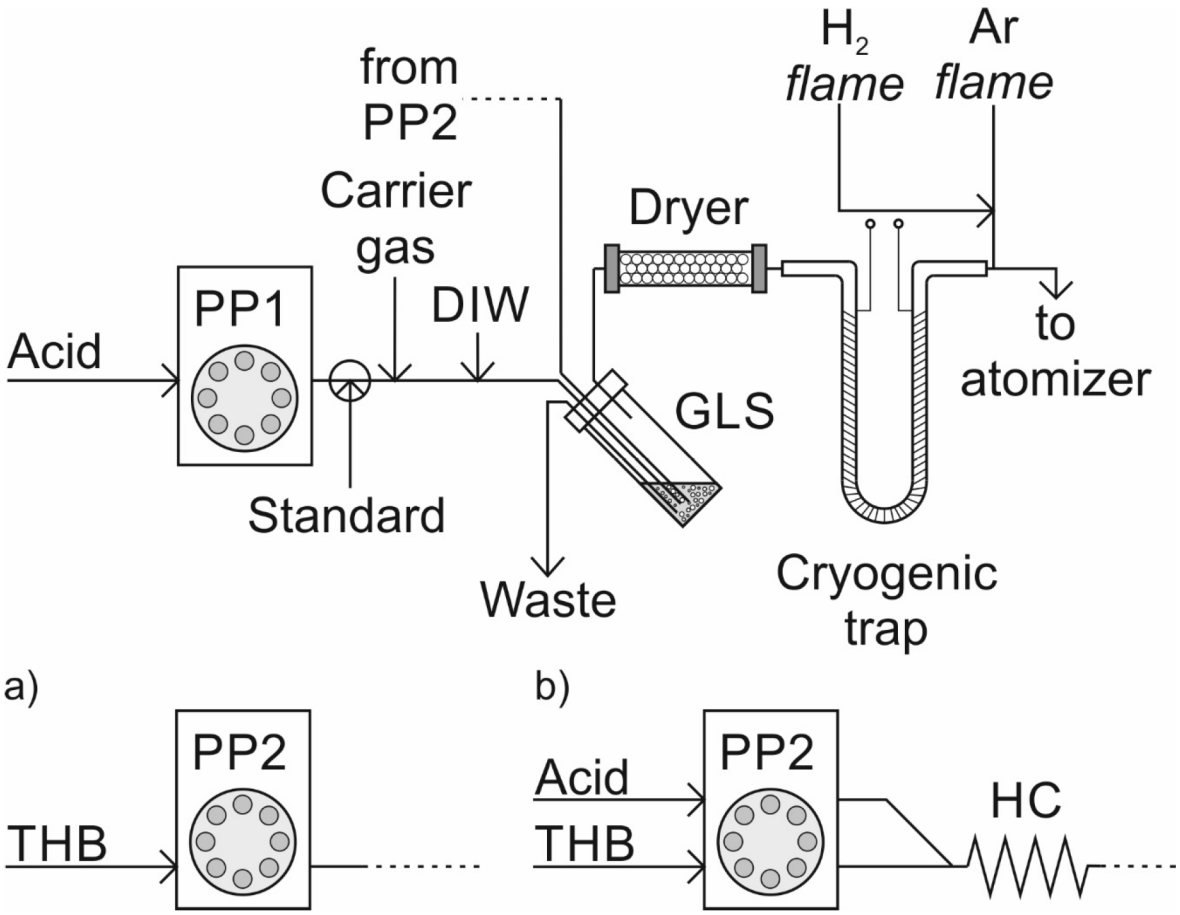

Figure 3 Experimental setup of the batch hydride generator with the CT with introduction of a) THB solution b) mixture of THB solution and acid: PP1/PP2 – peristaltic pumps, GLS – gas-liquid separator, HC – hydrolysis coil, THB – solution of sodium tetrahydridoborate(1–); DIW – deionized water. Reproduced with permission from Paper II. Copyright 2016 American Chemical Society.

3.3 Atomizer

The MDF was used as atomizer in all Papers (Papers I–III). MDF consisted of a vertical quartz tube (6 mm i.d. and 8.5 mm outer diameter (o.d.)) with a side inlet (2 mm i.d. and 3.75 mm o.d.) serving to introduce gases (Figure 4).

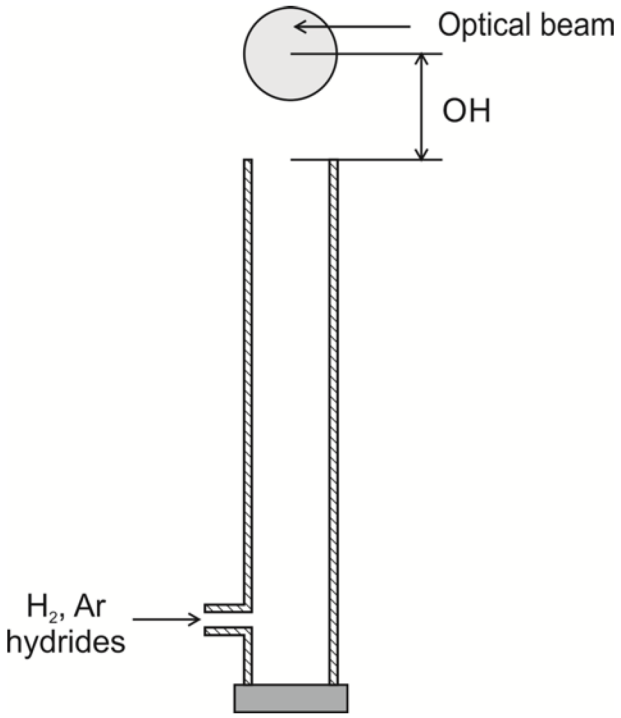

Figure 4 Scheme of MDF: OH – observation height. Adapted from Marschner K, *et al.*: *Spectrochimica Acta Part B: Atomic Spectroscopy*, **109**, 16–23 (2015), Copyright (2015), with permission from Elsevier.

4 Results

4.1 Optimization of Hydride Generation of Arsenic Species in Flow Injection Mode (Paper I)

The first part of Paper I describes the optimization of conditions of HG of iAs^{III}, iAs^{V}, MAs^{V}, and $DMAs^{V}$ in order to achieve the equal generation efficiency for all these species without any pre-reduction step in the flow injection mode. The relevant parameters of HG, *i.e.* HCl concentration (controlling pH of the reaction mixture), concentration of $NaBH_4$ and the volume of the RC (controlling the reaction time), were optimized. HCl concentration was tested in the range of 0.25 to 4 mol L^{-1}. Different trends were observed for individual arsenic species. For iAs^{III}, the signal remains almost constant (only a small positive effect of increased concentration of HCl was observed) while for iAs^{V} the positive effect of higher concentration of HCl was dramatic. The methylated species, MAs^{V} and $DMAs^{V}$, showed a different behavior. MAs^{V} had a maximum in the concentration range of 1–2 mol L^{-1} but the sensitivity at this maximum was still lower than for iAs^{III}. Increased concentration of HCl exhibited a strong negative effect on generation efficiency of $DMAs^{V}$. These dependencies correlate very well with the earlier works.[103,106,107,111,112] This different behavior of each arsenic species is the reason why achieving equal generation efficiency for all species has been unsuccessful yet. The concentration of 2 mol L^{-1} HCl was chosen for further optimization.

In order to increase reaction time, the volume of the RC was increased from 0.8 mL up to 8.9 mL. Increasing the volume to 3.5 mL was sufficient to reach the maximum MAs^{V} signal when it even reached the value of iAs^{III} signal. For iAs^{V} and $DMAs^{V}$, the signal gradually increased with the RC volume up to the maximum feasible volume of 8.9 mL.

To further improve HG efficiency of iAs^{V} and $DMAs^{V}$, the $NaBH_4$ concentration was increased from 1.0% up to 3.0% (m/v). The concentration higher than 2.0% is sufficient to unify HG efficiencies for all four arsenic species. A $NaBH_4$ concentration of 2.5% was chosen for further work. Assuming that the arsane is generated from iAs^{III} quantitatively in the optimized apparatus,[121] the HG efficiencies of iAs^{V}, MAs^{V}, and $DMAs^{V}$ were estimated as 100 ± 1%, 103 ± 2%, and 100 ± 2%, respectively.

Unfortunately, the high volume of the RC and high concentration of $NaBH_4$ had a negative effect on signal noise due to fluctuations of hydride supply into the atomizer. Several GLS units were tested (all details are described in Paper I). The system of two GLS

vessels (GLS unit IV) was found to be optimal. The first GLS was a small vessel (inner volume of approximately 3 mL) where the gas–liquid separation actually took place. The flame gases were introduced downstream of the small vessel and the dryer. The gas phase was further introduced to the second, larger GLS (inner volume of approximately 70 mL) which was connected to the atomizer.

This is for the first time that the equal hydride generation efficiency of iAs^{III}, iAs^{V}, MAs^{V}, and $DMAs^{V}$ in the flow injection mode (from acid medium without any pre-reduction step) has been reached.

4.2 The Post-column Hydride Generation for As Speciation Analysis (Paper I)

The second part of Paper I describes the practical use of developed HG for speciation analysis of arsenic by HPLC–HG–AFS. Firstly, the influence of a mobile phase on HG efficiency was tested. It was found that either mobile phase for ion pair chromatography (4.7 mmol L^{-1} tetrabutylammonium hydroxide, 2 mmol L^{-1} malonic acid in 4% methanol, pH adjusted to 5.85) or anion exchange chromatography (20 mmol L^{-1} phosphate buffer, pH adjusted to 6.00) had no effect on HG in the optimized hydride generator.

The separation of arsenics species in aqueous standard solution was successful when using ion pair chromatography as well as anion exchange chromatography. However, in the case of ion pair chromatography the resolution of arsenic species in undiluted urine samples was unsatisfactory. Peak tailing, overlapping and great shifting of retention times compared to standards in DIW was even observed. Ten times dilution was necessary to suppress the matrix effect. On the other hand, the anion exchange chromatography worked satisfactory, with excellent resolution of As species peaks, even for undiluted samples (Figure 5).

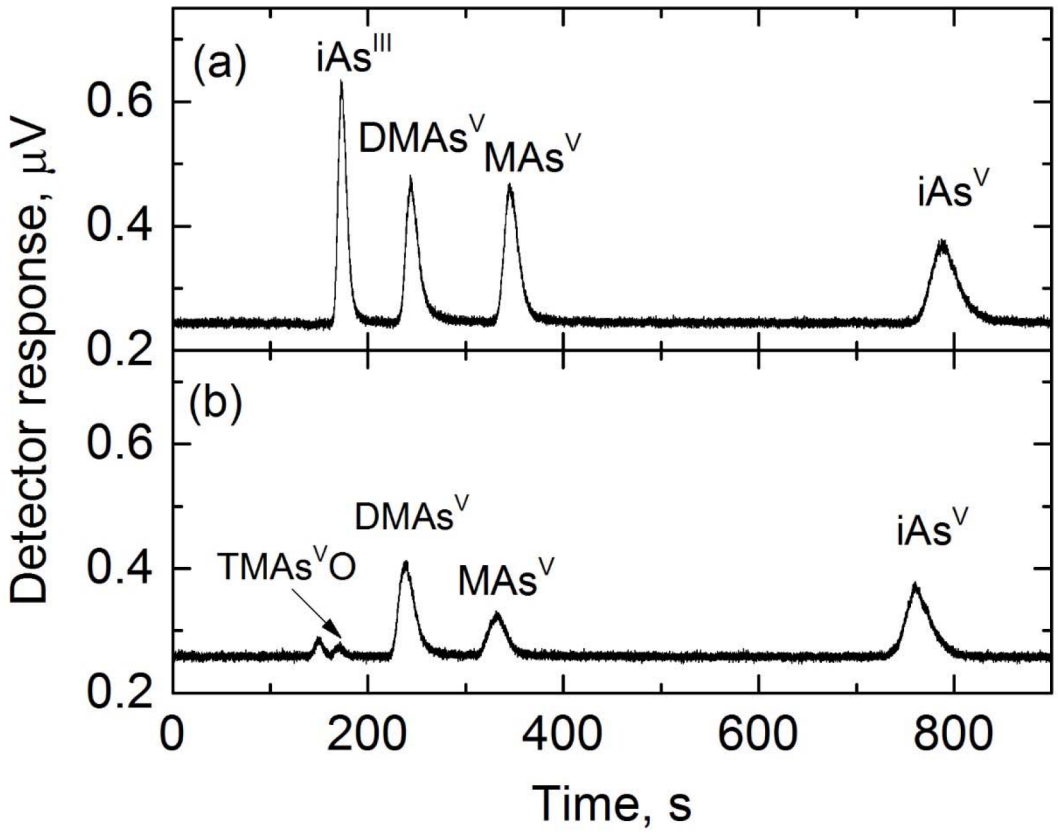

Figure 5 HPLC–HG–AFS chromatograms of (a) aqueous arsenic standards (5 ng mL^{-1} each), (b) urine SRM (NIST 2669 level I) with 3% H_2O_2; anion exchange chromatography with PRP-X100 column. Adapted with permission from Paper I. Copyright 2016 American Chemical Society.

Due to achieved 100% HG efficiency (chapter 4.1), the sensitivity evaluated from peak area was equal for all four species, the relative slopes of iAs^{III}, iAs^{V} and MAs^{V} (referred to DMAs^{V}) were 99 ± 2%, 102 ± 4%, and 100 ± 3%, respectively. Therefore, the calibration of DMAs^{V} could be used for quantification of other species. DMAs^{V} was chosen as a reference because it is a stable species and, in contrast to the inorganic species, it is not susceptible to reduction or oxidation. DMAs^{V} also elutes in the front part of the chromatogram so that the calibration can be obtained in much shorter time. It was found that only 350 s was necessary for measurement of calibration standard instead of 900 s for whole the chromatogram (see Figure 5a,b).

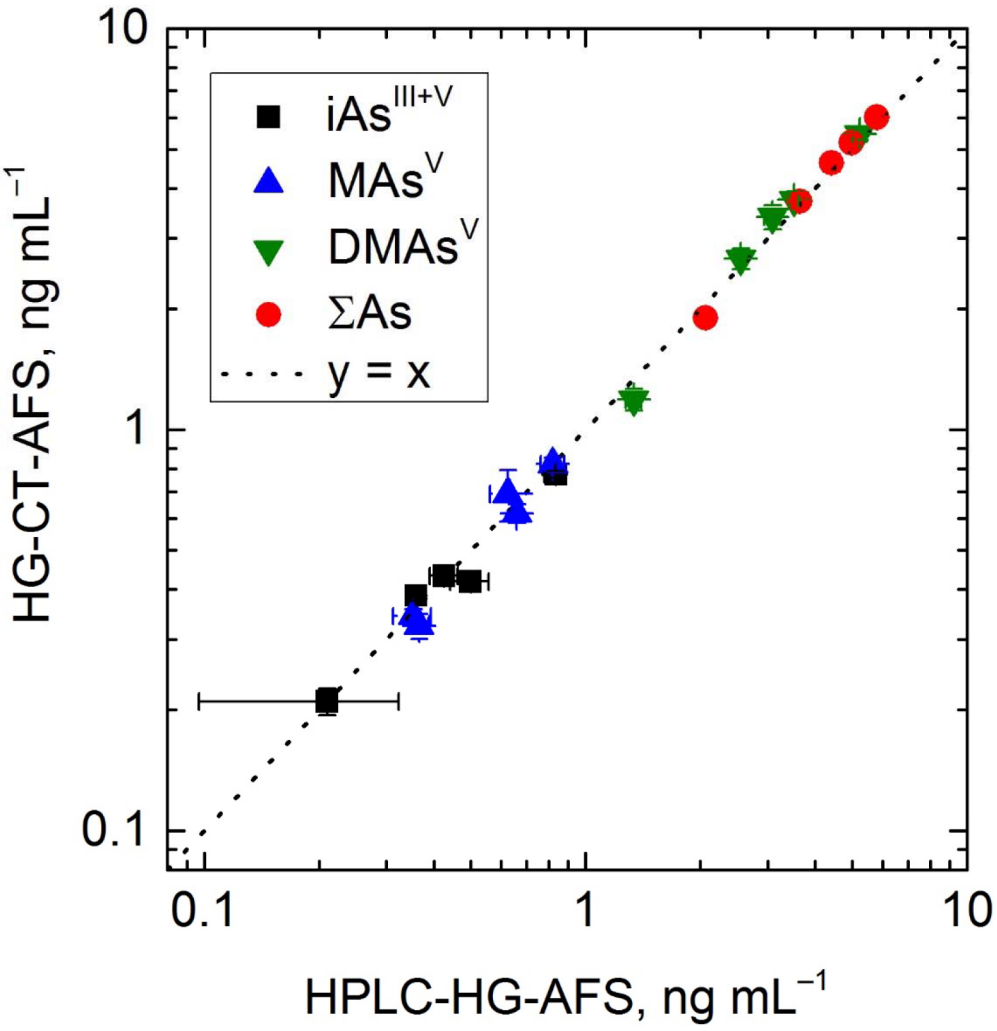

Figure 6. Comparison of results of analyses of human urine by HPLC-HG-AFS and HG-CT-AFS; ■ – iAs^{III+V}, ▲ – MAs^{V}, ▼ – DMAs^{V}, ● – ΣAs = (iAs^{III+V} + MAs^{V} + DMAs^{V}). Reproduced with permission from Paper I. Copyright 2016 American Chemical Society.

The determined absolute LODs for iAs^{III}, iAs^{V}, MAs^{V}, and DMAs^{V} were 2.0, 4.8, 2.9, and 2.8 pg, respectively. These LODs are much lower than those reported for other HPLC−HG−AFS instruments[122,123,124] and they are comparable with those reported for the HPLC−ICP-MS (typically from 0.3 to 24 pg).[125] The accuracy of the developed method was verified by analysis of standard reference material (SRM, NIST 2669, level I Arsenic species in frozen human urine) and by comparative analyses of five real samples of human urine of

five individuals using also HG–CT–AFS as a reference method (see Figure 6).[82]

4.3 Generation of Non-corresponding Substituted Arsanes (Paper II)

Paper II describes formation of the non-corresponding (less methylated) volatile products of HG of methylated arsenic species (MAs^V, $DMAs^V$, and $TMAs^VO$) in acidic media under analytical conditions in the batch mode. The main focus was on HCl medium because it is the most often used acid for HG of arsenic species.[32]

Firstly, the influence of HCl concentration on peak area of iAs^{III}, iAs^V, MAs^V, $DMAs^V$, and $TMAs^VO$ was optimized in the direct transfer mode. It was observed that all species were generated with the equal efficiency in the concentration range 0.5 to 1.0 mol L^{-1}. Increasing HCl concentration inevitably lead to broadening of the MAs^V, $DMAs^V$ and $TMAs^VO$ peaks and narrowing of iAs^{III} and iAs^V peaks. At HCl concentration of 2 mol L^{-1} or higher, the peak broadening resulted even in a decrease of normalized peak area of $TMAs^VO$. Although this could be compensated by addition of higher volume of 1% THB, it was not further employed due to pronounced increase of arsenic content in the blanks.

However, when the arsanes were generated from a mixed standard of iAs^{III}/iAs^V, MAs^V and $DMAs^V$ in the CT collection mode, a higher peak area of AsH_3 and lower peak areas for CH_3AsH_2 and $(CH_3)_2AsH$ were obtained. Namely, the use of 1 mol L^{-1} HCl and 1% THB resulted in 95 ± 3% and 77 ± 4% peak area for CH_3AsH_2 and $(CH_3)_2AsH$, respectively, relatively to the peak area of AsH_3. While this should be related to the exactly same normalized peak area of iAs^{III}/iAs^V, MAs^V and $DMAs^V$ in 1 mol L^{-1} HCl obtained in direct transfer mode. Two hypotheses were postulated related to this discrepancy: (i) individual arsenic species standards contain impurities of the other arsenic species, (ii) demethylation of MAs^V and $DMAs^V$ occurs during the HG step. The purity of the arsenic standards was confirmed by HPLC–ICP-MS as >99.9% for $DMAs^V$ and $TMAs^VO$, and 97.5% for MAs^V that contained 2.5% of inorganic arsenic (approximately half of iAs^{III} and half of iAs^V). Since the extent of the observed discrepancy (lower sensitivities of MAs^V and $DMAs^V$ using the CT collection mode) was much higher, the possibility of demethylation was further extensively studied.

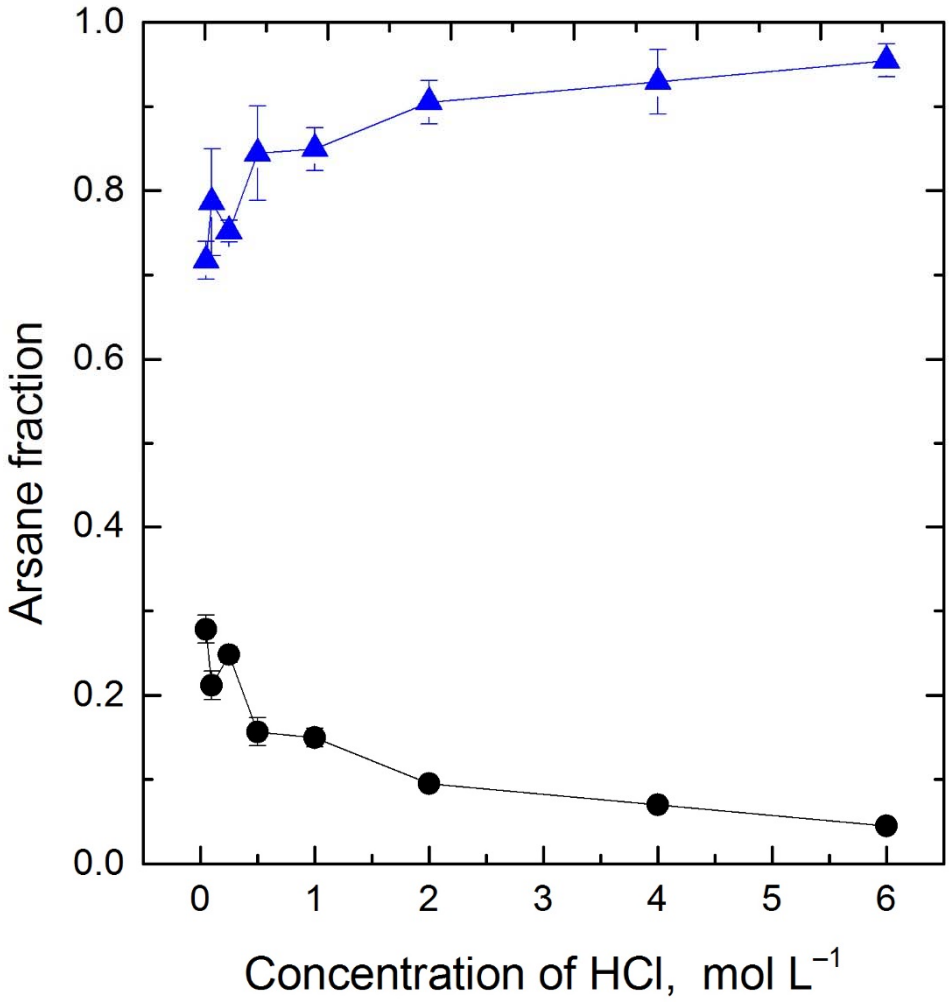

Figure 7. Dependence of arsane fraction formed from MAs^V on concentration of HCl; ● – AsH_3, ▲ – CH_3AsH_2; concentration of MAs^V was 0.5 ng mL^{-1}, 1 mL of 1% THB addition. Reproduced with permission from Paper II. Copyright 2016 American Chemical Society.

The dependence of demethylation (generation of methylsubstituted arsanes with lower degree of methylation) of MAs^V, $DMAs^V$, and $TMAs^VO$ on HCl concentration was studied in the range of 0.05 to 6.0 mol L^{-1}. For clarity, we define a term the "arsane fraction" as a peak area of the given arsane divided by the sum of peak areas of all arsanes quantified in the same chromatogram from single standard species. The dependence of arsane fraction for MAs^V is shown in Figure 7 and it clearly shows that the lower concentration of HCl leads to higher fraction of non-corresponding arsane (AsH_3) formed at the expense of CH_3AsH_2.

At the concentration of 0.05 mol L^{-1} HCl, 28 ± 2% of MAs^V is converted to AsH_3 instead of CH_3AsH_2.

The dependences for $DMAs^V$ and $TMAs^VO$ showed a similar trend as that for MAs^V. The yield of non-corresponding arsanes (at maximum) for $DMAs^V$ and $TMAs^VO$ was 37 ± 1% and 50 ± 2%, respectively. Higher HCl concentration is more suitable for generation of the corresponding arsane.

The dependence of demethylation of MAs^V, $DMAs^V$, and $TMAs^VO$ on THB solution concentration was also studied in the range of 0.25 to 4%. The maximum conversion to non-corresponding arsane was at 1–2% THB. The extent of demethylation for arsenic species was again in order $TMAs^VO > DMAs^V > MAs^V$, which can be attributed to the number of As–C bonds in the original species.

The above observations indicate that in the presence of HCl, THB (or some of its hydrolysis intermediates – equations 4–7) can cleave As–C bond. THB hydrolysis can be, to a certain extent, controlled when THB is on-line mixed with HCl solution in the HC before the mixture is pumped into the GLS (Figure 3b). The degree of THB hydrolysis is thus influenced by HCl concentration and by the reaction time which is proportional to the volume of the HC. The dependence of arsane fraction of MAs^V on HCl concentration used for pre-reaction of THB in the HC is shown in Figure 8. It clearly demonstrates that MAs^V demethylation extent reaches minimum (0.3 ± 0.2% of AsH_3) in the HCl concentration range from 0.25 to 1 mol L^{-1}. HCl concentration of 0.1 mol L^{-1} is obviously not high enough to pre-react 1% THB (0.28 mol L^{-1} together with KOH) sufficiently. Increasing HCl concentration above 1 mol L^{-1} leads to a slight but significant increase in demethylation: 5.0 ± 2.0% of AsH_3 from MAs^V. However, when the HC volume was increased from 40 to 825 µL (at 2 mol L^{-1} HCl) the demethylation of MAs^V decreased to 0.0 ± 0.7%. A similar behavior was observed also for $DMAs^V$ and $TMAs^VO$.

These experiments suggest that the "acid-resistant" hydridoboron species like $(H_2O)_2BH_2^+$ (equation (7)) can cleave the As–C bond while the next (and the last) hydridoboron species $(H_2O)BH(OH)_2$ cannot. $(H_2O)_2BH_2^+$ probably causes cleavage of As–C bond but it is not main responsible hydridoboron species for this action. The extent of demethylation at higher HCl concentration (used for pre-reaction) is much lower than without any HCl pre-reaction (Figure 8). Since BH_4^- is hydrolysed too fast, it is unlikely that this species can act as a derivatization agent for HG at all.[42] The $(HO)BH_3$ seems to be main hydridoboron species responsible for the demethylation process.

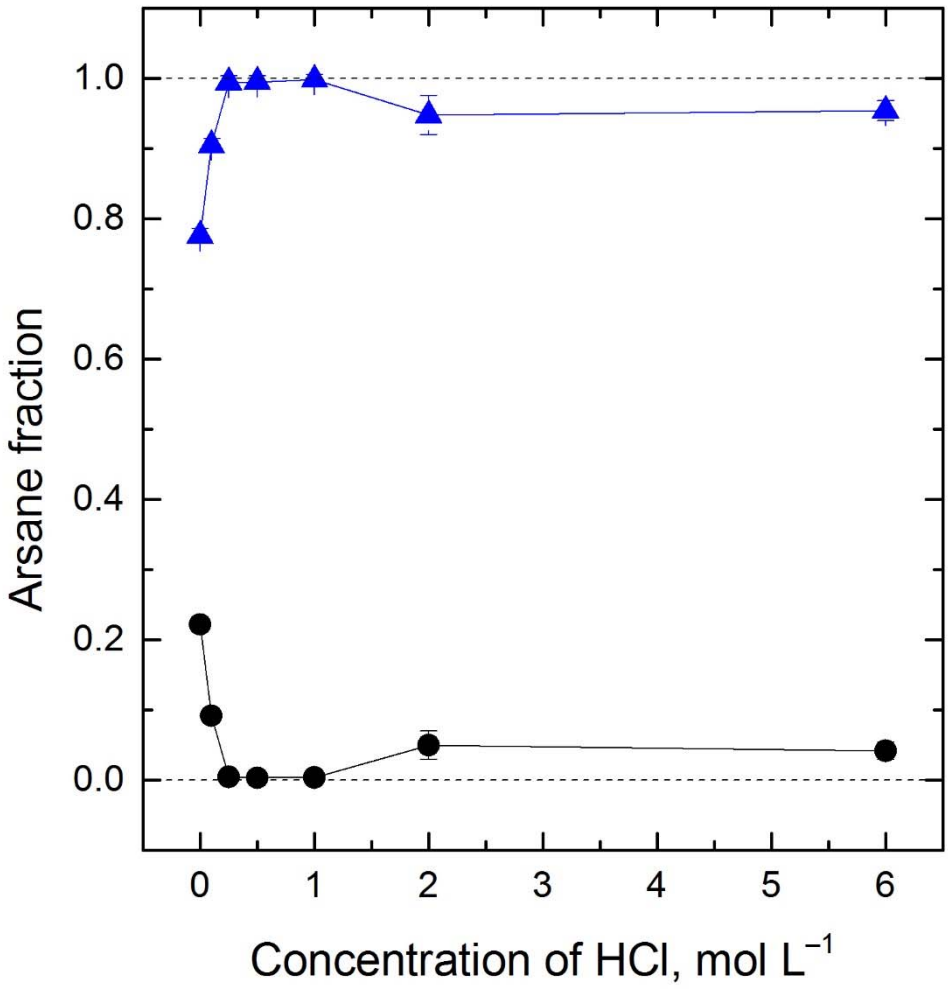

Figure 8. Dependence of arsane fractions formed from MAs^{V} on concentration of HCl used for pre-reaction of THB; ● – AsH_3, ▲ – CH_3AsH_2; HC volume was 40 µL, concentration of MAs^{V} was 0.5 ng mL^{-1}, 1 mL of 1% THB addition Reproduced with permission from Paper II. Copyright 2016 American Chemical Society.

The demethylation of arsenic species during HG was studied also in media of $HClO_4$, H_2SO_4, HNO_3, CH_3COOH, and from TRIS (pH 6.0) buffer after treatment with 2% L-cys. It was found that the demethylation of arsenic species was even greater in the medium of $HClO_4$ and H_2SO_4. In CH_3COOH or from TRIS buffer medium after L-cys pre-reduction of arsenic standard, no demethylation was observed for any species. An unusual situation was observed in the case of HNO_3 because the demethylation of MAs^{V} and $DMAs^{V}$ during HG was insignificant (lower than 1%). However, in the case of $TMAs^{V}O$ the demethylation to

the $(CH_3)_2AsH$ was observed and the arsane fraction of this non-corresponding arsane gradually increased with HNO_3 concentration. That is an opposite trend than for HCl (Figure 7).

The demethylation of arsenic species during HG does not bring any risk of incorrect results of the postcolumn HG (Paper I) since the resulting sensitivity does not depend on the degree of methylation of the resulting hydride. However, in the case of arsenic speciation analysis based on generation of substituted hydrides, the demethylation can endanger accuracy of arsenic speciation when HCl is employed as HG medium. This method of speciation analysis using HCl as the medium for HG has been used in the following published works.[126,127,128,129,130,131,132,133,134,135,136]

4.4 Generation of Arsanes from Arsenosugars (Paper III)

Paper III investigates the possibility of HG from arsenosugars with the aim to achieve as high HG efficiency as possible and to test the feasibility of this derivatization approach for speciation analysis by HPLC-HG-AFS.

The first problem with arsenosugars is that there are not commercially available or well characterized standards. They must be synthesized by a very complex procedure or extracted and purified from seaweed sources. Therefore, four seaweed samples (*Hijiki*, *Nori*, *Kombu*, and *Wakame*) were purchased at a local supermarket and milled to the fine powder. The extraction was performed by DIW in an ultrasonic bath. The identification of four arsenosugars (As-sugar-gly, As-sugar-PO_4, As-sugar-SO_3, and As-sugar-SO_4) was performed by HPLC–ESI–MS^2 and comparison of fragmentation spectra with published data.[137,138] It was found that the extract of *Nori* containes 98% of arsenic in the form of arsenosugars. Moreover, 94% of its arsenic content is in the form of As-sugar-PO_4. The diluted *Nori* extract was spiked with $DMAs^V$ and no matrix effect was observed on HG (the recovery was 100 ± 4%). Therefore, the diluted *Nori* extract was used as As-sugar-PO_4 "standard" for investigation of HG arsenosugars.

At first, HG activity of As-sugar-PO_4 was studied in the batch mode and it was found that 1 mol L^{-1} H_2SO_4 and 1% THB solution was optimal. HG efficiency under these conditions was 68 ± 1% while in HCl medium the maximum achieved HG efficiency was 35 ± 1%. This agrees with the results of Paper II reporting higher cleavage of As–C bond in H_2SO_4 than in HCl medium. The HG–CT–AFS technique was used for identification of

formed volatile arsanes from As-sugar-PO_4. 66 ± 3% was found in the form of $(CH_3)_2AsH$, 32 ± 3% as CH_3AsH_2 and 3 ± 1% as AsH_3. No traces of $(CH_3)_3As$ were detected.

The HG activity of As-sugar-PO_4 was also studied in the flow injection mode. The optimal conditions were 1.5 mol L^{-1} H_2SO_4 and 1% THB. The corresponding HG efficiency was 19 ± 1% while for 1.0 mol L^{-1} HCl and 2% THB the efficiency was 16.3 ± 0.2%. The HG efficiency achieved in the flow injection mode was dramatically lower than in the batch mode. This corresponds to the phenomenon observed in Paper II that only first two products of THB hydrolysis are capable to cleave As–C bond and therefore to form arsanes from arsenosugars. These two hydrolytic products are present in the batch mode during the whole time of analysis, since the analyte is continuously supplied with fresh solution of THB in the batch mode. In contrast, in the flow injection mode the first two hydrolytic products of THB are present only in the upstream part of the RC. In order to increase concentration of the first two hydrolytic products of THB and thus enhance the HG efficiency, a new design of hydride generator with two inlets of THB was constructed. This approach increased the HG efficiency of As-sugar-PO_4 in the flow injection mode to 29 ± 3%.

The mechanism of HG from arsenosugars was proposed. It is based on the formation of two kinds of analyte-borane-complex: the first one results in formation of volatile arsanes while the second decomposes back to the analyte (*i.e.* does not form the volatile arsanes).

The developed hydride generator was connected to HPLC for postcolumn HG. The seaweed extracts were analyzed by HPLC–HG–AFS (the chromatogram is shown in Figure 9) and from comparison with HPLC–ICP-MS the HG efficiencies for As-sugar-gly, As-sugar-PO_4, As-sugar-SO_3, and As-sugar-SO_4, were determined as 13 ± 1%, 28 ± 2%, 31 ± 3%, and 17 ± 1%, respectively. The absolute LODs were 41, 9.5, 13, and 19 pg for As-sugar-gly, As-sugar-PO_4, As-sugar-SO_3, and As-sugar-SO_4, respectively. These LODs are comparable to HPLC–UV-decomposition–HG–AFS approaches determined by other authors.[139,140,141]

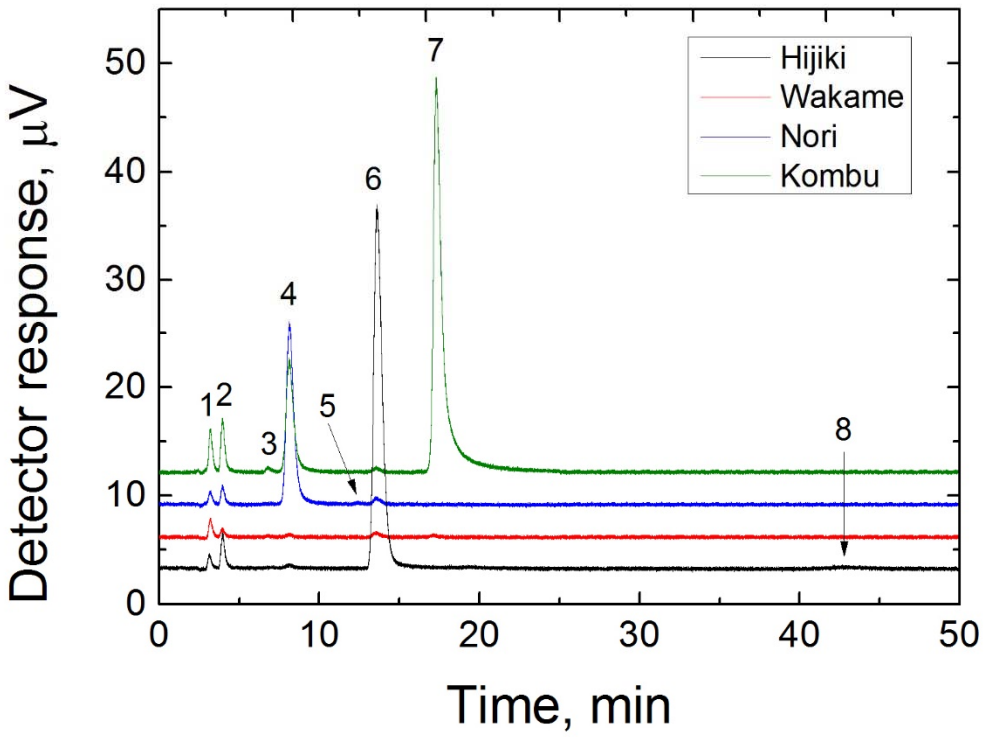

Figure 9 HPLC–HG–AFS chromatograms of four seaweed samples; HG conditions: 1.5 mol L^{-1} H_2SO_4, two inlets of 1% THB; 1 – As-sugar-gly, 2 – $DMAs^V$, 3 – MAs^V, 4 – As-sugar-PO_4, 5 – unknown, 6 – iAs^V, 7 – As-sugar-SO_3, 8 – As-sugar-SO_4.

5 Conclusion

The presented thesis is focused on HG of arsenic species. It brings a significant and previously unpublished progress in this field but also an analytical application of developed method. Two papers included in the thesis were published in the prestigious international scientific journal and one paper has been submitted. The achieved results were also presented at the conferences in the form of poster presentations (3) or as lectures (11). All objectives defined in the introduction part have been accomplished and are summarized in the following paragraphs.

The flow injection hydride generator which allows to generate iAs^{III}, iAs^{V}, MAs^{V}, and $DMAs^{V}$ with 100% efficiency was developed. The high noise which was the result of relatively high concentration of THB solution and large volume of RC was dramatically reduced by the newly developed design of the gas-liquid separator.

The developed hydride generator was successfully applied for post-column HG of arsenic species and used for determination of arsenic species in human urine samples. Due to equal HG efficiency of all four arsenic species the single species calibration could be used. That reduces the time for the calibration process by a factor of 2.6. The feasibility of this method was confirmed by analysis of a reference material and by comparative analysis of real samples.

The influence of conditions of HG from methylated arsenic species on the structure of their volatile form was studied in detail. A pronounced demethylation of MAs^{V}, $DMAs^{V}$, and $TMAs^{V}O$ during the reaction with THB in HCl, H_2SO_4, and $HClO_4$ media was observed. The demethylation appeared to be due to the action of specific hydrolytic products of THB. This behavior jeopardizes the accuracy of speciation analysis of arsenic employing generation of substituted arsanes.

Following the previous results, the possibility of generation of arsanes from arsenosugars was verified and optimized in the flow injection and batch modes. A probable reaction path was proposed which includes formation of two kinds of analyte-borane-complex: the first kind results in formation of volatile arsanes and the second one decomposes back to the analyte. Unfortunately, the lack of available standards makes this analysis currently impossible. Achieved HG efficiencies for As-sugars are similar or even better than those published up to now[13,142] depending on the mode of the generator used.

6 References

1. Hughes, M. F.: Arsenic toxicity and potential mechanisms of action. *Toxicology Letters,* **133**, 1-16 (2002).

2. Smith, A. H.; Lingas, E. O.; Rahman, M.: Contamination of drinking-water by arsenic in Bangladesh: a public health emergency. *Bulletin of the World Health Organization,* **78**, 1093-1103 (2000).

3. Tondel, M.; Rahman, M.; Magnuson, A.; Chowdhury, I. A.; Faruquee, M. H.; Ahmad, S. A.: The relationship of arsenic levels in drinking water and the prevalence rate of skin lesions in Bangladesh. *Environmental Health Perspectives,* **107**, 727-729 (1999).

4. Rahman, M.; Tondel, M.; Ahmad, S. A.; Axelson, O.: Diabetes Mellitus Associated with Arsenic Exposure in Bangladesh. *American Journal of Epidemiology,* **148**, 198-203 (1998).

5. Challenger, F.: Biological Methylation. *Chemical Reviews,* **36**, 315-361 (1945).

6. Hayakawa, T.; Kobayashi, Y.; Cui, X.; Hirano, S.: A new metabolic pathway of arsenite: arsenic-glutathione complexes are substrates for human arsenic methyltransferase Cyt19. *Archives of Toxicology,* **79**, 183-191 (2005).

7. Rehman, K.; Naranmandura, H.: Arsenic metabolism and thioarsenicals. *Metallomics,* **4**, 881-892 (2012).

8. Francesconi, K. A.: Arsenic species in seafood: Origin and human health implications. *Pure and Applied Chemistry* **82,** 373- (2010).

9. Nischwitz, V.; Pergantis, S. A.: Optimisation of an HPLC selected reaction monitoring electrospray tandem mass spectrometry method for the detection of 50 arsenic species. *Journal of Analytical Atomic Spectrometry,* **21**, 1277-1286 (2006).

10. Witt, B.; Meyer, S.; Ebert, F.; Francesconi, K. A.; Schwerdtle, T.: Toxicity of two classes of arsenolipids and their water-soluble metabolites in human differentiated neurons. *Archives of Toxicology,* 1-14 (2017).

11. Sele, V.; Sloth, J. J.; Lundebye, A. K.; Larsen, E. H.; Berntssen, M. H. G.; Amlund, H.: Arsenolipids in marine oils and fats: A review of occurrence, chemistry and future research needs. *Food Chemistry,* **133**, 618-630 (2012).

12. Niegel, C.; Matysik, F. M.: Analytical methods for the determination of arsenosugars-A review of recent trends and developments. *Analytica Chimica Acta,* **657**, 83-99 (2010).

13. Regmi, R.; Milne, B.; Feldmann, J.: Hydride generation activity of arsenosugars and thioarsenicals. *Anal Bioanal Chem,* **388**, 775-782 (2007).

14. D'Ulivo, A.; Dědina, J.; Mester, Z.; Sturgeon, R. E.; Wang, Q. Q.; Welz, B.: Mechanisms of chemical generation of volatile hydrides for trace element determination (IUPAC Technical Report). *Pure and Applied Chemistry,* **83**, 1283-1340 (2011).

15. Welz, B.; Sperling, M.: *Atomic Absorption Spectrometry.* Weinheim, Wiley-VCH (1999).

16. Dědina, J.: Generation of Volatile Compounds for Analytical Atomic Spectroscopy. In: *Encyclopedia of Analytical Chemistry*. Meyers, R.A. (ed.). Chichester: John Wiley and Sons Ltd., 2010, p. 1-39.

17. Luna, A. S.; Sturgeon, R. E.; de Campos, R. C.: Chemical Vapor Generation: Atomic Absorption by Ag, Au, Cu, and Zn Following Reduction of Aquo Ions with Sodium Tetrahydroborate(III). *Analytical Chemistry,* **72**, 3523-3531 (2000).

18. Sun, H.; Suo, R.; Lu, Y.: Determination of zinc in food using atomic fluorescence spectrometry by hydride generation from organized media. *Analytica Chimica Acta,* **457**, 305-310 (2002).

19. Sanz-Medel, A.; Valdes, H.; Bordel Garcia, N.; Fernandez de la Campa, M. R.: Generation of Cadmium Atoms at Room Temperature Using Vesicles and Its Application to Cadmium Determination by Cold Vapor Atomic Spectrometry. *Analytical Chemistry,* **67**, 2216-2223 (1995).

20. Xiao-Wei, G.; Xu-Ming, G.: Determination of cadmium at ultratrace levels by cold vapour atomic absorption spectrometry. *Journal of Analytical Atomic Spectrometry,* **10**, 987-991 (1995).

21. Pohl, P.; Jamroz, P.; Welna, M.; Szymczycha-Madeja, A.; Greda, K.: Chemical-vapor generation of transition metals through the reaction with tetrahydroborate in recent achievements in analytical atomic spectrometry. *TrAC Trends in Analytical Chemistry,* **59**, 144-155 (2014).

22. Sturgeon, R. E.; Guo, X.; Mester, Z.: Chemical vapor generation: are further advances yet possible? *Analytical and Bioanalytical Chemistry,* **382**, 881-883 (2005).

23. Guo, X.; Sturgeon, R. E.; Mester, Z.; Gardner, G. J.: Vapor Generation by UV Irradiation for Sample Introduction with Atomic Spectrometry. *Analytical Chemistry,* **76**, 2401-2405 (2004).

24. Guo, X.; Sturgeon, R. E.; Mester, Z.; Gardner, G. J.: UV Vapor Generation for Determination of Selenium by Heated Quartz Tube Atomic Absorption Spectrometry. *Analytical Chemistry,* **75**, 2092-2099 (2003).

25. Sturgeon, R. E.; Willie, S. N.; Berman, S. S.: Graphite furnace atomic absorption spectrometric determination of nickel at sub-ng g-1 levels in marine samples by carbonyl generation with in situ pre-concentration. *Journal of Analytical Atomic Spectrometry,* **4**, 443-446 (1989).

26. Grinberg, P.; Mester, Z.; Sturgeon, R. E.; Ferretti, A.: Generation of volatile cobalt species by UV photoreduction and their tentative identification. *Journal of Analytical Atomic Spectrometry,* **23**, 583-587 (2008).

27. Grinberg, P.; Sturgeon, R. E.; Gardner, G.: Identification of volatile iron species generated by UV photolysis. *Microchemical Journal,* **105**, 44-47 (2012).

28. Smichowski, P.; as, S.: Advantages and analytical applications of chloride generation. A review on vapor generation methods in atomic spectrometry. *Microchemical Journal,* **67**, 147-155 (2000).

29. Wu, P.; He, L.; Zheng, C.; Hou, X.; Sturgeon, R. E.: Applications of chemical vapor generation in non-tetrahydroborate media to analytical atomic spectrometry. *Journal of Analytical Atomic Spectrometry,* **25**, 1217-1246 (2010).

30. Rodriguez-Vázquez, J. A.: Quantitative inorganic analysis by gas chromatography. *Analytica Chimica Acta,* **73**, 1-32 (1974).

31. Tao, H.; Miyazaki, A.; Bansho, K.: Determination of osmium by inductively coupled plasma emission spectrometry with an oxide generation/condensation system. *Analytical Chemistry,* **60**, 1762-1765 (1988).

32. Dědina, J.; Tsalev, D. L.: *Hydride Generation Atomic Absorption Spectrometry.* Chichester, John Wiley & Sons, Inc. (1995).

33. Mester, Z.; Sturgeon, R. E.: Detection of volatile arsenic chloride species during hydride generation: a new prospectus. *Journal of Analytical Atomic Spectrometry,* **16**, 470-474 (2001).

34. Tesfalidet, S.; Irgum, K.: Volatilization of arsenic as the trichloride for sample introduction in atomic spectroscopy. *Analytical Chemistry,* **60**, 2031-2035 (1988).

35. Marsh, J.: Account of a Method of separating Small Quantities of Arsenic from Substances with which it may be mixed. *Edinb.N.Phil.Journ.,* **21**, 229-236 (1836).

36. Gutzeit, H.: Bemerkungen zur Revision der Pharmacopoea Germanica. *Pharmaceutische Zeitung,* **24**, 263-263 (1879).

37. Holak, W.: Gas-Sampling Technique for Arsenic Determination by Atomic Absorption Spectrophotometry. *Analytical Chemistry,* **41**, 1712-1713 (1969).

38. Braman, R. S.: Membrane probe-spectral emission type detection system for mercury in water. *Analytical Chemistry,* **43**, 1462-1467 (1971).

39. Braman, R. S.; Justen, L. L.; Foreback, C. C.: Direct volatilization-spectral emission type detection system for nanogram amounts of arsenic and antimony. *Analytical Chemistry,* **44**, 2195-2199 (1972).

40. Robbins, W. B.; Caruso, J. A.: Development of hydride generation methods for atomic spectroscopic analysis. *Analytical Chemistry,* **51**, 889A-898A (1979).

41. Laborda, F.; Bolea, E.; Baranguan, M. T.; Castillo, J. R.: Hydride generation in analytical chemistry and nascent hydrogen: when is it going to be over? *Spectrochimica Acta Part B-Atomic Spectroscopy,* **57**, 797-802 (2002).

42. D'Ulivo, A.: Mechanism of generation of volatile species by aqueous boranes Towards the clarification of most controversial aspects. *Spectrochimica Acta Part B-Atomic Spectroscopy,* **65**, 360-375 (2010).

43. D'Ulivo, A.; Baiocchi, C.; Pitzalis, E.; Onor, M.; Zamboni, R.: Chemical vapor generation for atomic spectrometry. A contribution to the comprehension of reaction mechanisms in the generation of volatile hydrides using borane complexes. *Spectrochimica Acta Part B: Atomic Spectroscopy,* **59**, 471-486 (2004).

44. D'Ulivo, A.: Chemical vapor generation by tetrahydroborate(III) and other borane complexes in aqueous media A critical discussion of fundamental processes and mechanisms involved in reagent decomposition and hydride formation. *Spectrochimica Acta, Part B: Atomic Spectroscopy,* **59B**, 793-825 (2004).

45. Wang, F. T.; Jolly, W. L.: Kinetic study of the intermediates in the hydrolysis of the hydroborate ion. *Inorganic Chemistry,* **11**, 1933-1941 (1972).

46. D'Ulivo, A.; Onor, M.; Pitzalis, E.: Role of hydroboron intermediates in the mechanism of chemical vapor generation in strongly acidic media. *Analytical Chemistry,* **76**, 6342-6352 (2004).

47. Laborda, F.; Bolea, E.; Castillo, J. R.: Electrochemical hydride generation as a sample-introduction technique in atomic spectrometry: fundamentals, interferences, and applications. *Analytical and Bioanalytical Chemistry,* **388**, 743-751 (2007).

48. Bloxam, C. L.: IV.-On the application of electrolysis to the detection of the poisonous metals in mixtures containing organic matters. *Quarterly Journal of the Chemical Society of London,* **13**, 12-22 (1861).

49. Bloxam, C. L.: XXXII.-On the electrolytic test for arsenic, and on the presence of that metal in certain reagents. *Quarterly Journal of the Chemical Society of London,* **13**, 338-343 (1861).

50. Lin, Y.; Wang, X.; Yuan, D.; Yang, P.; Huang, B.; Zhuang, Z.: Flow injection-electrochemical hydride generation technique for atomic absorption spectrometry. Invited lecture. *Journal of Analytical Atomic Spectrometry,* **7**, 287-291 (1992).

51. Brockmann, A.; Nonn, C.; Golloch, A.: New concept for hydride generation technique: electrochemical hydride generation. *Journal of Analytical Atomic Spectrometry,* **8**, 397-401 (1993).

52. Hraníček, J.; Červený, V.; Rychlovský, P.: Miniaturization of flow-through generation cells for electrochemical hydride generation in AAS. *Central European Journal of Chemistry,* **7**, 675-682 (2009).

53. Červený, V.; Rychlovský, P.; Netolická, J.; Šíma, J.: Electrochemical generation of mercury cold vapor and its in-situ trapping in gold-covered graphite tube atomizers. *Spectrochimica Acta Part B: Atomic Spectroscopy,* **62**, 317-323 (2007).

54. Arbab-Zavar, M. H.; Hashemi, M.: Evaluation of electrochemical hydride generation for spectrophotometric determination of As(III) by silver diethyldithiocarbamate. *Talanta,* **52**, 1007-1014 (2000).

55. He, Y.; Hou, X.; Zheng, C.; Sturgeon, R. E.: Critical evaluation of the application of photochemical vapor generation in analytical atomic spectrometry. *Analytical and Bioanalytical Chemistry,* **388**, 769-774 (2007).

56. Guo, X.; Sturgeon, R. E.; Mester, Z.; Gardner, G. J.: Photochemical alkylation of inorganic arsenic Part 1. Identification of volatile arsenic species. *Journal of Analytical Atomic Spectrometry,* **20**, 702-708 (2005).

57. Gil, S.; Lavilla, I.; Bendicho, C.: Ultrasound-Promoted Cold Vapor Generation in the Presence of Formic Acid for Determination of Mercury by Atomic Absorption Spectrometry. *Analytical Chemistry,* **78**, 6260-6264 (2006).

58. Braman, R. S.; Foreback, C. C.: Methylated Forms of Arsenic in the Environment. *Science,* **182**, 1247-1249 (1973).

59. Braman, R. S.; Johnson, D. L.; Foreback, C. C.; Ammons, J. M.; Bricker, J. L.: Separation and determination of nanogram amounts of inorganic arsenic and methylarsenic compounds. *Analytical Chemistry,* **49**, 621-625 (1977).

60. Matusiewicz, H.; Sturgeon, R. E.: Atomic spectrometric detection of hydride forming elements following in situ trapping within a graphite furnace. *Spectrochimica Acta Part B: Atomic Spectroscopy,* **51**, 377-397 (1996).

61. Haug, H. O.; Yiping, L.: Automated determination of tin by hydride generation using in situ trapping on stable coatings in graphite furnace atomic absorption spectrometry. *Spectrochimica Acta Part B: Atomic Spectroscopy,* **50**, 1311-1324 (1995).

62. Willie, S. N.: First order speciation of As using flow injection hydride generation atomic absorption spectrometry with in-situ trapping of the arsine in a graphite furnace. *Spectrochimica Acta Part B: Atomic Spectroscopy,* **51**, 1781-1790 (1996).

63. Kratzer, J.; Dědina, J.: In situ trapping of stibine in externally heated quartz tube atomizers for atomic absorption spectrometry. *Spectrochimica Acta Part B: Atomic Spectroscopy,* **60**, 859-864 (2005).

64. Kratzer, J.; Dědina, J.: In situ trapping of bismuthine in externally heated quartz tube atomizers for atomic absorption spectrometry. *Journal of Analytical Atomic Spectrometry,* **21**, 208-210 (2006).

65. Kratzer, J.; Dědina, J.: Arsine and selenium hydride trapping in a novel quartz device for atomic-absorption spectrometry. *Analytical and Bioanalytical Chemistry,* **388**, 793-800 (2007).

66. Kratzer, J.; Dědina, J.: Stibine and bismuthine trapping in quartz tube atomizers for atomic absorption spectrometry GÇö Method optimization and analytical applications. *Spectrochimica Acta Part B: Atomic Spectroscopy,* **63**, 843-849 (2008).

67. Kratzer, J.; Vobecky, M.; Dedina, J.: Stibine and bismuthine trapping in quartz tube atomizers for atomic absorption spectrometry. Part 2: a radiotracer study. *Journal of Analytical Atomic Spectrometry,* **24**, 1222-1228 (2009).

68. Dessuy, M. B.; Kratzer, J.; Vale, M. G.; Welz, B.; Dědina, J.: Hydride generation in-atomizer collection atomic absorption spectrometry for the determination of antimony in acetic acid leachates from pewter cups. *Talanta,* **87**, 255-261 (2011).

69. Průša, L.; Dědina, J.; Kratzer, J.: Ultratrace determination of tin by hydride generation in-atomizer trapping atomic absorption spectrometry. *Analytica Chimica Acta,* **804**, 50-58 (2013).

70. Ataman, O. Y.: Vapor generation and atom traps: Atomic absorption spectrometry at the ng/L level. *Spectrochimica Acta Part B: Atomic Spectroscopy,* **63**, 825-834 (2008).

71. Kula, I.; Arslan, Y.; Bakirdere, S.; Titretir, S.; Kendüzler, E.; Ataman, O. Y.: Determination and interference studies of bismuth by tungsten trap hydride generation atomic absorption spectrometry. *Talanta,* **80**, 127-132 (2009).

72. Alp, O.; Ertas, N.: In situ trapping of antimony hydride on iridium-coated tungsten coil and interference studies. *Journal of Analytical Atomic Spectrometry,* **23**, 976-980 (2008).

73. Kula, I.; Arslan, Y.; Bakirdere, S.; Ataman, O. Y.: A novel analytical system involving hydride generation and gold-coated W-coil trapping atomic absorption spectrometry for selenium determination at ng l-1 level. *Spectrochimica Acta Part B: Atomic Spectroscopy,* **63**, 856-860 (2008).

74. Titretir, S.; Kendüzler, E.; Arslan, Y.; Kula, I.; Bakirdere, S.; Ataman, O. Y.: Determination of antimony by using tungsten trap atomic absorption spectrometry. *Spectrochimica Acta Part B: Atomic Spectroscopy,* **63**, 875-879 (2008).

75. Matusiewicz, H.: Atom trapping and in situ preconcentration techniques for flame atomic absorption spectrometry. *Spectrochimica Acta Part B: Atomic Spectroscopy,* **52**, 1711-1736 (1997).

76. Matusiewicz, H.; Krawczyk, M.: Determination of cadmium and lead in reference materials by volatile species generation with in situ trapping flame atomic absorption spectrometry. *Microchemical Journal,* **83**, 17-23 (2006).

77. Ellwood, M. J.; Maher, W. A.: An automated hydride generation-cryogenic trapping-ICP-MS system for measuring inorganic and methylated Ge, Sb and As species in marine and fresh waters. *Journal of Analytical Atomic Spectrometry,* **17**, 197-203 (2002).

78. van Cleuvenbergen, R. J. A.; van Mol, W. E.; Adams, F. C.: Arsenic speciation in water by hydride cold trapping-quartz furnace atomic absorption spectrometry: an evaluation. *Journal of Analytical Atomic Spectrometry,* **3**, 169-176 (1988).

79. Musil, S.; Matoušek, T.: On-line pre-reduction of pentavalent arsenicals by thioglycolic acid for speciation analysis by selective hydride generation-cryotrapping-atomic absorption spectrometry. *Spectrochimica Acta, Part B: Atomic Spectroscopy,* **63B**, 685-691 (2008).

80. Matoušek, T.; Hernandez-Zavala, A.; Svoboda, M.; Langrová, L.; Adair, B. M.; Drobná, Z.; Thomas, D. J.; Stýblo, M.; Dědina, J.: Oxidation state specific generation of arsines from methylated arsenicals based on L-cysteine treatment in buffered media for speciation analysis by hydride generation-automated cryotrapping-gas chromatography-atomic absorption spectrometry with the multiatomizer. *Spectrochimica Acta, Part B: Atomic Spectroscopy,* **63B**, 396-406 (2008).

81. Matoušek, T.; Currier, J. M.; Trojánková, N.; Saunders, R. J.; Ishida, M. C.; Gonzalez-Horta, C.; Musil, S.; Mester, Z.; Stýblo, M.; Dědina, J.: Selective hydride generation-cryotrapping-ICP-MS for arsenic speciation analysis at picogram levels: analysis of river and sea water reference materials and human bladder epithelial cells. *Journal of Analytical Atomic Spectrometry,* **28**, 1456-1465 (2013).

82. Musil, S.; Matoušek, T.; Currier, J. M.; Stýblo, M.; Dědina, J.: Speciation Analysis of Arsenic by Selective Hydride Generation-Cryotrapping-Atomic Fluorescence Spectrometry with Flame-in-Gas-Shield Atomizer: Achieving Extremely Low Detection Limits with Inexpensive Instrumentation. *Analytical Chemistry,* **86**, 10422-10428 (2014).

83. Winefordner, J. D.; Vickers, T. J.: Atomic Fluorescence Spectrometry As Means of Chemical Analysis. *Analytical Chemistry,* **36**, 161-165 (1964).

84. Winefordner, J. D.; Staab, R. A.: Determination of Zinc Cadmium and Mercury by Atomic Fluorescence Flame Spectrometry. *Analytical Chemistry,* **36**, 165-168 (1964).

85. Tsujii, K.; Kitazume, E.: Depth profiles of arsenic in semiconductor silicon by chemical etching and non-dispersive atomic fluorescence spectrometry with hydride generation. *Analytica Chimica Acta,* **125**, 101-108 (1981).

86. Brandt, S.; Schütz, A.; Klute, F. D.; Kratzer, J.; Franzke, J.: Dielectric barrier discharges applied for optical spectrometry. *Spectrochimica Acta Part B: Atomic Spectroscopy,* **123**, 6-32 (2016).

87. Zhu, Z.; Liu, J.; Zhang, S.; Na, X.; Zhang, X.: Determination of Se, Pb, and Sb by atomic fluorescence spectrometry using a new flameless, dielectric barrier discharge atomizer. *Spectrochimica Acta Part B: Atomic Spectroscopy,* **63**, 431-436 (2008).

88. Xing, Z.; Kuermaiti, B.; Wang, J.; Han, G.; Zhang, S.; Zhang, X.: Simultaneous determination of arsenic and antimony by hydride generation atomic fluorescence spectrometry with dielectric barrier discharge atomizer. *Spectrochimica Acta Part B: Atomic Spectroscopy,* **65**, 1056-1060 (2010).

89. Xing, Z.; Wang, J.; Zhang, S.; Zhang, X.: Determination of bismuth in solid samples by hydride generation atomic fluorescence spectrometry with a dielectric barrier discharge atomizer. *Talanta,* **80**, 139-142 (2009).

90. Corns, W. T.; Stockwell, P. B.; Ebdon, L.; Hill, S. J.: Development of an atomic fluorescence spectrometer for the hydride-forming elements. *Journal of Analytical Atomic Spectrometry,* **8**, 71-77 (1993).

91. Dědina, J.; D'Ulivo, A.; Lampugnani, L.; Matoušek, T.; Zamboni, R.: Selenium hydride atomization, fate of free atoms and spectroscopic temperature in miniature diffusion flame atomizer studied by atomic absorption spectrometry. *Spectrochimica Acta Part B-Atomic Spectroscopy,* **53**, 1777-1790 (1998).

92. Dědina, J.; Rubeška, I.: Hydride atomization in a cool hydrogen-oxygen flame burning in a quartz tube atomizer. *Spectrochimica Acta Part B: Atomic Spectroscopy,* **35**, 119-128 (1980).

93. Dedina, J.; Welz, B.: Quartz tube atomizers for hydride generation atomic absorption spectrometry: mechanism for atomization of arsine. Invited lecture. *Journal of Analytical Atomic Spectrometry,* **7**, 307-314 (1992).

94. Cai, Y.: Speciation and analysis of mercury, arsenic, and selenium by atomic fluorescence spectrometry. *TrAC, Trends in Analytical Chemistry,* **19**, 62-66 (2000).

95. Correia, C. L. T.; Goncalves, R. A.; Azevedo, M. S.; Vieira, M. A.; Campos, R. C.: Determination of total arsenic in seawater by hydride generation atomic fluorescence spectrometry. *Microchemical Journal,* **96**, 157-160 (2010).

96. Sanchez-Rodas, D.; Corns, W. T.; Chen, B.; Stockwell, P. B.: Atomic Fluorescence Spectrometry: a suitable detection technique in speciation studies for arsenic, selenium, antimony and mercury. *Journal of Analytical Atomic Spectrometry,* **25**, 933-946 (2010).

97. Rahman, L.; Corns, W. T.; Bryce, D. W.; Stockwell, P. B.: Determination of mercury, selenium, bismuth, arsenic and antimony in human hair by microwave digestion atomic fluorescence spectrometry. *Talanta,* **52**, 833-843 (2000).

98. Chen, Y. W.; Belzile, N.: High performance liquid chromatography coupled to atomic fluorescence spectrometry for the speciation of the hydride and chemical vapour-forming elements As, Se, Sb and Hg: A critical review. *Analytica Chimica Acta,* **671**, 9-26 (2010).

99. Reyes, M. N. M.; Cervera, M. L.; de la Guardia, M.: Determination of total Sb, Se, Te, and Bi and evaluation of their inorganic species in garlic by hydride-generation-atomic-fluorescence spectrometry. *Analytical and Bioanalytical Chemistry,* **394**, 1557-1562 (2009).

100. Dědina, J.; D'Ulivo, A.: Argon shielded, highly fuel-rich, hydrogen-oxygen diffusion microflame - a new hydride atomizer. *Spectrochimica Acta Part B-Atomic Spectroscopy,* **52**, 1737-1746 (1997).

101. Dědina, J.: Atomization of volatile compounds for atomic absorption and atomic fluorescence spectrometry: on the way towards the ideal atomizer. *Spectrochimica Acta, Part B: Atomic Spectroscopy,* **62B**, 846-872 (2007).

102. Templeton, D. M.; Ariese, F.; Cornelis, R.; Danielsson, L.; Muntau, H.; van Leeuwen, H. P.; Lobinski, R.: Guidelines for terms related to chemical speciation and fractionation of elements. Definitions, structural aspects, and methodological approaches (IUPAC Recommendations 2000). *Pac* **72,** 1453- (2000).

103. Anderson, R. K.; Thompson, M.; Culbard, E.: Selective reduction of arsenic species by continuous hydride generation. Part I. Reaction media. *Analyst,* **111**, 1143-1152 (1986).

104. Devesa, V.; Maria Del Razo, L.; Adair, B.; Drobna, Z.; Waters, S. B.; Hughes, M. F.; Styblo, M.; Thomas, D. J.: Comprehensive analysis of arsenic metabolites by pH-specific hydride generation atomic absorption spectrometry. *Journal of Analytical Atomic Spectrometry,* **19**, 1460-1467 (2004).

105. Feldman, C.: Improvements in the arsine accumulation-helium glow detector procedure for determining traces of arsenic. *Analytical Chemistry,* **51**, 664-669 (1979).

106. Carrero, P.; Malave, A.; Burguera, J. L.; Burguera, M.; Rondon, C.: Determination of various arsenic species by flow injection hydride generation atomic absorption spectrometry: investigation of the effects of the acid concentration of different reaction media on the generation of arsines. *Analytica Chimica Acta,* **438**, 195-204 (2001).

107. Shraim, A.; Chiswell, B.; Olszowy, H.: Speciation of arsenic by hydride generation-atomic absorption spectrometry (HG-AAS) in hydrochloric acid reaction medium. *Talanta,* **50**, 1109-1127 (1999).

108. Donaldson, E. M.; Leaver, M. E.: Determination of arsenic in ores, concentrates and related materials by continuous hydride-generation atomic-absorption spectrometry after separation by xanthate extraction. *Talanta,* **35**, 297-300 (1988).

109. Haring, B. J. A.; van Delft, W.; Bom, C. M.: Determination of arsenic and antimony in water and soil by hydride generation and atomic absorption spectroscopy. *Fresenius' Zeitschrift F+-r Analytische Chemie,* **310**, 217-223 (1982).

110. Hoede, D.; Van Der Sloot, H. A.: Application of hydride generation for the determination of antimony and arsenic in biological material by neutron activation analysis. *Analytica Chimica Acta,* **111**, 321-325 (1979).

111. Le, X. C.; Cullen, W. R.; Reimer, K. J.: Effect of cysteine on the speciation of arsenic by using hydride generation atomic absorption spectrometry. *Analytica Chimica Acta,* **285**, 277-285 (1994).

112. Musil, S.; Pétursdóttir, Á. H.; Raab, A.; Gunnlaugsdóttir, H.; Krupp, E.; Feldmann, J.: Speciation without Chromatography Using Selective Hydride Generation: Inorganic Arsenic in Rice and Samples of Marine Origin. *Analytical Chemistry,* **86**, 993-999 (2014).

113. Howard, A. G.; Salou, C.: Cysteine enhancement of the cryogenic trap hydride AAS determination of dissolved arsenic species. *Analytica Chimica Acta,* **333**, 89-96 (1996).

114. Francesconi, K. A.; Kuehnelt, D.: Determination of arsenic species: A critical review of methods and applications, 2000-2003. *Analyst (Cambridge, United Kingdom),* **129**, 373-395 (2004).

115. Atallah, R. H.; Kalman, D. A.: On-line photo-oxidation for the determination of organoarsenic compounds by atomic-absorption spectrometry with continuous arsine generation. *Talanta,* **38**, 167-173 (1991).

116. Bin, H.; Gui-bin, J.; Xiao-bai, X.: Arsenic speciation based on ion exchange high-performance liquid chromatography hyphenated with hydride generation atomic fluorescence and on-line UV photo oxidation. *Fresenius' Journal of Analytical Chemistry,* **368**, 803-808 (2000).

117. Howard, A. G.; Hunt, L. E.: Coupled photooxidation-hydride AAS detector for the HPLC of arsenic compounds. *Analytical Chemistry,* **65**, 2995-2998 (1993).

118. Tsalev, D. L.; Sperling, M.; Welz, B.: Speciation determination of arsenic in urine by high-performance liquid chromatography-hydride generation atomic absorption spectrometry with on-line ultraviolet photooxidation[dagger]. *Analyst,* **123**, 1703-1710 (1998).

119. Tsalev, D. L.; Sperling, M.; Welz, B.: On-line UV-photooxidation with peroxodisulfate for automated flow injection and for high-performance liquid chromatography coupled to hydride generation atomic absorption spectrometry. *Spectrochimica Acta Part B: Atomic Spectroscopy,* **55**, 339-353 (2000).

120. Taurková, P.; Svoboda, M.; Musil, S.; Matoušek, T.: Loss of di- and trimethylarsine on Nafion membrane dryers following hydride generation. *Journal of Analytical Atomic Spectrometry,* **26**, 220-223 (2011).

121. Van Elteren, J. T.; Das, H. A.; Bax, D.: Radiotracer Examination of Gas-Liquid Separators Used in Arsenic Speciation by Hydride Generation - AAS. *Journal of Radioanalytical and Nuclear Chemistry-Articles,* **174**, 133-144 (1993).

122. Bohari, Y.; Astruc, A.; Astruc, M.; Cloud, J.: Improvements of hydride generation for the speciation of arsenic in natural freshwater samples by HPLC-HG-AFS. *Journal of Analytical Atomic Spectrometry,* **16**, 774-778 (2001).

123. Moreno E.; Cámara, C.; Corns, W. T.; Bryce, D. W.; Stockwell, P. B.: Arsenic speciation in beverages by direct injection-ion chromatography hydride generation atomic fluorescence spectrometry. *Journal of Automated Methods and Management in Chemistry,* **22**, 33-39 (2000).

124. Wei, C.; Liu, J.: A new hydride generation system applied in determination of arsenic species with ion chromatographyGÇôhydride generation-atomic fluorescence spectrometry (IC–HG-AFS). *Talanta,* **73**, 540-545 (2007).

125. Komorowicz, I.; Barałkiewicz, D.: Arsenic and its speciation in water samples by high performance liquid chromatography inductively coupled plasma mass spectrometry-Last decade review. *Talanta,* **84**, 247-261 (2011).

126. Drobná, Z.; Waters, S. B.; Devesa, V.; Harmon, A. W.; Thomas, D. J.; Stýblo, M.: Metabolism and toxicity of arsenic in human urothelial cells expressing rat arsenic (+3 oxidation state)-methyltransferase. *Toxicology and Applied Pharmacology,* **207**, 147-159 (2005).

127. Hughes, M. F.; Devesa, V.; Adair, B. M.; Styblo, M.; Kenyon, E. M.; Thomas, D. J.: Tissue dosimetry, metabolism and excretion of pentavalent and trivalent monomethylated arsenic in mice after oral administration. *Toxicology and Applied Pharmacology,* **208**, 186-197 (2005).

128. Wen, W.; Wen, J.; Lu, L.; Liu, H.; Yang, J.; Cheng, H.; Che, W.; Li, L.; Zhang, G.: Metabolites of arsenic and increased DNA damage of p53 gene in arsenic plant workers. *Toxicology and Applied Pharmacology,* **254**, 41-47 (2011).

129. Devesa, V.; Adair, B. M.; Liu, J.; Waalkes, M. P.; Diwan, B. A.; Styblo, M.; Thomas, D. J.: Arsenicals in maternal and fetal mouse tissues after gestational exposure to arsenite. *Toxicology,* **224**, 147-155 (2006).

130. Valenzuela, O. L.; Borja-Aburto, V. H.; Garcia-Vargas, G. G.; Cruz-Gonzalez, M. B.; Garcia-Montalvo, E. A.; Calderon-Aranda, E. S.; Del Razo, L. M.: Urinary Trivalent Methylated Arsenic Species in a Population Chronically Exposed to Inorganic Arsenic. *Environmental Health Perspectives,* **113**, 250-254 (2005).

131. Hernandez-Zavala, A.; Valenzuela, O. L.; Matoušek, T.; Drobná, Z.; Dědina, J.; Garcia-Vargas, G. G.; Thomas, D. J.; Del Razo, L. M.; Stýblo, M.: Speciation of Arsenic in Exfoliated Urinary Bladder Epithelial Cells from Individuals Exposed to Arsenic in Drinking Water. *Environmental Health Perspectives,* **116**, 1656-1660 (2008).

132. Sun, G. F.; Xu, Y. Y.; Li, X.; Jin, Y. P.; Li, B.; Sun, X. C.: Urinary arsenic metabolites in children and adults exposed to arsenic in drinking water in Inner Mongolia, China. *Environmental Health Perspectives,* **115**, 648-652 (2007).

133. Calatayud, M.; Bralatei, E.; Feldmann, J.; Devesa, V.; Vélez, D.: Transformation of Arsenic Species during in Vitro Gastrointestinal Digestion of Vegetables. *Journal of Agricultural and Food Chemistry,* **61**, 12164-12170 (2013).

134. Calatayud, M.; Vázquez, M.; Devesa, V.; Vélez, D.: In Vitro Study of Intestinal Transport of Inorganic and Methylated Arsenic Species by Caco-2/HT29-MTX Cocultures. *Chemical Research in Toxicology,* **25**, 2654-2662 (2012).

135. Calatayud, M.; Vélez, D.; Devesa, V.: Metabolism of Inorganic Arsenic in Intestinal Epithelial Cell Lines. *Chemical Research in Toxicology,* **25**, 2402-2411 (2012).

136. Zhao, R.; Zhao, M.; Wang, H.; Taneike, Y.; Zhang, X.: Arsenic speciation in moso bamboo shoot – A terrestrial plant that contains organoarsenic species. *Science of The Total Environment,* **371**, 293-303 (2006).

137. Gallagher, A.; Wei, X.; Shoemaker, A.; Brockhoff, A.; Creed, T.: Detection of arsenosugars from kelp extracts via IC-electrospray ionization-MS-MS and IC membrane hydride generation ICP-MS. *Journal of Analytical Atomic Spectrometry,* **14**, 1829-1834 (1999).

138. McSheehy, S.; Marcinek, M.; Chassaigne, H.; Szpunar, J.: Identification of dimethylarsinoyl-riboside derivatives in seaweed by pneumatically assisted electrospray tandem mass spectrometry. *Analytica Chimica Acta,* **410**, 71-84 (2000).

139. Garcia-Salgado, S.; Quijano, M. A.; Bonilla, M. M.: Arsenic speciation in edible alga samples by microwave-assisted extraction and high performance liquid chromatography coupled to atomic fluorescence spectrometry. *Analytica Chimica Acta,* **714**, 38-46 (2012).

140. Schaeffer, R.; Soeroes, C.; Ipolyi, I.; Fodor, P.; Thomaidis, N. S.: Determination of arsenic species in seafood samples from the Aegean Sea by liquid chromatography-(photo-oxidation)-hydride generation-atomic fluorescence spectrometry. *Analytica Chimica Acta,* **547**, 109-118 (2005).

141. Simon, S.; Tran, H.; Pannier, F.; Potin-Gautier, M.: Simultaneous determination of twelve inorganic and organic arsenic compounds by liquid chromatography-ultraviolet irradiation-hydride generation atomic fluorescence spectrometry. *Journal of Chromatography A,* **1024**, 105-113 (2004).

142. Schmeisser, E.; Goessler, W.; Kienzl, N.; Francesconi, K. A.: Volatile Analytes Formed from Arsenosugars: Determination by HPLC-HG-ICPMS and Implications for Arsenic Speciation Analyses. *Analytical Chemistry,* **76**, 418-423 (2004).

Appendix I – Achieving 100% Efficient Postcolumn Hydride Generation for As Speciation Analysis by Atomic Fluorescence Spectrometry

analytical chemistry

Article

pubs.acs.org/ac

Achieving 100% Efficient Postcolumn Hydride Generation for As Speciation Analysis by Atomic Fluorescence Spectrometry

Karel Marschner,*[,†,‡] Stanislav Musil,[†] and Jiří Dědina[†]

[†]Institute of Analytical Chemistry of the CAS, v. v. i., Veveří 97, 602 00 Brno, Czech Republic

[‡]Charles University in Prague, Faculty of Science, Department of Analytical Chemistry, Albertov 6, 128 43 Prague, Czech Republic

Supporting Information

ABSTRACT: An experimental setup consisting of a flow injection hydride generator coupled to an atomic fluorescence spectrometer was optimized in order to generate arsanes from tri- and pentavalent inorganic arsenic species (iAs^{III}, iAs^{V}), monomethylarsonic acid (MAs^{V}), and dimethylarsinic acid ($DMAs^{V}$) with 100% efficiency with the use of only HCl and $NaBH_4$ as the reagents. The optimal concentration of HCl was 2 mol L^{-1}; the optimal concentration of $NaBH_4$ was 2.5% (m/v), and the volume of the reaction coil was 8.9 mL. To prevent excessive signal noise due to fluctuations of hydride supply to an atomizer, a new design of a gas−liquid separator was implemented. The optimized experimental setup was subsequently interfaced to HPLC and employed for speciation analysis of arsenic. Two chromatography columns were tested: (i) ion-pair chromatography and (ii) ion exchange chromatography. The latter offered much better results for human urine samples without a need for sample dilution. Due to the equal hydride generation efficiency (and thus the sensitivities) of all As species, a single species standardization by $DMAs^{V}$ standard was feasible. The limits of detection for iAs^{III}, iAs^{V}, MAs^{V}, and $DMAs^{V}$ were 40, 97, 57, and 55 pg mL^{-1}, respectively. Accuracy of the method was tested by the analysis of the standard reference material (human urine NIST 2669), and the method was also verified by the comparative analyses of human urine samples collected from five individuals with an independent reference method.

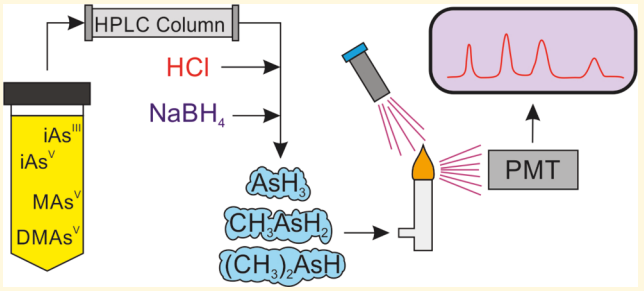

For speciation analysis of arsenic, anion exchange high performance liquid chromatography (HPLC) coupled with an inductively coupled plasma mass spectrometry (ICPMS) detector is the most common and powerful method.[1] The alternative and also more economic approach is to substitute ICPMS with atomic fluorescence spectrometry (AFS). Hydride generation (HG) is used for postcolumn derivatization to convert As species to volatile arsanes that can be subsequently atomized in atomizers for AFS. Due to high sensitivity of the AFS instruments, the combination of HPLC−HG−AFS can approach the low limits of detection (LOD) typical of HPLC−ICPMS.[2]

The HG step itself offers a number of advantages, but it also brings some disadvantages. As for the advantages, it reduces matrix interference and substantially increases sensitivity because As species are converted to volatile arsanes with much higher efficiency (up to 100%) in comparison to the efficiency of nebulization that is a typical analyte introduction technique for the ICPMS. The disadvantage of HG with respect to arsenic lies in the limited number of hydride active As species, i.e., species that can be converted to their corresponding arsanes, arsenous acid (iAs^{III}) and arsenic acid (iAs^{V}) to arsane, monomethylarsonic acid (MAs^{V}) to methylarsane, dimethylarsinic acid ($DMAs^{V}$) to dimethylarsane, and trimethylarsane oxide ($TMAs^{V}O$) to trimethylarsane. Other As species can not be simply converted to arsanes (or with very low efficiencies)[3,4] and can not be thus determined using HG without their previous conversion, e.g., by UV decomposition. Furthermore, HG efficiency of the above listed species strongly depends on the conditions of HG, mainly on the concentration of the acid. HCl is the most common choice for HG, but a different optimal concentration was reported for each species to reach 100% yield.[5−8] For example, iAs^{III} can be converted to arsane quantitatively in a wide concentration range while iAs^{V} needs higher concentrations of HCl, but still, typically, much lower HG efficiency is obtained than for iAs^{III}. MAs^{V} and $DMAs^{V}$ are efficiently converted to the corresponding arsanes at lower HCl concentration, but with increasing concentration, the HG efficiency gradually decreases (conversion of $DMAs^{V}$ can be even almost completely suppressed).[9] This is why it is difficult to achieve 100% HG efficiencies for all these As species under the same conditions of HG. Up to now, two approaches have been reported to unify HG efficiencies of individual hydride active As species in the flow arrangement: (i) Pentavalent As species are online prereduced to their trivalent analogues which can be then more easily converted to their corresponding arsanes. Additional equipment such as prereduction coils (even heated) is required, and/or highly toxic

Received: January 28, 2016
Accepted: March 2, 2016
Published: March 3, 2016

DOI: 10.1021/acs.analchem.6b00370
Anal. Chem. 2016, 88, 4041−4047

substances have to be employed.[10,11] (ii) For the purpose of postcolumn HG, Tian et al.[12] used a gradient HG when a higher concentration of HCl (6 M) was used during iAs^{III}, iAs^{V}, and MAs^{V} elution from the column while a much lower concentration (0.6 M) was used during $DMAs^{V}$ and $TMAs^{V}O$ elution. However, this approach requires complicated equipment and a sophisticated operational scheme to switch between the acids at the right time. A different approach is postcolumn online UV decomposition[13−17] converting As species mostly to iAs^{V}.[13] Additional accessories (at least a UV reactor with a coil) and chemicals are required as well and, mainly, chromatographic peaks are broadened due to dispersion in the UV reactor resulting in a worse resolution.[14,16] As mentioned above, iAs^{V} is usually generated with lower HG efficiency.[5−9]

The aim of the present work is (i) to optimize the flow HG arrangement in order to convert iAs^{III}, iAs^{V}, MAs^{V}, and $DMAs^{V}$ to their corresponding arsanes quantitatively with the use of only HCl and $NaBH_4$ as the reagents (to our best knowledge, 100% HG efficiencies of all pentavalent species under these conditions have never been reported in the literature); (ii) to interface the optimized hydride generator to HPLC and employ it for speciation analysis of human urine samples.

EXPERIMENTAL SECTION

Standards and Reagents. Deionized water (DIW; <0.2 μS cm^{-1}, Ultrapur, Watrex, USA) was used for the preparation of all solutions. A 1000 mg L^{-1} As standard solution (Merck, Germany) was used as iAs^{V} stock standard solution. Stock solutions of 1000 mg L^{-1} As were prepared for iAs^{III}, MAs^{V}, $DMAs^{V}$, and $TMAs^{V}O$ species in DIW using the following compounds: As_2O_3 (Lachema, Czech Republic); $Na_2CH_3AsO_3 \cdot 6H_2O$ (Chem. Service, USA); $(CH_3)_2As(O)OH$ (Strem Chemicals, Inc., USA); $(CH_3)_3AsO$ was obtained by courtesy of Dr. William Cullen (University of British Columbia, Canada). The total As content of methylated arsenic species standards was confirmed by liquid sampling graphite furnace-atomic absorption spectrometry as described previously.[18] A reducing solution of $NaBH_4$ (Fluka, Germany) in 0.1% KOH (Lach-Ner, Czech Republic) was prepared fresh daily. For HG, HCl (Merck, Germany) or tris(hydroxymethyl)aminomethane (TRIS) buffer were used. TRIS buffer was prepared from Trizma hydrochloride (Sigma, Germany); pH was adjusted to 6.00 by KOH (Lach-Ner, Czech Republic). L-Cysteine hydrochloride monohydrate (Merck, Germany) for prereduction of As species was used. Mobile phase for ion pair chromatography was 4.7 mmol L^{-1} tetrabutylammonium hydroxide (Fluka, Germany) and 2 mmol L^{-1} malonic acid (Sigma-Aldrich, Germany) in 4% methanol (Sigma-Aldrich, Germany); pH was adjusted to 5.85 by KOH.[19] Mobile phase for anion exchange chromatography was 20 mmol L^{-1} phosphate buffer (from KH_2PO_4 (Merck, Germany) and K_2HPO_4 (Xenon Lodz, Poland)), pH adjusted to 6.00.[20] Solid NaOH (Lach-Ner, Czech Republic) in the form of 3 mm pearls was used as a filling of a NaOH dryer.[21]

Hydride Generation. Two modes of HG were employed: (i) the flow injection (FI) mode and (ii) the postcolumn mode. (i) In the FI mode, the sample was injected into the flow of DIW by a six-port injection valve (Rheodyne, USA) with 0.6 mL sample loop volume. See Figure 1 for the scheme of the hydride generator. The manifold was built from polytetrafluorethylene (PTFE) tubing and polyetheretherketone (PEEK) T-junctions (Cole Parmer, USA). $NaBH_4$, HCl, and DIW were pumped by a peristaltic pump Reglo Digital (Ismatec,

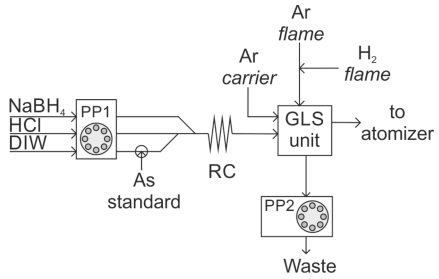

Figure 1. Scheme of the hydride generator in the flow injection mode; PP1/PP2, peristaltic pumps; RC, reaction coil; GLS, gas−liquid separator.

Switzerland) at the flow rates of 1 mL min^{-1}. PTFE reaction coils of various length and inner diameter (i.d.) were used: 1 mm i.d. for 0.8 mL and 1.85 mm i.d. for 3.5 and 8.9 mL. A 5 cm long PEEK capillary of 0.25 mm i.d. (not shown) was employed downstream the reaction coil to introduce 80 mL min^{-1} of argon (argon carrier) in order to reduce pressure fluctuations in the apparatus. Arsanes were separated from the liquid phase in various gas−liquid separator (GLS) units (see the following section for details) and transported by a flow of gas formed by the argon carrier, by a supplementary argon flow (flame argon), and by a hydrogen flow (flame hydrogen) to the atomizer. An additional hydrogen flow originated from the $NaBH_4$ decomposition at the rate controlled by the $NaBH_4$ concentration (from 24 to 71 mL min^{-1}). Argon carrier, flame argon, and flame hydrogen flows were controlled by the mass flow controllers (Omega engineering, USA). The second peristaltic pump (identical as PP1) was used for waste removal from the GLS units. (ii) In the postcolumn mode of HG, the injection valve and the channel for DIW were replaced by the outlet from the chromatography column. HPLC system Agilent 1200 (USA) was employed, and 50 μL of sample was injected by an autosampler. Two columns were tested for speciation analysis in water and human urine samples, C18−ODS-3 column (150 × 4.6 mm, 3 μm particle size, Phenomenex, USA) with a guard column and PRP-X100 column (250 × 4.6 mm, 10 μm particle size, Hamilton, USA) with a guard column.

GLS Units. See Figure 2 for the actual designs of the GLS units employed. The individual units consisted of the GLS vessel(s), NaOH dryer (10 cm long polypropylene tube of 1.7 cm i.d. filled with solid NaOH),[21] and connecting PTFE tubing and PEEK T-junctions.

GLS vessel of the unit I was made of glass with volume of ca. 18 mL. Stable liquid level (one-third of the vessel volume) was maintained by the PP2. Flame argon and hydrogen were introduced downstream of the GLS vessel and the dryer.

GLS unit II differed from the unit I only in the point of introduction of the flame gases (argon and hydrogen), that were introduced into the GLS vessel.

GLS vessel of the unit III was that of HG accessories from Agilent 7700 series for ICPMS. Its inner volume was ca. 70 mL, and it also contained a membrane filter. Instead of using a standard concentric nebulizer for reaction mixture introduction into this GLS, a 7 cm long PTFE tube (1.6 mm i.d.) sealed by a rubber was used as the inlet. The flame gases were introduced together with argon carrier upstream the GLS vessel and the dryer.

GLS unit IV contained two GLS vessels. The first one was a small vessel where the gas−liquid separation took place.[22] Briefly, it consisted of an open quartz tube ending with a

DOI: 10.1021/acs.analchem.6b00370
Anal. Chem. 2016, 88, 4041−4047

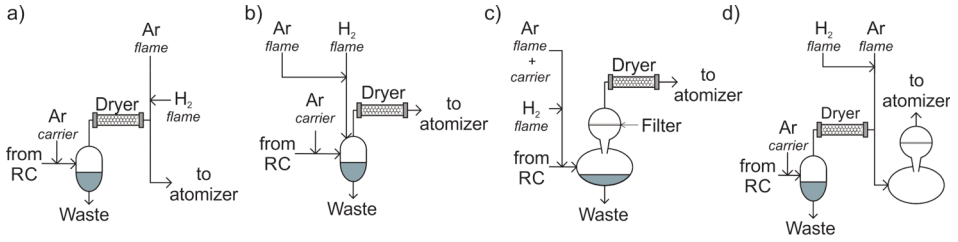

Figure 2. Schemes of GLS units; a) GLS unit I, b) GLS unit II, c) GLS unit III and d) GLS unit IV.

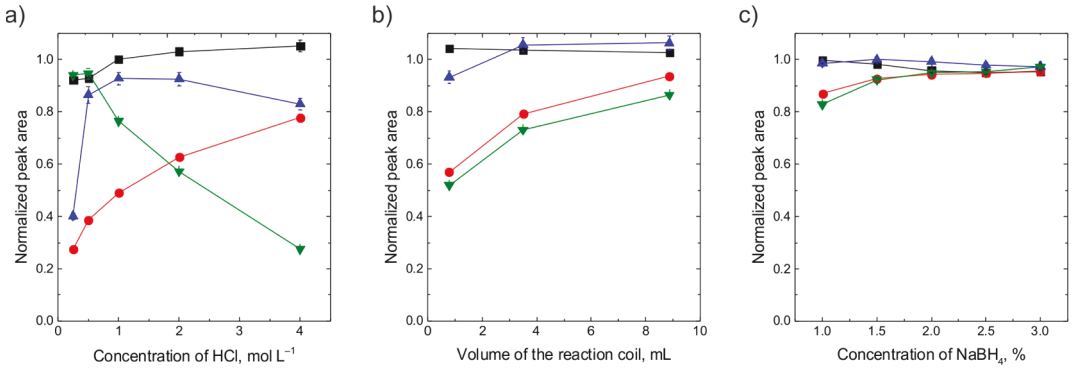

Figure 3. Dependence of the normalized peak area on (a) concentration of HCl, (b) volume of the reaction coil, and (c) concentration of $NaBH_4$; 2 ng mL^{-1} of ■, iAs^{III}; red ●, iAs^{V}; blue ▲, MAs^{V}; green ▼, $DMAs^{V}$; (a) 1% $NaBH_4$, volume of the reaction coil, 0.8 mL, (b) 2 mol L^{-1} HCl, 1% $NaBH_4$, and (c) 2 mol L^{-1} HCl, volume of the reaction coil, 8.9 mL.

standard joint where it was closed by a quartz stopper. The bottom of the vessel was constructed from a rubber septum, through which two PTFE tubes passed, one from the reaction coil and the other for removing liquid to waste. The inner volume was approximately 3 mL. The flame gases were introduced downstream of the small vessel and the dryer. The gas phase was further introduced to the second GLS vessel which was actually the GLS vessel of the unit III with the same inlet as mentioned above.

Atomizer. A miniature diffusion flame (MDF) was used as the atomizer. The atomizer optimum observation height (7 mm), flow rates of flame hydrogen (200 mL min^{-1}), and flame argon (600 mL min^{-1}) were optimized previously.[23]

Spectrometer. The in-house assembled research grade nondispersive atomic fluorescence spectrometer was employed as the detector. The experimental setup is described elsewhere.[18,23] Briefly, the instrument was equipped with an As electrodeless discharge lamp (EDL system II, PerkinElmer, USA) as a radiation source, an interference filter (193 nm, full width at half-maximum 18.7 nm, CVI Melles Griot, USA) to isolate fluorescence radiation from the atomizer, and a solar blind photomultiplier (165−320 nm, PerkinElmer Optoelectronics, USA) as the detector.

HG−Cryotrapping−AFS. A completely different hydride generator system (using a plastic GLS capable of handling overpressure, not shown) employing a cryotrapp and coupled to AFS detection (HG−CT−AFS) was used as a reference method for analyses of real samples. The method is described in ref. 18: briefly, arsanes are generated from TRIS buffer medium by $NaBH_4$ and then trapped in a U-tube cooled to −196 °C (liquid N_2). After trapping, the U-tube is electrically heated up; arsanes are gradually released (and separated) from the U-tube according to the differences in their boiling points. iAs^{III+V}, MAs^{V}, and $DMAs^{V}$ are quantified in the replicate which was prereduced by L-cysteine.

Real Samples. Standard reference material (SRM) NIST 2669 Level I,II (As species in frozen human urine) and real human urine samples were analyzed. Urine samples were collected from five volunteers (adult men), filtered through a syringe filter (PTFE, 25 mm, pore size 0.2 μm, Agilent, USA), and stored frozen at −18 °C before the analysis. If explicitly stated, the urine samples were diluted with the mobile phase before analysis and/or spiked with H_2O_2 (to 3%) to oxidize iAs^{III} to iAs^{V}. Quantification of As species was performed against external calibration of aqueous $DMAs^{V}$ standards.

For HG−CT−AFS analyses, urine samples were diluted ten times by DIW and prereduced by 2% L-cysteine at least 1 h prior to analysis. External calibration of aqueous mixed standards treated with 2% L-cysteine was employed.

Procedure and Data Evaluation. The postcolumn mode was used to analyze real samples while the FI mode was exclusively used for the method optimization. Peak area was invariably employed as the analytical quantity. Since the AFS detector output yields a response (in μV units) specific to actual detector settings, peak area values can not be simply related to those yielded under different detector settings. Therefore, for FI experiments, we deal with normalized peak areas, related to that of 2 ng mL^{-1} iAs^{III} generated by 1% $NaBH_4$ from 1 mol L^{-1} HCl medium in the generator using the reaction coil of 0.8 mL.

RESULTS AND DISCUSSION

HG Efficiency. To optimize the flow HG arrangement, the influence of its relevant parameters, i.e., HCl concentration (controlling pH of the reaction mixture), concentration of $NaBH_4$, and the volume of the reaction coil (controlling the reaction time) on the FI mode signals of individual arsenic species, was investigated employing the GLS unit I.

Concentration of HCl. Concentration of HCl was tested in the range from 0.25 to 4 mol L^{-1}. Figure 3a shows different

DOI: 10.1021/acs.analchem.6b00370
Anal. Chem. 2016, 88, 4041−4047

trends for all As species. There is a positive effect of increased concentration of HCl for iAs^V while for iAs^{III} the signal remains almost unchanged. For methylated species, MAs^V and $DMAs^V$, there is a signal decrease in HG efficiencies at higher concentrations of HCl, much more pronounced for $DMAs^V$ which well correlates with the earlier works.[5−9] Different behavior and different optimum with the highest sensitivity for each species indicates how difficult it can be to achieve equal HG efficiency for all these species without the prereduction step (see the introduction). Two mol L^{-1} of HCl was chosen for subsequent experiments as a compromise between $DMAs^V$ and iAs^V signals.

Volume of the Reaction Coil. In order to provide more time for reactions of analytes with the hydroboron reducing species, various volumes of the reaction coil were tested. Figure 3b shows that increasing the volume of the reaction coil to 3.5 mL is enough to reach the maximum MAs^V signal. For iAs^V and $DMAs^V$, the signal gradually increases with the reaction coil volume up to the maximum feasible volume of 8.9 mL. This reaction coil volume was chosen for further work. Only negligible effect on the peak shape (almost no change in the peak width and height, only the noise slightly increased) and a small (around 20 s) shift of the time of peak maximum was observed when using an 8.9 mL coil compared to the coil with a volume of 0.8 mL. This can be explained by two effects that are both related to hydrogen that is formed from the decomposition of $NaBH_4$. The bubbles of hydrogen in the reaction coil form a segmented flow of the reaction mixture which prevents analyte dispersion in the coil. Since the degree of $NaBH_4$ decomposition and thus the size of bubbles in the reaction conduit are also driven by the volume of the reaction coil, the residence time in the reaction coil is not simply proportional to the reaction coil volume and to the flow rate of the reagents. Therefore, the residence time in the reaction coil is much lower than in the case when the reaction coil is filled only by liquid phase.

Concentration of $NaBH_4$. The influence of concentration of $NaBH_4$ was tested in the range from 1% to 3% (m/v). Figure 3c shows that a $NaBH_4$ concentration higher than 2.0% is compatible with the same sensitivity of all species. A $NaBH_4$ concentration of 2.5% was chosen for further work. Assuming that arsane is generated from iAs^{III} quantitatively, HG efficiencies of iAs^V, MAs^V, and $DMAs^V$ were estimated as 100 ± 1%, 103 ± 2%, and 100 ± 2%, respectively.

Design of the GLS. Although both the concentration of $NaBH_4$ and high volume of the reaction coil enabled the generation of all species quantitatively, very noisy peaks were observed (Figure 4a), due to fluctuations of hydride supply to the atomizer. Several designs of the GLS units were tested to reduce these fluctuations. At first, all the flame gases were introduced directly to the GLS vessel (GLS unit II, Figure 2b). The higher gas flow rate through the GLS vessel improved the noise significantly (Figure 4b). When the flame gases were introduced into the GLS unit III (Figure 2c) with much higher inner volume, the noise improvement was even more pronounced (Figure 4c). The disadvantage of units II and III is the high gas flow rate through the GLS vessels (ca. 900 mL min^{-1} compared to ca. 80 mL min^{-1} in the case of the GLS unit I) carrying more moisture from the GLS vessels which could not be efficiently dried out by the NaOH dryer. The NaOH dryer was thus saturated within 1 h, and the cartridge had to be replaced. This was why the GLS unit IV with two GLS vessels (Figure 2d) was designed. The first small GLS vessel

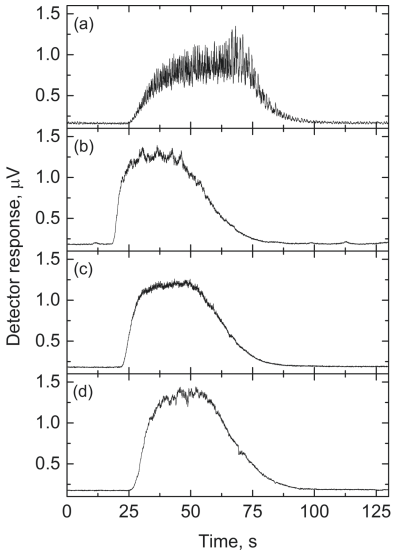

Figure 4. Peak profiles for different GLS unit designs in FI mode; (a) GLS unit I, (b) GLS unit II, (c) GLS unit III, and (d) GLS unit IV; 2 ng mL^{-1} iAs^{III}, 2.5% $NaBH_4$, 2 mol L^{-1} HCl, 8.9 mL volume of the reaction coil.

(approximately 3 mL) allowed for the gas liquid separation with a low gas flow rate (80 mL min^{-1}). The separated gaseous phase was efficiently dried by the NaOH dryer which thus provided a longer lifetime of one working day. The second GLS vessel served just to increase the dead volume. As it is seen in Figure 4d, the peaks were sufficiently smooth.

Postcolumn Mode Measurements. *Influence of the Mobile Phase.* Before interfacing the hydride generator to HPLC for speciation analysis, the influence of mobile phases on the signals of all As species was investigated, 4.7 mmol L^{-1} tetrabutylammonium hydroxide, 2 mmol L^{-1} malonic acid in 4% methanol (pH adjusted to 5.85) for ion pair chromatography,[19] and 20 mmol L^{-1} phosphate buffer (pH 6.00) for anion exchange chromatography.[20] Problems can arise during HG when HG efficiency can be decreased but also during atomization in the MDF. For example, alcohol has been reported to decrease the efficiency of arsane atomization or to quench the AFS signal which can limit the arsenic determination in alcoholic beverages.[24] With the present experimental setup, the signal suppression for all species was observed only when the liquid phase contained methanol but only in the GLS unit designs II and III that used high gas flow rate (900 mL min^{-1}) for the gas−liquid separation. There was no signal suppression in the tested range up to 10% (v/v) methanol with the GLS unit designs I and IV where much lower gas flow rate was used for the gas−liquid separation (80 mL min^{-1}). It can be concluded that (i) the methanol interference mechanism is not a suppression of efficiency of HG but of atomization, (ii) a very high gas flow rate through the gas−liquid separation vessel is required to release methanol vapor at a concentration high enough to interfere with atomization in the present design of the MDF, and (iii) GLS unit design IV is optimum for determination of arsenic in alcoholic solutions. As the result of the above measurements, optimal hydride generator parameters, summarized in Table 1, were chosen for further work.

Separation of As Species. The reversed-phase C18−ODS-3 column for ion pair chromatography and mobile phase consisting of tetrabutylammonium hydroxide, malonic acid,

DOI: 10.1021/acs.analchem.6b00370
Anal. Chem. 2016, 88, 4041−4047

Table 1. Optimal Parameters of Hydride Generator

parameter	value
concentration of HCl	2.0 mol L^{-1}
concentration of $NaBH_4$ (m/v)	2.5%
volume of the reaction coil	8.9 mL
hydride generator design	GLS unit IV

and methanol was tested first since this combination was used by other laboratories in combination with the ICPMS or HG-AFS for analysis of As species in aqueous solutions,[25] human urine,[19,26−28] or cells.[29,30] In the present work, a very good separation of all 4 species was obtained for aqueous standards; however, separation of undiluted urine SRM (NIST 2669, Level I) was unsatisfactory: overlapping, tailing of peaks, and shifting of retention times. Ten times dilution of the SRM with the mobile phase was necessary for sufficient resolution (See Supporting Information for details).

The anion exchange chromatography (PRP-X100 column) with phosphate buffer as the mobile phase was found to be more suitable for the analysis of arsenic species in urine. Better separation (compared to ion-pair chromatography) of all species was obtained in the SRM (NIST 2669) with almost no tailing and shifting in retention times in comparison to arsenic aqueous standards (compare Figure 5a,b). Since

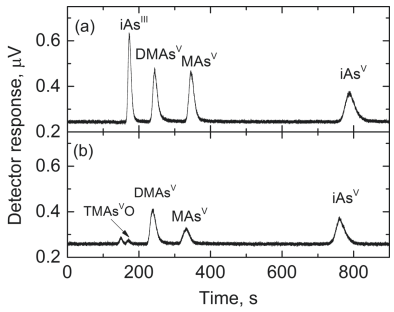

Figure 5. HPLC−HG−AFS chromatograms of (a) aqueous arsenic standards (5 ng mL^{-1} each) and (b) urine SRM (NIST 2669 Level I) with 3% H_2O_2; anion exchange chromatography with PRP X-100 column.

$TMAs^{V}O$ can be present in the chromatogram as a minor species in urine samples, troubles can arise for determination of iAs^{III} because $TMAs^{V}O$ and iAs^{III} elute both close to the dead time of the column; see Figure 5b. $TMAs^{V}O$ was identified again by spiking with the $TMAs^{V}O$ standard. HG efficiency of $TMAs^{V}O$ under these conditions was found to be 43 ± 1%.

Analytical Performance. The comparison of slopes of calibration curves of individual species showed good uniformity of sensitivities expressed as peak areas measured for aqueous standards of 0, 0.5, 1, 2, and 5 ng mL^{-1} of As. The relative sensitivities for iAs^{III}, iAs^{V}, and MAs^{V} referred to $DMAs^{V}$ were 99 ± 2%, 102 ± 4%, and 100 ± 3%, respectively, which corresponds to the above-discussed equal and 100% HG efficiency. These results enable standardization on single species for quantification of all other As species. $DMAs^{V}$ was chosen as a reference because it is the stable species, not susceptible to reduction or oxidation as both iAs species in the aqueous environment. $DMAs^{V}$ elutes in the front part of the chromatogram, and calibration can be obtained in much shorter time; only 350 s was found necessary for complete $DMAs^{V}$ elution in comparison to 900 s for the whole chromatography record. The blank values were insignificant; i.e., they could not be distinguished from the baseline which was controlled by the contamination of As from reagents.

LODs for individual species are in Table 2 and compared with those reported in the literature for HPLC−HG−AFS measurements. The present LODs are slightly better than those reported by Bohari et al.,[31] and they are substantially better than those reached by other authors. The superior LODs should be due to the quantitative conversion of all As species to arsanes and/or to the excellent performance of the employed atomic fluorescence spectrometer (EDL lamp, optical path, etc.).[23]

Accuracy. The accuracy of the developed analytical method was verified by speciation analysis of human urine SRM (NIST 2669, Level I) and of urine samples collected from five individuals. As it is seen in Table 3, a good agreement between the certified and determined As species concentrations in the SRM was reached. The results of analyses of the collected urine samples were compared with results obtained by the reference method HG−CT−AFS. This method utilizes a different type of hydride generator, different conditions of HG (TRIS buffer medium instead of HCl), and mainly a different separation process, which is not based on separation of As species in the

Table 3. Determination of Arsenic Species in SRM (NIST 2669, Level I) by HPLC−HG−AFS with Anion Exchange Column (PRP X-100)[a]

species	determined (ng mL^{-1})	certified (ng mL^{-1})
iAs^{III+V}	4.10 ± 0.45	3.88 ± 0.32
MAs^{V}	1.85 ± 0.12	1.87 ± 0.39
$DMAs^{V}$	3.81 ± 0.22	3.47 ± 0.41

[a] iAs^{III+V} quantified as the sum after addition of 3% H_2O_2.

Table 2. Comparison of Achieved LODs with Other HPLC−HG−AFS Methods

	LOD, pg mL^{-1} (absolute LOD, pg)			
reference	iAs^{III}	iAs^{V}	MAs^{V}	$DMAs^{V}$
this work	40 (2.0)	97 (4.8)	57 (2.9)	55 (2.8)
ref 31	50 (5)	60 (6)	50 (5)	70 (7)
ref 32	160 (32)	570 (114)	320 (64)	330 (66)
ref 33	1000 (20)	8500 (170)	2150 (43)	2250 (45)
ref 24	120 (12)	270 (27)	150 (15)	130 (13)
ref 34	3000 (300)	2000 (200)	2000 (200)	4000 (400)
ref 35	130 (13)	100 (10)	260 (26)	80 (8)
ref 36	500 (10)	800 (16)	400 (8)	700 (14)

DOI: 10.1021/acs.analchem.6b00370
Anal. Chem. 2016, 88, 4041−4047

liquid phase but on separation of generated arsanes in the gaseous phase. The found concentrations of As species determined by these two methods are presented in Figure 6.

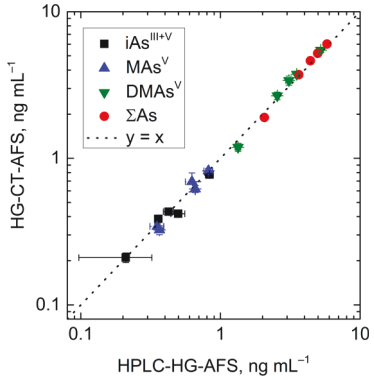

Figure 6. Comparison of results of analyses of human urine by HPLC−HG−AFS and HG−CT−AFS; ■, iAs^{III+V}; blue ▲, MAs^{V}; green ▼, DMAs^{V}; red ●, ΣAs = (iAs^{III+V} + MAs^{V} + DMAs^{V}).

There was a good linearity between the results with the slope close to 1 (0.994 ± 0.026 with R^2 = 0.9965 for iAs^{III+V}, 0.967 ± 0.021 with R^2 = 0.9976 for MAs^{V}, 1.027 ± 0.032 with R^2 = 0.9950 for DMAs^{V}, and 1.012 ± 0.025 with R^2 = 0.9969 for ΣAs which is the sum of iAs^{III+V}, MAs^{V}, and DMAs^{V}). These agreements (with SRM and HG−CT−AFS method) indicate that 100% HG efficiency is reached also for real samples.

CONCLUSION

The flow HG arrangement was optimized to reach 100% HG efficiency of all tested As species (iAs^{III}, iAs^{V}, MAs^{V}, and DMAs^{V}). The main impact had the use of high volume of the reaction coil. Also, the GLS design was modified in order to reduce the signal noise caused by hydrogen evolution. The optimized hydride generator was subsequently interfaced to HPLC and employed for speciation analysis of human urine samples. The ion pair chromatography did not offer good separation of As species in urine samples; however, the anion exchange provided satisfactory performance. The absolute LODs were in the range of 2.0 and 4.8 pg, much lower than those reported for other HPLC−HG−AFS instruments, and this LOD is comparable with the HPLC−ICPMS instrument at which it ranges typically from 0.3 to 24 pg.[37] 100% efficient postcolumn generation of arsanes from all tested As species, besides being reflected in excellent sensitivity (and thus LOD), makes possible single species standardization. This is extremely useful for two reasons: (i) it is sufficient to determine sensitivity in a standard solution of a single As species; (ii) the choice of DMAs^{V} as the reference reduces the time for the calibration process by a factor of 2.6.

ASSOCIATED CONTENT

Supporting Information

The Supporting Information is available free of charge on the ACS Publications website at DOI: 10.1021/acs.analchem.6b00370.

Details on speciation analysis of As in urine by ion-pair chromatography. (PDF)

AUTHOR INFORMATION

Corresponding Author

*E-mail: karel.marschner@biomed.cas.cz.

Notes

The authors declare no competing financial interest.

ACKNOWLEDGMENTS

This work was supported by GA CR (grant no. P206/14-23532S), Institute of Analytical Chemistry of the CAS, v. v. i. (project no. RVO: 68081715), and Charles University in Prague (project SVV260317).

REFERENCES

(1) Francesconi, K. A.; Kuehnelt, D. *Analyst* **2004**, *129*, 373−395.
(2) Sánchez-Rodas, D.; Corns, W. T.; Chen, B.; Stockwell, P. B. *J. Anal. At. Spectrom.* **2010**, *25*, 933−946.
(3) Schmeisser, E.; Goessler, W.; Kienzl, N.; Francesconi, K. A. *Anal. Chem.* **2004**, *76*, 418−423.
(4) Regmi, R.; Milne, B.; Feldmann, J. *Anal. Bioanal. Chem.* **2007**, *388*, 775−782.
(5) Anderson, R. K.; Thompson, M.; Culbard, E. *Analyst* **1986**, *111*, 1143−1152.
(6) Le, X. C.; Cullen, W. R.; Reimer, K. J. *Anal. Chim. Acta* **1994**, *285*, 277−285.
(7) Shraim, A.; Chiswell, B.; Olszowy, H. *Talanta* **1999**, *50*, 1109−1127.
(8) Carrero, P.; Malavé, A.; Burguera, J. L.; Burguera, M.; Rondón, C. *Anal. Chim. Acta* **2001**, *438*, 195−204.
(9) Musil, S.; Pétursdóttir, Á. H.; Raab, A.; Gunnlaugsdóttir, H.; Krupp, E.; Feldmann, J. *Anal. Chem.* **2014**, *86*, 993−999.
(10) Tsalev, D. L.; Sperling, M.; Welz, B. *Talanta* **2000**, *51*, 1059−1068.
(11) Musil, S.; Matoušek, T. *Spectrochim. Acta, Part B* **2008**, *63*, 685−691.
(12) Tian, Y.; Chen, M. L.; Chen, X. W.; Wang, J. H.; Hirano, Y.; Sakamoto, H.; Setsu, I. *J. Anal. At. Spectrom.* **2010**, *25*, 48−54.
(13) Atallah, R. H.; Kalman, D. A. *Talanta* **1991**, *38*, 167−173.
(14) Bin, H.; Gui-bin, J.; Xiao-bai, X. *Fresenius' J. Anal. Chem.* **2000**, *368*, 803−808.
(15) Tsalev, D. L.; Sperling, M.; Welz, B. *Analyst* **1998**, *123*, 1703−1710.
(16) Howard, A. G.; Hunt, L. E. *Anal. Chem.* **1993**, *65*, 2995−2998.
(17) Tsalev, D. L.; Sperling, M.; Welz, B. *Spectrochim. Acta, Part B* **2000**, *55*, 339−353.
(18) Musil, S.; Matoušek, T.; Currier, J. M.; Stýblo, M.; Dědina, J. *Anal. Chem.* **2014**, *86*, 10422−10428.
(19) Gong, Z. L.; Lu, X. F.; Cullen, W. R.; Le, X. C. *J. Anal. At. Spectrom.* **2001**, *16*, 1409−1413.
(20) Viñas, P.; López-García, I.; Merino-Meroño, N.; Campillo, N.; Hernández-Córdoba, M. *Chromatographia* **2003**, *57*, 611−616.
(21) Taurková, P.; Svoboda, M.; Musil, S.; Matoušek, T. *J. Anal. At. Spectrom.* **2011**, *26*, 220−223.
(22) Matoušek, T.; Johansson, M.; Dědina, J.; Frech, W. *Spectrochim. Acta, Part B* **1999**, *54*, 631−643.
(23) Marschner, K.; Musil, S.; Dědina, J. *Spectrochim. Acta, Part B* **2015**, *109*, 16−23.
(24) Karadjova, I. B.; Lampugnani, L.; Onor, M.; D'Ulivo, A.; Tsalev, D. L. *Spectrochim. Acta, Part B* **2005**, *60*, 816−823.
(25) Shraim, A.; Sekaran, N. C.; Anuradha, C. D.; Hirano, S. *Appl. Organomet. Chem.* **2002**, *16*, 202−209.
(26) Le, X. C.; Lu, X. F.; Ma, M. S.; Cullen, W. R.; Aposhian, H. V.; Zheng, B. S. *Anal. Chem.* **2000**, *72*, 5172−5177.
(27) Rabieh, S.; Hirner, A. V.; Matschullat, J. *J. Anal. At. Spectrom.* **2008**, *23*, 544−549.
(28) Wang, Z. W.; Zhou, J.; Lu, X. F.; Gong, Z.; Le, X. C. *Chem. Res. Toxicol.* **2004**, *17*, 95−103.

DOI: 10.1021/acs.analchem.6b00370
Anal. Chem. 2016, 88, 4041−4047

(29) Hippler, J.; Zdrenka, R.; Reichel, R. A. D.; Weber, D. G.; Rozynek, P.; Johnen, G.; Dopp, E.; Hirner, A. V. *J. Anal. At. Spectrom.* **2011**, *26*, 2396−2403.
(30) Currier, J. M.; Saunders, R. J.; Ding, L.; Bodnar, W.; Cable, P.; Matoušek, T.; Creed, J. T.; Stýblo, M. *J. Anal. At. Spectrom.* **2013**, *28*, 843−852.
(31) Bohari, Y.; Astruc, A.; Astruc, M.; Cloud, J. *J. Anal. At. Spectrom.* **2001**, *16*, 774−778.
(32) Moreno, E.; Cámara, C.; Corns, W. T.; Bryce, D. W.; Stockwell, P. B. *J. Autom. Methods Manage. Chem.* **2000**, *22*, 33−39.
(33) Wei, C. J.; Liu, J. *Talanta* **2007**, *73*, 540−545.
(34) Lindberg, A. L.; Goessler, W.; Grandér, M.; Nermell, B.; Vahter, M. *Toxicol. Lett.* **2007**, *168*, 310−318.
(35) Ruiz-Chancho, M. J.; Sabé, R.; López-Sánchez, J. F.; Rubio, R.; Thomas, P. *Microchim. Acta* **2005**, *151*, 241−248.
(36) Le, X. C.; Ma, M. S. *Anal. Chem.* **1998**, *70*, 1926−1933.
(37) Komorowicz, I.; Barałkiewicz, D. *Talanta* **2011**, *84*, 247−261.

DOI: 10.1021/acs.analchem.6b00370
Anal. Chem. 2016, 88, 4041−4047

Achieving 100% Efficient Postcolumn Hydride Generation for As Speciation Analysis by Atomic Fluorescence Spectrometry

Karel Marschner[1,2,*], Stanislav Musil[1], Jiří Dědina[1]

[1]Institute of Analytical Chemistry of the CAS, v. v. i., Veveří 97, 602 00 Brno, Czech Republic

[2]Charles University in Prague, Faculty of Science, Department of Analytical Chemistry, Albertov 8, 128 43 Prague, Czech Republic

*Corresponding author; E-mail: karel.marschner@biomed.cas.cz

Abstract of Supporting Information

Supporting information includes details on speciation analysis of As in urine by HPLC-HG-AFS using ion-pair chromatography by C18 – ODS-3 column (4.7 mmol L^{-1} tetrabutylammonium hydroxide, 2 mmol L^{-1} malonic acid in 4% methanol (pH adjusted to 5.85) as mobile phase).

Separation of As Species

The use of ion-pair chromatography on aqueous standard leads to very good separation of all 4 species (Figure S-1a). Separation of undiluted urine SRM (NIST 2669, Level I), however, leads to unsatisfactory resolution (overlapping of $DMAs^V$ with MAs^V and MAs^V with iAs^V, even to multiple peaks of iAs^V and to shifting of retention time, Figure S-1b). Therefore SRM was diluted with mobile phase 5 times (Figure S-1c) and 10 times (Figure S-1d). Retention times were still shifted compared to aqueous standards but no overlapping or multiple peaks

for iAs^{V} were observed. Due to co-elution of $TMAs^{V}O$ and iAs^{III}, iAs^{III} was oxidized to iAs^{V} with 3% H_2O_2. 10 times dilution worsened method LODs accordingly but it lead to satisfactory analytical performance demonstrated by the accurate results of determination of SRM (NIST 2669, Level II) (see Table S-1). All the species were determined using calibration on $DMAs^{V}$.

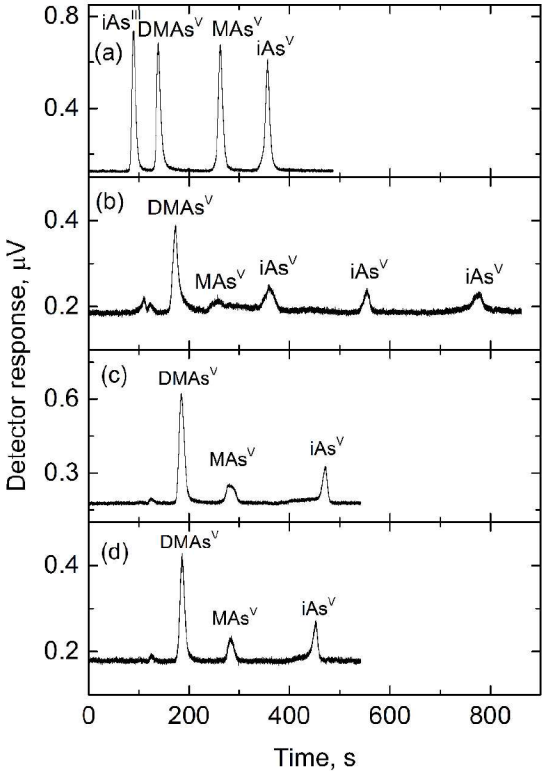

Figure S-1. HPLC–HG–AFS chromatograms of (a) aqueous arsenic standard (5 ng mL^{-1} each), (b) urine SRM (NIST 2669, Level I) with 3% H_2O_2, (c) urine SRM (NIST 2669, Level II) 5x diluted with 3% H_2O_2 and (d) urine SRM (NIST 2669, Level II) 10x diluted with 3% H_2O_2; ion pair chromatography C18 –ODS-3 column.

Table S-1. Determination of arsenic species in SRM (NIST 2669, Level II) by HPLC-HG-AFS with ion pair chromatography C18 – ODS-3 column; iAs^{III+V} quantified as the sum after addition of 3% H_2O_2

Species	Determined (ng mL^{-1})	Certified (ng mL^{-1})
iAs^{III+V}	12.0 ± 1.1	11.2 ± 1.0
MAs^{V}	6.64 ± 0.73	7.18 ± 0.56
$DMAs^{V}$	25.9 ± 1.1	25.3 ± 0.7

Appendix II – Demethylation of Methylated Arsenic Species During Generation of Arsanes with Tetrahydridoborate(1–) in Acidic Media

analytical chemistry

Article

pubs.acs.org/ac

Demethylation of Methylated Arsenic Species during Generation of Arsanes with Tetrahydridoborate(1−) in Acidic Media

Karel Marschner,*[,†,‡] Stanislav Musil,[†] and Jiří Dědina[†]

[†]Institute of Analytical Chemistry of the CAS, v. v. i., Veveří 97, 602 00 Brno, Czech Republic

[‡]Department of Analytical Chemistry, Faculty of Science, Charles University in Prague, Albertov 8, 128 43 Prague, Czech Republic

Supporting Information

ABSTRACT: Demethylation during generation of volatile hydrides (HG), i.e. formation of noncorresponding arsanes from monomethylarsonic acid (MAs^V), dimethylarsinic acid ($DMAs^V$), and trimethylarsine oxide ($TMAs^VO$) by the reaction of sodium tetrahydridoborate(1−) (THB) with different acids under analytical conditions, was investigated and characterized. Pronounced demethylation of MAs^V, $DMAs^V$, and $TMAs^VO$ was found during the reaction of THB with HCl, H_2SO_4, and $HClO_4$, while HG from CH_3COOH or TRIS buffer after prereduction with L-cysteine resulted in the formation of only the corresponding hydrides. In the case of HNO_3 formation of corresponding hydrides was preserved for MAs^V and $DMAs^V$ but not for $TMAs^VO$. The extent of demethylation strongly depends on concentration of the acid and THB. It can be strongly suppressed in HCl medium by partial hydrolysis of THB with optimal concentration of acid before it reacts with MAs^V, $DMAs^V$, or $TMAs^VO$. It appears that the demethylation is due to the action of specific hydrolytic products of THB (most probably by the first and second one).

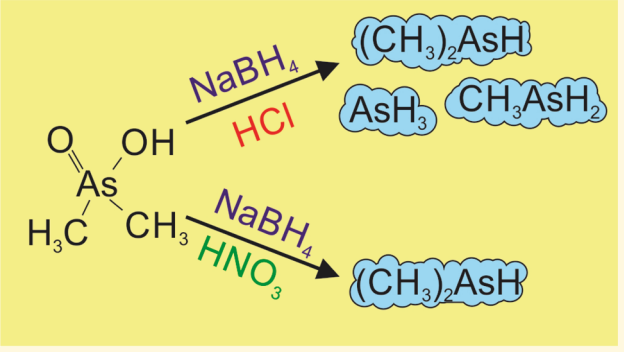

Generation of volatile hydrides (HG) is a popular sample introduction technique for trace element and speciation analysis of "hydride forming" elements As, Se, Sb, Sn, Bi, Pb, Te, and Ge.[1] The reaction between tetrahydridoborate(1−) (THB) and acid is almost exclusively used for HG when an analyte in the liquid phase is converted to volatile hydride that is released from the liquid matrix and subsequently introduced in the gaseous phase into a detector, typically atomic or mass spectrometers.

THB in acidic medium is stepwise hydrolyzed to boric acid and hydrogen. Hydride active As species are converted to arsanes by reactions with THB and/or with its hydrolyzed intermediates. This can be described by the following schemes 1 and 2[2]

$$BH_4^- + H_3O^+ + 2H_2O \rightarrow \text{intermediates} \rightarrow B(OH)_3 + 4H_2 \quad (1)$$

$$\text{As (hydride active species)} + BH_4^-/\text{intermediates} \rightarrow \text{arsanes} + B(OH)_3 \quad (2)$$

Hydrolysis of THB under strong acidic conditions in aqueous medium is described by the following reactions 3−6 postulated by D'Ulivo et al.[2]

$$BH_4^- + H_3O^+ \rightarrow BH_3(H_2O) + H_2 \quad (3)$$

$$BH_3(H_2O) + H_2O \rightarrow (H_2O)BH_2OH + H_2 \quad (4)$$

$$(H_2O)BH_2OH + H_2O \rightarrow (H_2O)BH(OH)_2 + H_2 \quad (5)$$

$$(H_2O)BH(OH)_2 \rightarrow B(OH)_3 + H_2 \quad (6)$$

In fact this scheme is simplified. For example dihydridoboron species should be written as $L_2BH_2^n$, where L could be one or more groups among H_2O, OH^-, and Cl^- and n is the charge (−1, 0, or +1). Other hydridoboron species may be treated similarly.[3]

Wang and Jolly[4] studied THB hydrolysis in water−methanol at lower temperature, and they found that $BH_3(H_2O)$ could generate two hydridoboron species $(H_2O)_2BH_2^+$ and $(H_2O)BH_2OH$, with an equilibrium between these species

$$H_3O^+ + (H_2O)BH_2OH \rightleftarrows (H_2O)_2BH_2^+ + H_2O \quad (7)$$

Only $(H_2O)BH_2OH$ species undergoes hydrolysis. Therefore, hydrolysis of THB is much faster when $[H_3O^+] < 0.5$ mol L^{-1}. That is in agreement with results of D'Ulivo et al.[5] who found that increasing acidity from 0.2 to 10 mol L^{-1} H_3O^+ decreased the decomposition rate of THB.

Among approaches of employing HG for As speciation analysis, the generation of substituted arsanes provides several essential advantages.[6] Its general scheme consists of two steps. The first step is generation of (substituted) arsanes from hydride active species, i.e. AsH_3 is formed from arsenite (iAs^{III}) and arsenate (iAs^V), CH_3AsH_2 from monomethylarsonic acid

Received: February 24, 2016
Accepted: May 31, 2016
Published: May 31, 2016

DOI: 10.1021/acs.analchem.6b00735
Anal. Chem. 2016, 88, 6366−6373

(MAs^V), $(CH_3)_2AsH$ from dimethylarsinic acid ($DMAs^V$), and $(CH_3)_3As$ from trimethylarsine oxide ($TMAs^VO$).[7] The second step is the separation of generated arsanes. There are practically only two ways employed to separate arsanes: (i) cryotrapping (CT) when arsanes are trapped in a liquid nitrogen cooled U-trap and subsequently volatilized gradually according to their different boiling points,[8−15] or (ii) gas chromatography (GC) when arsanes are injected into a GC column.[16−18] The advantage of HG−CT is possibility to achieve low detection limits, due to preconcentration of arsanes in CT. The disadvantage is the laboriousness of this method.

The explicit relation between a hydride active species and its corresponding arsane, for example between MAs^V and CH_3AsH_2, is a necessary condition for reaching accurate results of the speciation analysis. It is generally assumed that an As−C bond (in methylated species) is not cleaved during reaction 2 under analytical conditions and therefore that As species are converted only to their corresponding arsanes.[7,19] However, some kind of molecular rearrangement of methylated As species was investigated under nonanalytical conditions recently.[19] There were also scarce reports from the past indicating As species rearrangement: Talmi and Bostick[20] and Van Elteren et al.[21] observed that $DMAs^V$ species was converted not only to its corresponding hydride, $(CH_3)_2AsH$, but also to AsH_3 and CH_3AsH_2. MAs^V was converted not only to CH_3AsH_2 but also partly to AsH_3 and even $(CH_3)_2AsH$. These experiments were performed in the medium of HCl, and Talmi and Bostick[20] referred to the fact that the conversion to the noncorresponding hydride was pH dependent. A different example of cleavage of the As−C bond by HG in HCl medium is known for arsenosugars that contain, however, a much longer side chain than methyl.[22] The volatile product was identified as $(CH_3)_2AsH$ with a very low yield of 6−9%.[23] The authors explained this cleavage by formation of the analyte-borane complex which withdrew electron density from methylene making it more susceptible to hydride attack. This indicates that As speciation analysis based on the generation of substituted arsanes in the HCl media (which is the most used acid for HG) could provide inaccurate speciation information.

The aim of the present work was to (i) characterize the noncorresponding volatile products of HG of methylated As species (MAs^V, $DMAs^V$, and $TMAs^VO$) in acidic media under analytical conditions and (ii) find how the conditions of HG influence the formation of corresponding and noncorresponding arsanes. For separation and detection of generated gaseous arsanes CT with atomic fluorescence detection was used.

EXPERIMENTAL SECTION

Standards and Reagents. Deionized water (DIW; < 0.2 $\mu S\ cm^{-1}$, Ultrapur, Watrex, USA) was used for the preparation of all solutions. A 1000 $\mu g\ mL^{-1}$ As standard solution (Merck, Germany) was used as iAs^V stock standard solution. Stock solutions of 1000 $\mu g\ mL^{-1}$ As were prepared for iAs^{III}, MAs^V, $DMAs^V$, and $TMAs^VO$ species in DIW using the following compounds: As_2O_3 (Lachema, Czech Republic); $Na_2CH_3AsO_3 \cdot 6H_2O$ (Chem. Service, USA); $(CH_3)_2As(O)OH$ (Strem Chemicals, Inc., USA); and $(CH_3)_3AsO$ (obtained by courtesy of Dr. William Cullen, University of British Columbia, Canada). The total As content of methylated arsenic species standards was confirmed by liquid sampling graphite furnace-atomic absorption spectrometry as described previously.[24] The purity of all species was confirmed by HPLC-ICPMS as >99.9% for $DMAs^V$ and $TMAs^VO$ and 97.5% for MAs^V that contained 2.5% inorganic arsenic (approximately half of iAs^{III} and half of iAs^V). The solution of $NaBH_4$ (THB, Fluka, Germany) in 0.1% KOH (Lach-Ner, Czech Republic) was prepared fresh daily. HCl (p.a., Merck, Germany), H_2SO_4 (suprapure, Merck, Germany), $HClO_4$ (p.a., Merck, Germany), HNO_3 (semiconductor grade, Sigma-Aldrich, Germany), CH_3COOH (Lachema, Czech Republic), and tris(hydroxymethyl)aminomethane (TRIS) buffer were used for HG. TRIS buffer was prepared from Trizma hydrochloride (Sigma, Germany) - pH was adjusted to 6.00 by KOH (Lach-Ner, Czech Republic). L-Cysteine hydrochloride monohydrate (Merck, Germany) for prereduction of As species was added to the As standard 1 h prior to analysis. Solid NaOH (Lach-Ner, Czech Republic) in the form of 3 mm pearls was used as a filling of a NaOH dryer.[25]

When explicitly stated, solutions of THB, HCl, DIW, and As standards used for HG were purged by Ar for 30 min to remove dissolved oxygen.

Hydride Generator. The generator (Figure 1) consisted of peristaltic pumps (PP1 and PP2, Reglo Digital, Ismatec, Switzerland), a glass gas−liquid separator (GLS) with a forced outlet of total volume of 7 mL, a chemifold between the pumps and the GLS, the dryer (10 cm long polypropylene tube of 1.7 cm i.d. filled with solid NaOH pellets), and a cryogenic trap (CT). The chemifold was built using polytetrafluorethylene (PTFE) tubes (0.75 mm i.d.) and polyetheretherketone T-junctions. The CT was described previously,[15,24] and it consisted of a 300 mm glass U-tube (2.4 mm i.d.) packed with Chromosorb WAW-DMCS 45/60, 15% OV-3 (Supelco, USA). The U-tube was wrapped with a resistance wire for gradual heating by an appropriate voltage of 21 V (~1 A).

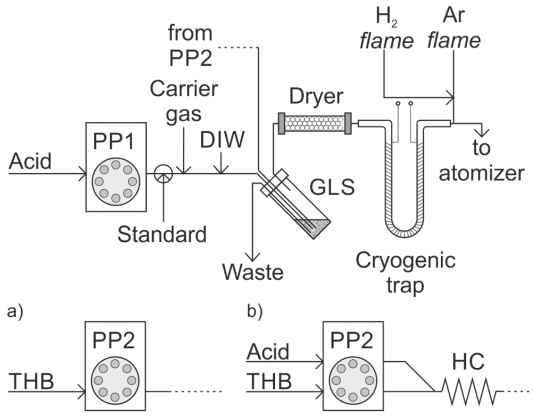

Figure 1. Batch hydride generator (a) without and (b) with hydrolysis coil (HC); PP1/PP2 − peristaltic pumps, DIW − deionized water, GLS − gas−liquid separator, HC − hydrolysis coil.

Acid was pumped by the pump PP1 at the flow rate of 4 mL min^{-1}. As standard was introduced into the acid channel by a six-port injection valve (Rheodyne, USA) with a 0.6 mL loop volume. A carrier gas (argon or helium) merged the acid channel downstream to the standard introduction point. The mixture was then introduced to the bottom of the GLS so that carrier gas could bubble through the liquid. The acid channel was provided with an additional T-junction upstream with the GLS that served for cleaning of the GLS with DIW manually by a syringe. Another channel was used to remove liquid waste from the GLS manually by a syringe. The solution of THB was pumped by the pump PP2 at the flow rate of 1 mL min^{-1} (see Figure 1a), and it was introduced to the bottom of the GLS

DOI: 10.1021/acs.analchem.6b00735
Anal. Chem. 2016, 88, 6366−6373

below the liquid level. If explicitly stated the THB flow was mixed with the other acid flow and pumped by the second channel of the pump PP2, at the flow rate of 1 mL min^{-1} (Figure 1b). THB was thus partially decomposed (hydrolyzed) in a hydrolysis coil (HC) downstream the point of mixing the THB flow with the other acid flow. The output of the gases from the GLS was connected to the dryer. The filling of the dryer was changed approximately every 3 days.[25]

The generator was operated either in the direct transfer mode or in the collection one. (i) In the direct transfer mode – the carrier gas was argon, and the NaOH dryer was directly connected to the T-junction serving to introduce hydrogen (flame hydrogen) and argon (flame argon) for an atomizer (not shown in Figure 1). (ii) The setup of the CT collection mode is shown in Figure 1 – the carrier gas was helium.

Atomizer. A miniature diffusion flame (MDF) was used as the atomizer. The atomizer optimum observation height (7 mm), flow rates of flame hydrogen (200 mL min^{-1}), and flame argon (600 mL min^{-1}) were optimized previously – see ref 26 for details.

Spectrometer. The in-house assembled research grade nondispersive AFS was employed. The experimental setup of AFS is described elsewhere.[24,26] Briefly, the instrument was equipped with an As electrodeless discharge lamp (EDL system II, PerkinElmer, USA) as a radiation source, an interference filter (193 nm, full width at half-maximum 18.7 nm, CVI Melles Griot, USA) to isolate fluorescence radiation from the atomizer, and a solar blind photomultiplier (165–320 nm, PerkinElmer Optoelectronics, USA) as the detector.

Procedure and Data Evaluation. *Direct Transfer Mode.* A standard (concentration of 2 ng mL^{-1}) was injected into the flow of acid, and it was dosed (by PP1) into the GLS. The total volume of liquid was 1.2 mL (0.6 mL of standard and 0.6 mL of acid). Subsequently, recording of the fluorescence signal was switched on (210 s read time), and 2 mL of THB was being pumped into the GLS. After recording had been completed, the remaining liquid was removed from the GLS, and the GLS was cleaned with DIW.

CT Collection Mode. Dosing of standard (concentration of 0.5 or 2.0 ng mL^{-1} in the case of $TMAs^{V}O$ when the HG efficiency was low) and acid (1.2 mL total) was the same as in the direct transfer mode. Then approximately 3/4 of the U-tube was manually immersed into liquid N_2. Immediately thereafter 1 mL of THB was added. If explicitly stated, acid was pumped and mixed with THB in the HC as illustrated in Figure 1b. After introduction of THB had been accomplished, another 150 s was allowed to complete the reaction and for transport of arsanes from the GLS to the CT. The volatilization step started by removing the flask with liquid N_2 and switching on heating of the U-tube. The signal (chromatogram) was recorded during the entire volatilization step (90 s read time). Finally, the heating was switched off, the remaining liquid was removed, and the GLS was cleaned in the same way as in the direct transfer mode.

Peak area was invariably employed as the analytical quantity. Since the AFS detector output yields a response in μV units that are specific to the instrument, peak area values cannot be simply related to those yielded by different instruments. Therefore, in the direct transfer mode, we deal with normalized peak areas – related to that of 2 ng mL^{-1} iAs^{III} that was generated by 1% THB from 1 mol L^{-1} of the used acid (HCl, HNO_3, and CH_3COOH). In the most experiments in the CT collection mode, only single species standards (MAs^{V}, $DMAs^{V}$, or $TMAs^{V}O$) were treated. In these cases, we present "arsane fraction" which is defined as a peak area of the given arsane divided by the sum of peak areas of all arsanes recorded in the same chromatogram. Arsane fractions were corrected (subtracted) to inorganic arsenic impurities in the MAs^{V} standard. When appropriate, we deal with sensitivity. In the direct transfer mode it is expressed as the peak area of a given species related to its concentration. In the CT collection mode, it means sum of the peak areas (of the single chromatogram) related to the concentration of the standard. All measurements were performed at least in triplicate and error bars in the figures mean standard deviations.

RESULTS AND DISCUSSION

Effect of HCl Concentration. Figure 2 shows dependence of the normalized peak area of iAs^{III}, iAs^{V}, MAs^{V}, $DMAs^{V}$, and

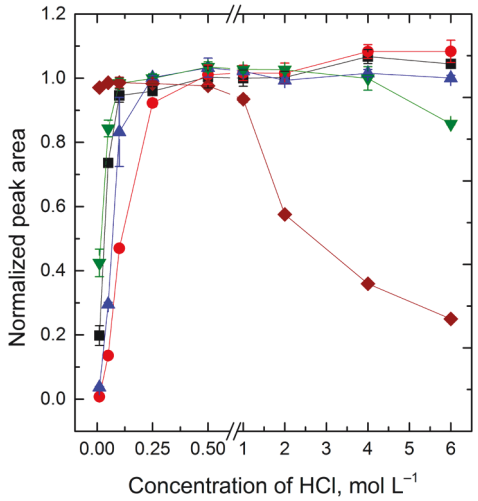

Figure 2. Dependence of normalized peak area of As species on concentration of HCl; (black) ■ – iAs^{III}, (red) ● – iAs^{V}, (blue) ▲ – MAs^{V}, (green) ▼ – $DMAs^{V}$, (brown) ♦ – $TMAs^{V}O$; concentration of As species was 2 ng mL^{-1}, 2 mL of 1% THB addition.

$TMAs^{V}O$ on concentration of HCl measured in the direct transfer mode. Taking into account that the atomization efficiency of all arsanes in the MDF is equal[24] and that iAs^{III} can be converted to the arsane with 100% efficiency under optimized conditions of HG,[27] it is evident that all the As species except $TMAs^{V}O$ are completely converted to arsanes in the range from 0.5 to 4 mol L^{-1} of HCl, while $TMAs^{V}O$ is completely converted to arsanes when concentration 1 mol L^{-1} or lower is used. It should be highlighted that increasing HCl concentration inevitably leads to broadening MAs^{V}, $DMAs^{V}$, and $TMAs^{V}O$ peaks and narrowing of iAs^{III} and iAs^{V} peaks. At HCl concentration of 2 mol L^{-1} or higher, the peak broadening resulted even to a decrease of normalized peak area of $TMAs^{V}O$ (Figure 2). Although this could be compensated with addition of a higher volume of 1% THB, it was not further employed due to a pronounced increase of iAs content in the blanks.

However, in the CT collection mode when arsanes were generated from a mixed standard containing the same concentrations of iAs^{III}/iAs^{V}, MAs^{V}, and $DMAs^{V}$, a higher peak area of AsH_3 and lower peak areas for CH_3AsH_2 and $(CH_3)_2AsH$ were obtained. Namely, the use of 1 mol L^{-1} HCl and 1% THB resulted in 95 ± 3% and 77 ± 4% peak area for

DOI: 10.1021/acs.analchem.6b00735
Anal. Chem. 2016, 88, 6366–6373

MAs^V and $DMAs^V$, respectively, relative to the peak area of AsH_3. This should be related to exactly the same normalized peak area of iAs^{III+V}, MAs^V, and $DMAs^V$ in 1 mol L^{-1} HCl (Figure 2). This discrepancy suggests a demethylation of MAs^V and $DMAs^V$ under the employed HG conditions.

Fractions of all arsanes arising from MAs^V, $DMAs^V$, and $TMAs^VO$ were determined in the concentration range from 0.05 to 6.0 mol L^{-1} of HCl. Dependence for MAs^V is shown in Figure 3. (The dependences for $DMAs^V$ and $TMAs^VO$ are in the Supporting Information – Figure S-1a,b). Typical chromatograms of volatile products from $DMAs^V$ using 0.25 and 1.0 mol L^{-1} of HCl are shown in Figure 4a,b. In the case of MAs^V at a lower concentration of HCl a higher fraction of noncorresponding hydride (AsH_3) is formed at the expense of CH_3AsH_2: almost 28% of MAs^V is converted to AsH_3 at 0.05 mol L^{-1} HCl (Figure 3). The dependence for $DMAs^V$ and $TMAs^VO$ showed a similar trend as MAs^V. A minimum for the fraction of $(CH_3)_2AsH$ formed from $DMAs^V$ was found in the region 0.1–0.25 mol L^{-1} HCl with the value of 63 ± 1%. The fraction of $(CH_3)_3As$ from $TMAs^VO$ had a minimum at 0.1 mol L^{-1} HCl with the value of 50 ± 3%. Higher HCl concentration is more suitable for generation of the corresponding hydride. In contrast to Talmi and Bostick,[20] neither formation of $(CH_3)_2AsH$ from MAs^V nor $(CH_3)_3As$ from $DMAs^V$ was observed in the whole concentration range. This could be ascribed to different concentrations of standards which were used in this work (0.5 ng mL^{-1}), while Talmi and Bostick worked with concentrations 2 to 5 orders of magnitude higher.

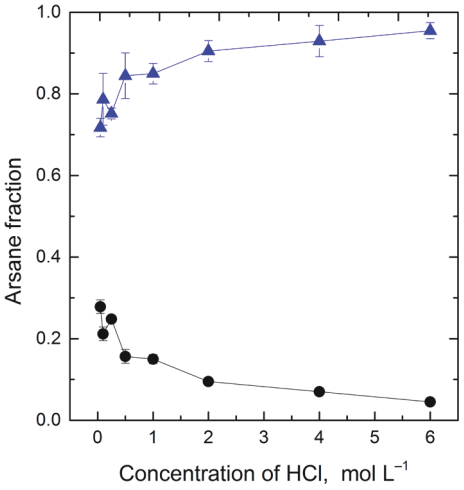

Figure 3. Dependence of arsane fractions formed from MAs^V on concentration of HCl; (black) ● – AsH_3, (blue) ▲ – CH_3AsH_2; concentration of MAs^V was 0.5 ng mL^{-1}, 1 mL of 1% THB addition.

Effect of THB Concentration. The effect of THB concentration on demethylation was investigated in the concentration range from 0.25 to 4% at three different concentrations of HCl – 0.25, 1.0, and 6.0 mol L^{-1}. Figure 5 shows the dependence of volatile products formed from MAs^V at 0.25 mol L^{-1} HCl. The maximum conversion to AsH_3 occurs at 2% of THB; an increasing or decreasing concentration of THB leads to a lower fraction of AsH_3. The dependences were similar for 1.0 and 6.0 mol L^{-1} of HCl – just the extent of conversion to noncorresponding hydrides was lower – in agreement with Figure 3. Similar influence of THB at 0.25 mol L^{-1} HCl was observed for $DMAs^V$ and $TMAs^VO$. Maximum conversion to CH_3AsH_2 from $DMAs^V$ occurred at 2% of THB with a small fraction of AsH_3 as well, and $TMAs^VO$ had the maximum conversion to noncorresponding hydride at 1% (see the Supporting Information for Figures S-2a,b). Maximum conversion to noncorresponding hydride was always observed at 1–2% of THB. Since the demethylation dependences on the concentration of HCl and THB were similar for MAs^V, $DMAs^V$, and $TMAs^VO$, we suppose that the demethylation is caused by the influence of hydrolytic products of THB.

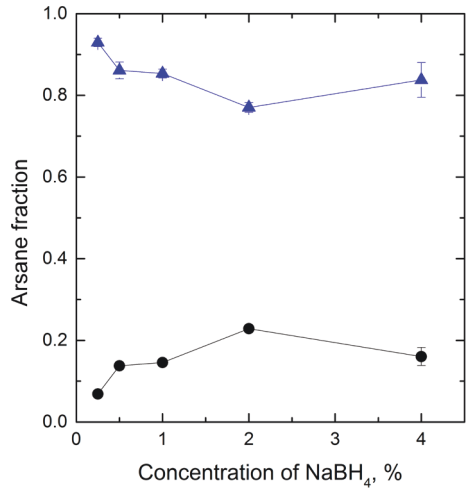

Figure 5. Dependence of arsane fractions formed from MAs^V on concentration of THB; (black) ● – AsH_3, (blue) ▲ – CH_3AsH_2; concentration of MAs^V was 0.5 ng mL^{-1}, 0.25 mol L^{-1} HCl, 1 mL of THB addition.

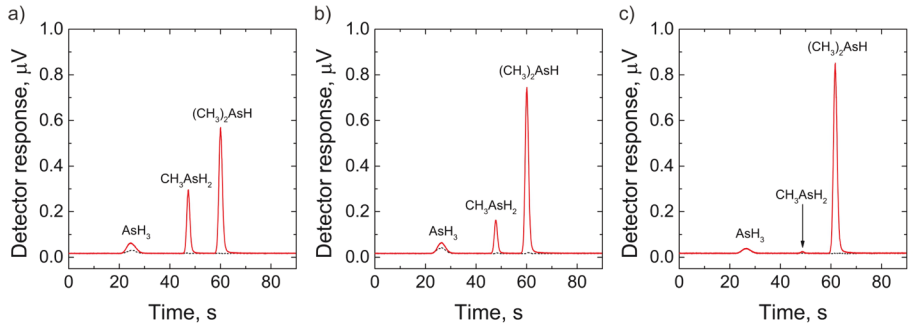

Figure 4. HG–CT–AFS chromatograms of volatile products generated from $DMAs^V$ using (a) 0.25 mol L^{-1} HCl, (b) 1.0 mol L^{-1} HCl, (c) 1.0 mol L^{-1} HNO_3; red solid line – $DMAs^V$ standard, black dashed line – blank; concentration of $DMAs^V$ was 0.5 ng mL^{-1}, 1 mL of 1% THB addition.

DOI: 10.1021/acs.analchem.6b00735
Anal. Chem. 2016, 88, 6366–6373

The above observations indicate that in the presence of HCl, THB (or some of its hydrolysis intermediates) can cleave the As−C bond. The extent of demethylation for As species was always in the order of $TMAs^{V}O$ > $DMAs^{V}$ > MAs^{V}; this can be attributed to the number of As−C bonds in the molecule.

Effect of Dissolved Oxygen and Day-to-Day Repeatability. Talmi and Bostick[20] reported that removing dissolved oxygen from all reagents strongly suppressed the demethylation extent. To check the potential oxygen role, all solutions were purged by Ar to remove dissolved oxygen. Demethylation for both species (MAs^{V} and $DMAs^{V}$) decreased by one-third (at 0.25 mol L^{-1} HCl with 1% THB) indicating that dissolved oxygen plays some role, but it is not a dominant factor.

Demethylation was quite repeatable during the day (relative standard deviation of the arsane fraction was typically below 1%); however, day-to-day repeatability was significantly worse (e.g., demethylation of MAs^{V} in 1 mol L^{-1} HCl and 1% THB ranged between 8−17% during the days). This could be ascribed to differing oxygen concentrations in reagents.

Prereaction of THB with HCl. THB hydrolysis can be, to a certain extent, controlled when THB is online mixed with HCl solution in the HC before the mixture is pumped into the GLS. The degree of THB hydrolysis is thus influenced by HCl concentration and by the reaction time which is proportional to the volume of the HC. Unfortunately, there are no kinetic data on THB hydrolysis in acidic aqueous media at ambient temperature. The reactions are too fast to measure; therefore, it is quite speculative to determine which hydrolytic product is a dominant species after partial hydrolysis, but it is certainly not BH_4^- because hydrolysis of BH_4^- is too fast (Theoretically 99% of BH_4^- is hydrolyzed in less than 3 μs at pH 0, but the usual mixing time in the HG reaction system is approximately 20−30 ms.).[7,28] Due to the design of the hydride generator the minimal volume of the HC was approximately 40 μL; this corresponded to the residence time between 0.12 and 0.17 s (calculated on the assumption that two or three molecular hydrogens arise − reactions 3−5).

Using the 40 μL of HC, 1% THB with 0.1% KOH (0.28 mol L^{-1} together) was mixed online with HCl at a concentration from 0 to 6 mol L^{-1}. Sensitivity during these measurements was constant and equal for both MAs^{V} and $DMAs^{V}$ with the exception of 6 mol L^{-1} HCl when the sensitivity for $DMAs^{V}$ decreased to approximately 54% of the maximum. In the case of $TMAs^{V}O$ the sensitivity decreased exponentially from a concentration of 0.5 mol L^{-1} (at the 6 mol L^{-1} the sensitivity was only 7% of the maximum). Figure 6 demonstrates that demethylation decreased for MAs^{V} with a higher concentration of HCl reaching a minimum in the range from 0.25 to 1 mol L^{-1}. These minima correspond to 0.3 ± 0.2% of AsH_3 formed from MAs^{V}. HCl concentration of 0.1 mol L^{-1} of HCl is obviously not high enough to prereact THB sufficiently. For 2.0 mol L^{-1} HCl and higher there is a slight but significant increase in demethylation: 5.0 ± 2.0% of AsH_3 from MAs^{V}. This can be caused by hydridoboron intermediates which are more "acid-resistant" like $L_2BH_2^n$ (eq 7). The similar behavior was also observed for $DMAs^{V}$ and $TMAs^{V}O$ which had a minimum at 0.5 mol L^{-1} yielding 1.3 ± 0.2% of CH_3AsH_2 and 1.4 ± 0.0% of $(CH_3)_2AsH$, respectively. The increase in fractions of non-corresponding arsanes at 2.0 mol L^{-1} to values 3.8 ± 0.1% of CH_3AsH_2 from DMAs and 4.7 ± 0.3% $(CH_3)_2AsH$ from $TMAs^{V}O$ was also evident (see the Supporting Information for Figures S-3a,b).

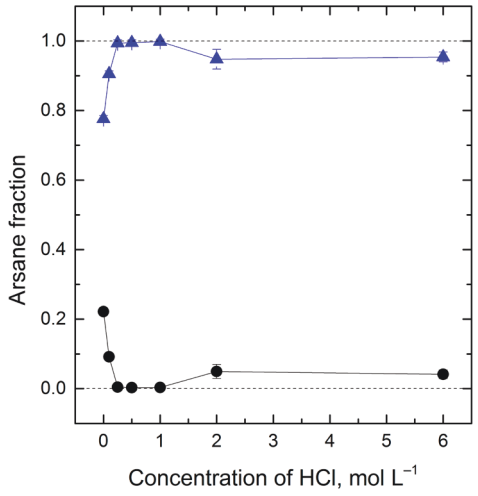

Figure 6. Dependence of arsane fractions formed from MAs^{V} on concentration of HCl used for prereaction of THB; (black) ● − AsH_3, (blue) ▲ − CH_3AsH_2; HC volume was 40 μL, concentration of MAs^{V} was 0.5 ng mL^{-1}, 1 mL of 1% THB addition, 0.6 mL of 0.25 mol L^{-1} HCl added with standard.

When the HC was enlarged to 825 μL (2 mol L^{-1} HCl was mixed with THB in the HC), the demethylation decreased to 0.0 ± 0.7%, 1.2 ± 0.3%, and 1.7 ± 0.2% for MAs^{V}, $DMAs^{V}$, and $TMAs^{V}O$, respectively, and no decrease of sensitivity was observed for MAs^{V} and $DMAs^{V}$. The sensitivity for $TMAs^{V}O$ decreased to 72%. The decrease in demethylation with the larger HC could be caused by hydrolysis of an "acid-resistant" hydridoboron species − $L_2BH_2^n$. The next and last hydrolytic product which can react with analyte is L_3BH^n. These results suggest that L_3BH^n species does not cleave the As−C bond. $L_2BH_2^n$ species probably can cleave the As−C bond but is not mainly responsible for demethylation. Since BH_4^- is hydrolyzed too fast, it is unlikely that this species can act as a derivatization agent for HG at all.[3] Therefore, it is even more unlikely that it cleaves the As−C bond. Consequently, LBH_3^n seems to be responsible for the demethylation process. This is supported by the fact that $(HO)BH_3^-$ species has an even higher reduction power than BH_4^-.[2]

Influence of identity of a ligand (H_2O, OH^-, and Cl^-) in LBH_3^n on the demethylation effect is not considered here, because there are no data on which one of those species should be present in the majority.

Other Acids. The use of other acids was also investigated with respect to demethylation during HG − $HClO_4$, HNO_3, H_2SO_4, and CH_3COOH. HG from TRIS buffer after treatment with 2% L-cysteine, which was found suitable for speciation studies,[15,24] was also tested and compared.

Perchloric and Sulfuric Acid. The volatile products of MAs^{V}, $DMAs^{V}$, and $TMAs^{V}O$ formed from the reaction of THB with $HClO_4$, H_2SO_4, and HCl (for comparison) are shown in Table 1. One mol L^{-1} $HClO_4$ shows a similar demethylation effect on MAs^{V} compared to HCl, and the effect is slightly higher in the case of $DMAs^{V}$ and $TMAs^{V}O$. In the case of 0.5 mol L^{-1} H_2SO_4 the demethylation of MAs^{V}, $DMAs^{V}$, and $TMAs^{V}O$ was even higher. Sensitivities were almost identical with those achieved in HCl medium. The mechanism of demethylation in the case of $HClO_4$ and H_2SO_4 is probably similar as for HCl. However, in the presence of these acids only hydridoboron species with ligand H_2O and OH^- are formed because perchlorate, sulfate, and hydrogensulfate are weakly coordinating anions. Since the

DOI: 10.1021/acs.analchem.6b00735
Anal. Chem. 2016, 88, 6366−6373

Table 1. Volatile Products Formed from Methylated Arsenic Species by Reaction of THB with Different Acids

	MAs^V		$DMAs^V$			$TMAs^VO$			
acid (mol L^{-1})	AsH_3	CH_3AsH_2	AsH_3	CH_3AsH_2	$(CH_3)_2AsH$	AsH_3	CH_3AsH_2	$(CH_3)_2AsH$	$(CH_3)_3As$
HCl (1)	12 ± 1%	88 ± 3%	4 ± 1%	15 ± 1%	81 ± 1%	1 ± 0%	4 ± 0%	19 ± 2%	76 ± 5%
$HClO_4$ (1)	12 ± 1%	88 ± 1%	3 ± 0%	20 ± 0%	77 ± 1%	1 ± 0%	7 ± 0%	24 ± 1%	67 ± 3%
H_2SO_4 (0.5)	28 ± 1%	72 ± 2%	5 ± 3%	27 ± 3%	67 ± 3%	3 ± 0%	12 ± 0%	26 ± 1%	60 ± 0%

demethylation effect of HCl is the lowest from these acids (at the same acidity), the hydridoboron species with chloride ligand probably suppresses the demethylation.

Acetic Acid. First, sensitivity of iAs^{III} in 1 mol L^{-1} of acetic acid did not significantly differ from that in 1 mol L^{-1} HCl. Figure 7 shows dependence of the normalized peak area

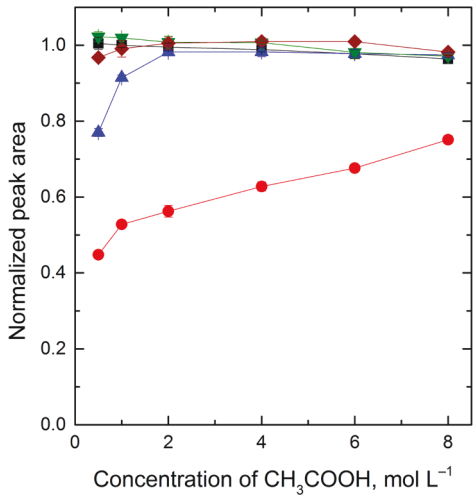

Figure 7. Dependence of normalized peak area of As species on concentration of CH_3COOH; (black) ■ – iAs^{III}, (red) ● – iAs^V, (blue) ▲ – MAs^V, (green) ▼ – $DMAs^V$, (brown) ♦ – $TMAs^VO$; concentration of As species was 2 ng mL^{-1}, 2 mL of 1% THB addition.

obtained in the direct transfer mode of iAs^{III}, iAs^V, MAs^V, $DMAs^V$, and $TMAs^VO$ on the concentration of acetic acid. iAs^{III}, $DMAs^V$, and $TMAs^VO$ are easily converted to the arsanes in the whole range. MAs^V is completely converted to arsane at concentrations 2 mol L^{-1} and higher. The most important is that even 8 mol L^{-1} is not enough to generate iAs^V quantitatively. This could be explained by the fact that acetic acid is a weak acid (pK_a = 4.8) in comparison to iAs^V (pK_a = 2.3). This correlates well with the assumption that As species must be present in an undissociated form to be efficiently converted to hydrides by the reaction with THB and/or its hydrolyzed intermediates.[29−31]

In the CT collection mode experiments, no demethylation of MAs^V, $DMAs^V$, and $TMAs^VO$ using acetic acid was observed in the whole concentration range from 0.5 to 6.0 mol L^{-1}.

When acetic acid reacts with THB, hydrolytic products are different compared to HCl[2]

$$CH_3COOH + BH_4^- \rightarrow (CH_3COO)BH_3^- + H_2 \quad (8)$$

$$(CH_3COO)BH_3^- + CH_3COOH \rightarrow (CH_3COO)_2BH_2^- + H_2 \quad (9)$$

$$(CH_3COO)_2BH_2^- + CH_3COOH \rightarrow (CH_3COO)_3BH^- + H_2 \quad (10)$$

$$(CH_3COO)_3BH^- + CH_3COOH \rightarrow (CH_3COO)_4B^- + H_2 \quad (11)$$

Our results indicate that none of these intermediates can cleave the As−C bond. To test whether demethylation caused by HCl could be prevented in the presence of CH_3COOH its addition to 1 mol L^{-1} HCl was investigated. A significant but not complete suppression of demethylation was found. Both 0.25 and 1 mol L^{-1} of CH_3COOH addition to HCl suppressed demethylation of MAs^V by 50%. As for demethylation of $DMAs^V$ the addition of 0.25 mol L^{-1} and 1 mol L^{-1} of CH_3COOH suppressed demethylation by 60% and 80%, respectively. This can be explained by the competing reactions during THB hydrolysis giving rise to formation of (CH_3COO)-BH_3^- and LBH_3^n (from HCl).

To conclude, acetic acid from the demethylation point of view could be more useful for speciation analysis of arsenic; however, an incomplete generation efficiency from MAs^V and mainly from iAs^V should be expected. The addition of acetic acid to HCl solves the problem partially.

Nitric Acid. Nitric acid appears to be convenient for HG since all the investigated arsenic species yielded a uniform normalized peak area at the HNO_3 concentration of 1 mol L^{-1} (Figure 8). Moreover, the corresponding sensitivity did not

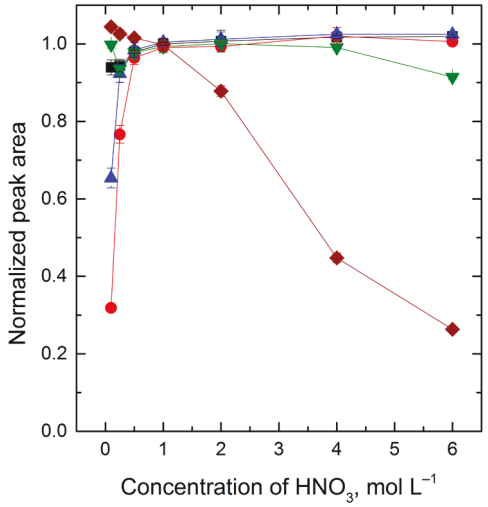

Figure 8. Dependence of normalized peak area of As species on concentration of HNO_3; (black) ■ – iAs^{III}, (red) ● – iAs^V, (blue) ▲ – MAs^V, (green) ▼ – $DMAs^V$, (brown) ♦ – $TMAs^VO$; concentration of As species 2 ng mL^{-1}, 2 mL of 1% THB addition.

significantly differ from that in 1 mol L^{-1} HCl. This dependence is quite similar to that for HCl, but in contrast to HCl there is no marked demethylation for MAs^V and $DMAs^V$: the fraction of noncorresponding arsanes formed from $DMAs^V$ in the whole studied concentration range from 0.1 to 6.0 mol L^{-1} was lower than 1%. In the case of MAs^V it was also under 1% with the only exception of concentration of 0.1 mol L^{-1} when it was 3 ± 1%. Typical chromatogram of volatile

DOI: 10.1021/acs.analchem.6b00735
Anal. Chem. 2016, 88, 6366−6373

products generated from $DMAs^V$ standard using a 1.0 mol L^{-1} of HNO_3 is shown in Figure 4c.

Nevertheless, the situation for $TMAs^VO$ was completely different. At the concentration 0.1 mol L^{-1} the fraction of $(CH_3)_2AsH$ was 1.4 ± 0.4%. A further increase of HNO_3 concentration caused a gradual increase of $(CH_3)_2AsH$ fraction. At the concentration of 6 mol L^{-1} it was 37 ± 5% of $(CH_3)_2AsH$ (the dependence of demethylation on the acid concentration was linear in the range 0.1−6 mol L^{-1} − see Supporting Information Figure S-4). The formation of other noncorresponding hydrides (AsH_3, CH_3AsH_2) was not observed, which is in agreement with the measurements for $DMAs^V$ where only the corresponding arsane was formed. The demethylation of $TMAs^VO$ probably proceeds via a different mechanism and may be associated with the reaction rate of $(CH_3)_3As$ formation. As indicated by the low yield at a higher HNO_3 concentration the reaction is slower. Therefore, $TMAs^VO$ remains for a longer time in the liquid phase, and the demethylation becomes more efficient. The difference between HNO_3 and other acids is not easy to explain, because nitrate ions are weakly coordinating anions compared to chloride and in the postulated reaction scheme of the analyte-borane complex[23] there is no influence of acid (or anions) considered.

L-Cysteine Prereduction. Analogously, no demethylation was also observed when As species (with the exception of $TMAs^VO$) were prereduced with L-cysteine to generate corresponding hydrides from 0.75 mol L^{-1} TRIS buffer medium (pH adjusted to 6.0) which is in agreement with our previous work using these generation conditions for speciation analysis by HG-CT coupled to AAS, AFS, or ICPMS detectors.[15,24,32] The L-cysteine changes the nature of the substrate (reduces to trivalent arsenic species and forms thiolate complexes) as well as changes the nature of hydridoboron species (e.g., $RS-BH_3^-$).[33,34] In the case of $TMAs^VO$, HG is performed only from TRIS buffer medium, and no L-cysteine is used for prereduction because $TMAs^VO$ is thus gradually reduced to $(CH_3)_3As$ and consequently lost from the solution.[35] No demethylation was also observed at these conditions as well.

CONCLUSION

Demethylation of MAs^V, $DMAs^V$, and $TMAs^VO$ during the reaction with THB under analytical conditions in the presence of HCl, $HClO_4$, and H_2SO_4 was characterized. It should be highlighted that the demethylation does not bring any risk of incorrect results of the postcolumn HG since the resulting sensitivity does not depend on the degree of methylation of the resulting hydride.[36] However, in the case of As speciation analysis based on generation of substituted hydrides, the demethylation can endanger accuracy of the resulting speciation namely in the case when HCl medium is employed for HG.[37−47]

In principle, even in the case of HCl medium, the demethylation can be almost completely eliminated when using the mixing coil to partially hydrolyze THB (to minimize concentrations of LBH_3^n and $L_2BH_2^n$). However, this requires a more complicated setup of the hydride generator. In the CH_3COOH medium the degree of methylation is preserved, but generation efficiency from iAs^V and MAs^V is unsatisfactory. In the case of HNO_3 the methylation (i.e., speciation information) is preserved for MAs^V and $DMAs^V$, but $TMAs^VO$ is partially demethylated to form $(CH_3)_2AsH$. Therefore, HNO_3 appears to be a suitable acid for HG of arsenic (when $TMAs^VO$ is not present in the samples) because (i) methylation of As species is preserved and (ii) equal generation efficiencies are obtained for all species. The HG system with L-cysteine prereduction and TRIS buffer medium leads only to formation of corresponding hydrides for all As species.

ASSOCIATED CONTENT

Supporting Information

The Supporting Information is available free of charge on the ACS Publications website at DOI: 10.1021/acs.analchem.6b00735.

Details on demethylation of $DMAs^V$ and $TMAs^VO$ (PDF)

AUTHOR INFORMATION

Corresponding Author

*E-mail: karel.marschner@biomed.cas.cz.

Notes

The authors declare no competing financial interest.

ACKNOWLEDGMENTS

This work was supported by GA CR (grant no. P206/14-23532S), by the Institute of Analytical Chemistry of the CAS, v. v. i. (project no. RVO: 68081715) and by Charles University in Prague (project SVV260317).

REFERENCES

(1) Dědina, J.; Tsalev, D. L. *Hydride Generation Atomic Absorption Spectrometry*; John Wiley & Sons: Chichester, UK, 1995.
(2) D'Ulivo, A. *Spectrochim. Acta, Part B* **2004**, *59*, 793−825.
(3) D'Ulivo, A. *Spectrochim. Acta, Part B* **2010**, *65*, 360−375.
(4) Wang, F. T.; Jolly, W. L. *Inorg. Chem.* **1972**, *11*, 1933−1941.
(5) D'Ulivo, A.; Onor, M.; Pitzalis, E. *Anal. Chem.* **2004**, *76*, 6342−6352.
(6) Dědina, J. In *Encyclopedia of Analytical Chemistry, Supplementary Vols. S1-S3*; Meyers, R. A., Ed.; John Wiley & Sons: Chichester, UK, 2011; pp 897−936.
(7) D'Ulivo, A.; Dědina, J.; Mester, Z.; Sturgeon, R. E.; Wang, Q. Q.; Welz, B. *Pure Appl. Chem.* **2011**, *83*, 1283−1340.
(8) Braman, R. S.; Foreback, C. C. *Science* **1973**, *182*, 1247−1249.
(9) Howard, A. G.; Salou, C. *Anal. Chim. Acta* **1996**, *333*, 89−96.
(10) Cabon, J. Y.; Cabon, N. *Fresenius' J. Anal. Chem.* **2000**, *368*, 484−489.
(11) Ellwood, M. J.; Maher, W. A. *J. Anal. At. Spectrom.* **2002**, *17*, 197−203.
(12) Hsiung, T. M.; Wang, J. M. *J. Anal. At. Spectrom.* **2004**, *19*, 923−928.
(13) Devesa, V.; Del Razo, L. M.; Adair, B.; Drobná, Z.; Waters, S. B.; Hughes, M. F.; Stýblo, M.; Thomas, D. J. *J. Anal. At. Spectrom.* **2004**, *19*, 1460−1467.
(14) Narváez, J.; Richter, P.; Toral, M. I. *Anal. Bioanal. Chem.* **2005**, *381*, 1483−1487.
(15) Matoušek, T.; Currier, J. M.; Trojánková, N.; Saunders, R. J.; Ishida, M. C.; González-Horta, C.; Musil, S.; Mester, Z.; Stýblo, M.; Dědina, J. *J. Anal. At. Spectrom.* **2013**, *28*, 1456−1465.
(16) Tseng, C. M.; Amouroux, D.; Brindle, I. D.; Donard, O. F. X. *J. Environ. Monit.* **2000**, *2*, 603−612.
(17) Prohaska, T.; Pfeffer, M.; Tulipan, M.; Stingeder, G.; Mentler, A.; Wenzel, W. W. *Fresenius' J. Anal. Chem.* **1999**, *364*, 467−470.
(18) Feldmann, J.; Grümping, R.; Hirner, A. V. *Fresenius' J. Anal. Chem.* **1994**, *350*, 228−234.
(19) D'Ulivo, A.; Meija, J.; Mester, Z.; Pagliano, E.; Sturgeon, R. E. *Anal. Bioanal. Chem.* **2012**, *402*, 921−933.
(20) Talmi, Y.; Bostick, D. T. *Anal. Chem.* **1975**, *47*, 2145−2150.

DOI: 10.1021/acs.analchem.6b00735
Anal. Chem. 2016, 88, 6366−6373

(21) Van Elteren, J. T.; Das, H. A.; De Ligny, C. L.; Agterdenbos, J.; Bax, D. *J. Radioanal. Nucl. Chem.* **1994**, *179*, 211−219.
(22) Schmeisser, E.; Goessler, W.; Kienzl, N.; Francesconi, K. A. *Anal. Chem.* **2004**, *76*, 418−423.
(23) Regmi, R.; Milne, B. F.; Feldmann, J. *Anal. Bioanal. Chem.* **2007**, *388*, 775−782.
(24) Musil, S.; Matoušek, T.; Currier, J. M.; Stýblo, M.; Dědina, J. *Anal. Chem.* **2014**, *86*, 10422−10428.
(25) Taurková, P.; Svoboda, M.; Musil, S.; Matoušek, T. *J. Anal. At. Spectrom.* **2011**, *26*, 220−223.
(26) Marschner, K.; Musil, S.; Dědina, J. *Spectrochim. Acta, Part B* **2015**, *109*, 16−23.
(27) Van Elteren, J. T.; Das, H. A.; Bax, D. *J. Radioanal. Nucl. Chem.* **1993**, *174*, 133−144.
(28) D'Ulivo, A.; Baiocchi, C.; Pitzalis, E.; Onor, M.; Zamboni, R. *Spectrochim. Acta, Part B* **2004**, *59*, 471−786.
(29) Braman, R. S.; Johnson, D. L.; Foreback, C. C.; Ammons, J. M.; Bricker, J. L. *Anal. Chem.* **1977**, *49*, 621−625.
(30) Anderson, R. K.; Thompson, M.; Culbard, E. *Analyst* **1986**, *111*, 1143−1152.
(31) Howard, A. G. *J. Anal. At. Spectrom.* **1997**, *12*, 267−272.
(32) Matoušek, T.; Hernández-Zavala, A.; Svoboda, M.; Langrová, L.; Adair, B. M.; Drobná, Z.; Thomas, D. J.; Stýblo, M.; Dědina, J. *Spectrochim. Acta, Part B* **2008**, *63*, 396−406.
(33) Brindle, I. D.; Le, X. C. *Anal. Chim. Acta* **1990**, *229*, 239−247.
(34) Pitzalis, E.; Ajala, D.; Onor, M.; Zamboni, R.; D'Ulivo, A. *Anal. Chem.* **2007**, *79*, 6324−6333.
(35) Musil, S.; Matoušek, T. *Spectrochim. Acta, Part B* **2008**, *63*, 685−691.
(36) Marschner, K.; Musil, S.; Dědina, J. *Anal. Chem.* **2016**, *88*, 4041−4047.
(37) Drobná, Z.; Waters, S. B.; Devesa, V.; Harmon, A. W.; Thomas, D. J.; Stýblo, M. *Toxicol. Appl. Pharmacol.* **2005**, *207*, 147−159.
(38) Hughes, M. F.; Devesa, V.; Adair, B. M.; Styblo, M.; Kenyon, E. M.; Thomas, D. J. *Toxicol. Appl. Pharmacol.* **2005**, *208*, 186−197.
(39) Wen, W. H.; Wen, J. H.; Lu, L.; Liu, H.; Yang, J.; Cheng, H. R.; Che, W. J.; Li, L.; Zhang, G. *Toxicol. Appl. Pharmacol.* **2011**, *254*, 41−47.
(40) Devesa, V.; Adair, B. M.; Liu, J.; Waalkes, M. P.; Diwan, B. A.; Styblo, M.; Thomas, D. J. *Toxicology* **2006**, *224*, 147−155.
(41) Valenzuela, O. L.; Borja-Aburto, V. H.; Garcia-Vargas, G. G.; Cruz-Gonzalez, M. B.; Garcia-Montalvo, E. A.; Calderon-Aranda, E. S.; Del Razo, L. M. *Environ. Health Perspect.* **2005**, *113*, 250−254.
(42) Hernandéz-Zavala, A.; Valenzuela, O. L.; Matoušek, T.; Drobná, Z.; Dědina, J.; Garcia-Vargas, G. G.; Thomas, D. J.; Del Razo, L. M.; Stýblo, M. *Environ. Health Perspect.* **2008**, *116*, 1656−1660.
(43) Sun, G. F.; Xu, Y. Y.; Li, X.; Jin, Y. P.; Li, B.; Sun, X. C. *Environ. Health Perspect.* **2007**, *115*, 648−652.
(44) Calatayud, M.; Bralatei, E.; Feldmann, J.; Devesa, V.; Vélez, D. *J. Agric. Food Chem.* **2013**, *61*, 12164−12170.
(45) Calatayud, M.; Vázquez, M.; Devesa, V.; Vélez, D. *Chem. Res. Toxicol.* **2012**, *25*, 2654−2662.
(46) Calatayud, M.; Vélez, D.; Devesa, V. *Chem. Res. Toxicol.* **2012**, *25*, 2402−2411.
(47) Zhao, R.; Zhao, M. X.; Wang, H.; Taneike, Y.; Zhang, X. R. *Sci. Total Environ.* **2006**, *371*, 293−303.

DOI: 10.1021/acs.analchem.6b00735
Anal. Chem. 2016, 88, 6366−6373

Demethylation of Methylated Arsenic Species during Generation of Arsanes with Tetrahydridoborate(1–) in Acidic Media

Karel Marschner*[,†,‡], Stanislav Musil[†], Jiří Dědina[†]

[†]Institute of Analytical Chemistry of the CAS, v. v. i., Veveří 97, 602 00 Brno, Czech Republic

[‡]Department of Analytical Chemistry, Faculty of Science, Charles University in Prague, Albertov 8, 128 43 Prague, Czech Republic

*Corresponding author; E-mail: karel.marschner@biomed.cas.cz

Abstract of Supporting Information

Supporting Information includes details on dependences of demethylation of $DMAs^V$ and $TMAs^VO$. Namely, it contains dependences on concentration of HCl, THB, experiments with hydrolysis coil (HC), and demethylation of $TMAs^VO$ on concentration of HNO_3.

Effect of HCl Concentration

The dependences of arsane fractions formed from $DMAs^V$ and $TMAs^VO$ on concentration of HCl are shown in Figure S-1(a,b).

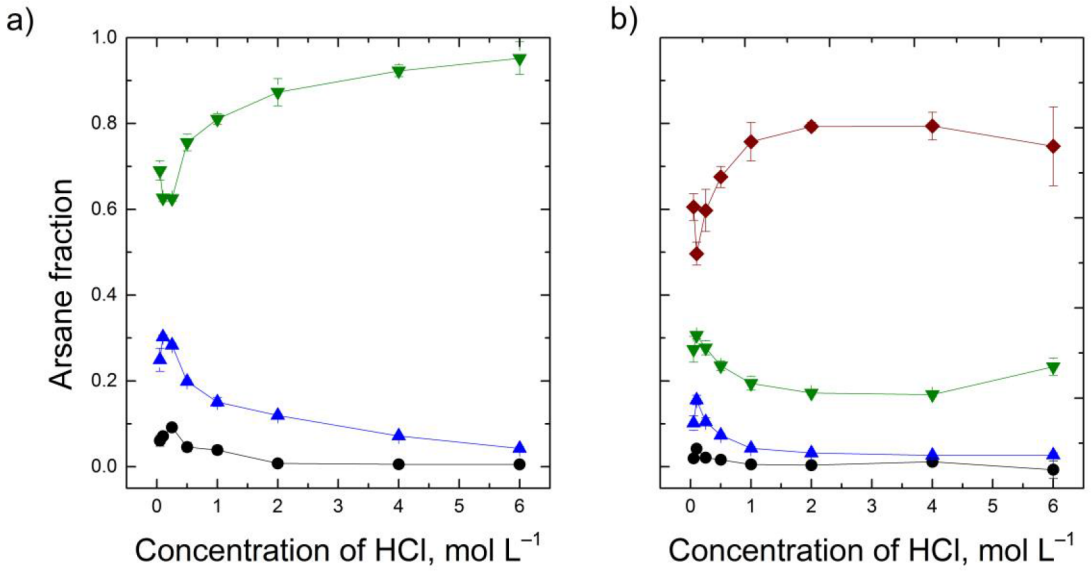

Figure S-1 Dependence of arsane fractions formed from (a) $DMAs^V$ and (b) $TMAs^VO$ on concentration of HCl; (black) ● – AsH_3, (blue) ▲ – CH_3AsH_2, (green) ▼ – $(CH_3)_2AsH$ and (brown) ♦ – $(CH_3)_3As$; concentration of $DMAs^V$ species was 0.5 ng mL^{-1}, concentration of $TMAs^VO$ was 0.5 ng mL^{-1} for HCl concentration range from 0.05 to 1.0 mol L^{-1} and 2.0 ng mL^{-1} for HCl concentration range from 2.0 to 6.0 mol L^{-1}, 1 mL of 1% THB addition.

Effect of THB Concentration

The dependences of arsane fractions formed from $DMAs^V$ and $TMAs^VO$ on concentration of THB are shown in Figure S-2(a,b).

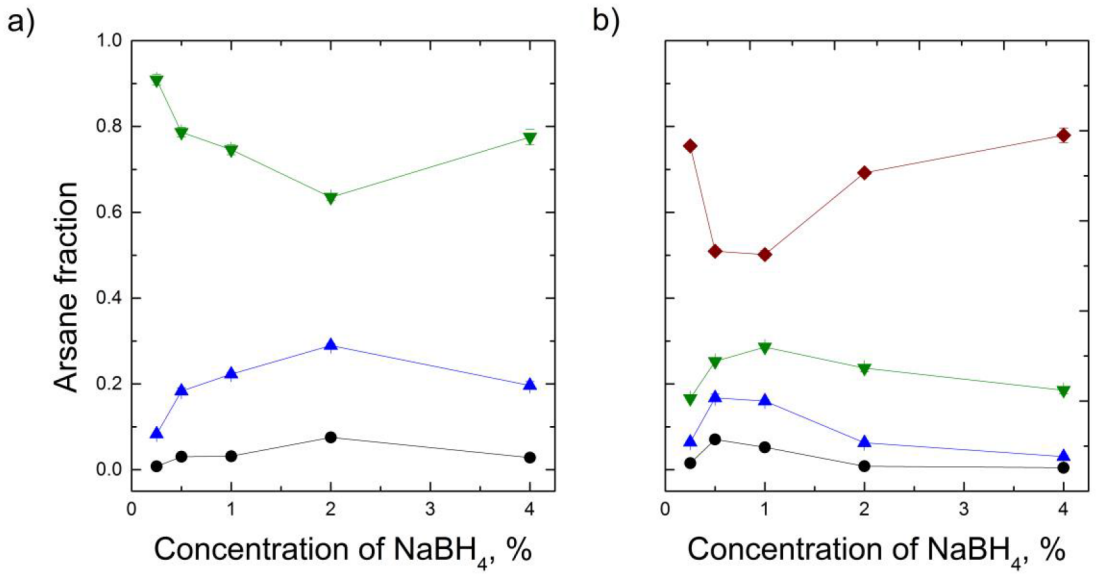

Figure S-2 Dependence of arsane fractions formed from (a) $DMAs^V$ and (b) $TMAs^VO$ on concentration of THB; (black) ● – AsH_3, (blue) ▲ – CH_3AsH_2, (green) ▼ – $(CH_3)_2AsH$ and (brown) ♦ – $(CH_3)_3As$; concentration of As species was 0.5 ng mL^{-1}, 0.25 mol L^{-1} HCl, 1 mL of 1% THB addition.

Prereaction of THB with HCl

The dependences of arsane fractions formed from $DMAs^V$ and $TMAs^VO$ on concentration of HCl used for prereaction are shown in Figure S-3(a,b).

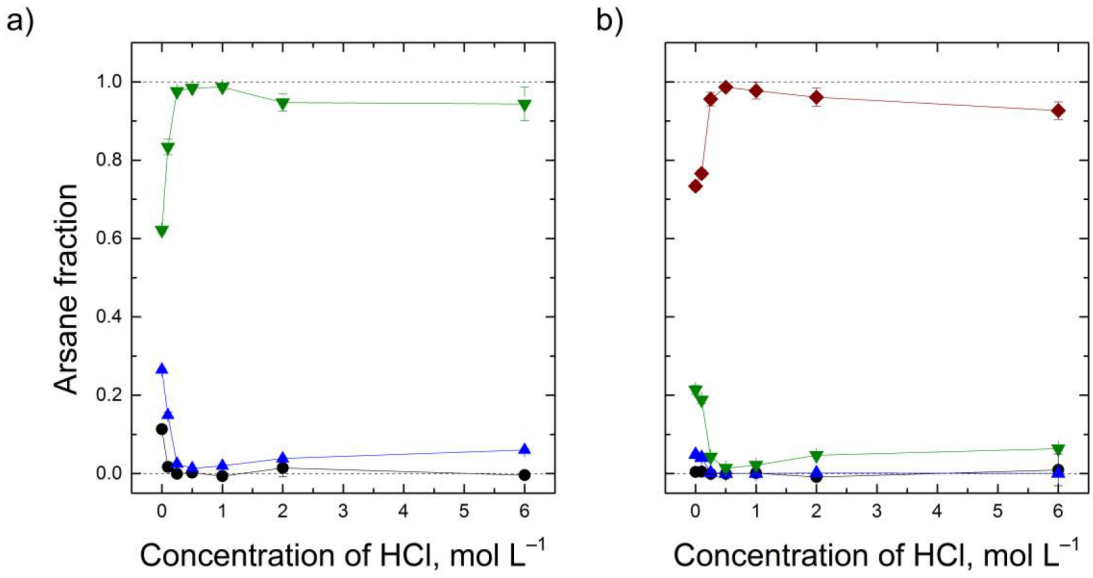

Figure S-3 Dependence of arsane fractions formed from (a) $DMAs^V$ and (b) $TMAs^VO$ on concentration of HCl used for prereaction of THB; (black) ● – AsH_3, (blue) ▲ – CH_3AsH_2, (green) ▼ – $(CH_3)_2AsH$ and (brown) ♦ – $(CH_3)_3As$; HC volume was 40 µL, concentration of $DMAs^V$ species was 0.5 ng mL^{-1}, concentration of $TMAs^VO$ was 0.5 ng mL^{-1} for HCl concentration range from 0 to 1.0 mol L^{-1} and 2.0 ng mL^{-1} for HCl concentration range from 2.0 to 6.0 mol L^{-1}, 1 mL of 1% THB addition, 0.6 mL of 0.25 mol L^{-1} HCl added with standard.

Nitric Acid

The dependences of arsane fractions formed from $TMAs^VO$ on concentration of HNO_3 are shown in Figure S-4. The linear regression of points for $(CH_3)_3As$ gives an equation $y = -0.061x + 0.998$ with $R^2 = 0.9902$ while for $(CH_3)_2AsH$ it gives an equation $y = 0.059x + 0.006$ with $R^2 = 0.9902$. This shows good linearity between demethylation and concentration of HNO_3.

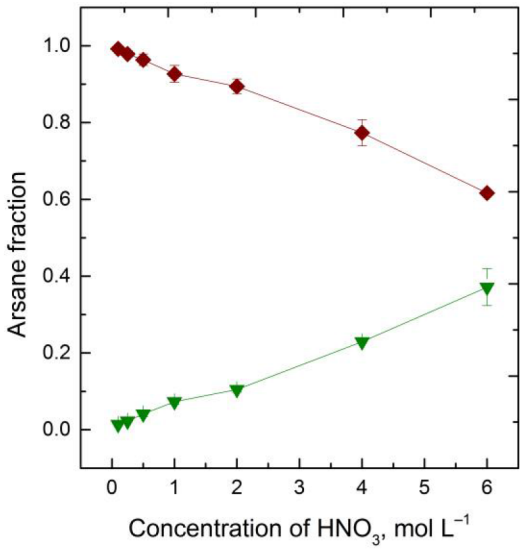

Figure S-4 Dependence of arsane fractions formed from $TMAs^{V}O$ on concentration of HNO_3; (green) ▼ – $(CH_3)_2AsH$ and (brown) ♦ – $(CH_3)_3As$; concentration of $DMAs^{V}$ species was 0.5 ng mL^{-1}, concentration of $TMAs^{V}O$ was 0.5 ng mL^{-1} for HNO_3 concentration range from 0.1 to 1.0 mol L^{-1} and 2.0 ng mL^{-1} for HNO_3 concentration range from 2.0 to 6.0 mol L^{-1}, 1 mL of 1% THB addition.

Appendix III – Hydride generation from arsenosugars

Submitted to *Journal of Analytical Atomic Spectrometry*.

Hydride Generation from Arsenosugars

Karel Marschner[1,2,*], Stanislav Musil[1], Ivan Mikšík[3], Jiří Dědina[1]

[1]Institute of Analytical Chemistry of the CAS, v. v. i., Veveří 97, 602 00 Brno, Czech Republic

[2]Charles University, Faculty of Science, Department of Analytical Chemistry, Albertov 8, 128 43 Prague, Czech Republic

[3]Institute of Physiology of the CAS, v.v.i., Vídeňská 1083, 142 20 Prague, Czech Republic

*Corresponding author; E-mail: karel.marschner@biomed.cas.cz

Abstract

Hydride generation (HG) from arsenosugars (dimethylarsinoylribosides) was studied in the batch and flow injection modes. It was found to be more efficient in H_2SO_4 medium than in HCl and with higher efficiency in the batch mode than in the flow injection mode. To increase the HG efficiency in the flow injection mode a new generator with two inlets of $NaBH_4$ solution was designed. This modified generator was implemented between a HPLC column (postcolumn HG) and an atomic fluorescence detector. The absolute limits of detection for glycerol-ribose, phosphate-ribose, sulfonate-ribose, and sulfate-ribose were 41, 9.5, 13, and 19 pg, respectively. HG efficiencies for these arsenosugars were only in the range from 13 to 30% most probably due to a more complicated mechanism of HG. It includes formation of two kinds of analyte-borane-complexes and only one of them leads to formation of volatiles arsanes (dimethylarsane, methylarsane, and arsane were identified).

1 Introduction

Determination of arsenic and its species is an important task due to their abundances in the environment and impact on health. More than fifty arsenic species have been reported in marine organisms[1,2] but the species strongly differ in their toxicity. Arsenite (iAs^{III}), and arsenate (iAs^{V}) are carcinogens of group one. Methylated species, methylarsonate (MAs^{V}), dimethylarsinate ($DMAs^{V}$), and trimethylarsine oxide ($TMAs^{V}O$), are less toxic. Arsenobetaine (AsB) and arsenocholine are considered as non-toxic.[3] The toxicity of arsenosugars (As-sugars)[4] and arsenolipids[5,6] is still a subject of research.

The lack of commercially available or well characterized standards of As-sugars makes their analysis difficult. The chemical synthesis is possible but the procedure is complex. It involves between six and ten reaction steps. Therefore, stock solutions are usually extracted from various seaweed sources and purified by a number of preparative chromatography.[7]

The majority of analytical methods for determination of As-sugars (see Fig. 1 for structures of the most common species) are based on high performance liquid chromatography (HPLC) coupled with inductively coupled plasma mass spectrometry (ICP-MS).[7] Due to the absence of calibration standards, As-sugars can be quantified according to the calibration curves of the nearest eluting standard species.[8,9] Sensitive detection is not limited only to ICP-MS as element specific detector, but also atomic fluorescence spectrometry (AFS) can be realized for detection after postcolumn on-line decomposition and hydride generation (HG).[10,11,12]

HG is a derivatization and sample introduction technique for analytical atomic spectrometry. Nowadays, it is almost exclusively based on the reaction of tetrahydridoborate(1–) (THB) in acidic media with hydride forming elements (As, Se, Sb, Sn, Bi, Pb, Te and Ge).[13] THB is stepwise hydrolysed to boric acid and hydrogen in acidic media:[14]

$$[BH_4]^- \rightarrow [LBH_3]^n \rightarrow [L_2BH_2]^n \rightarrow [L_3BH]^n \rightarrow H_3BO_3 \qquad (1)$$

, where *L* could be one or more groups among H_2O, OH^-, and Cl^- and *n* is the charge (–1, 0, or +1). THB and its hydrolysed products, *i.e.* hydridoboron species, react with the hydride forming elements to produce an analyte-borane complex (ABC) from which a volatile hydride is formed.[14]

In the case of arsenic, the inorganic species $iAs^{III,V}$ and methylated MAs^V, $DMAs^V$, and $TMAs^VO$ species can be easily converted to volatile hydrides (arsane or mono-, di- and trimethyl substituted arsanes) via the reaction of THB in acidic media which is also typically utilized for speciation analysis[15]. It has been believed for a long time that the other organically bound species could not be converted to the volatile arsanes because the As-C bond could not be cleaved during HG. Sánchez-Rodas *et al.*[11] probably observed low but significant HG activity of As-sugars which they however explained by a partial degradation of As-sugars to $DMAs^V$ under the acidic conditions. Later Schmeisser *et al.*[16] proved that As-sugars were prone to conversion to volatile hydrides with an efficiency strongly dependent on the conditions of HG. The cleavage of As-C bond during HG was subsequently confirmed by Regmi *et al.*[17] who found 6–9% conversion of As-sugars to $(CH_3)_2AsH$. It was explained by a formation of ABC making methylene group more susceptible to hydride attack. Very recently, the cleavage of As–C bond during HG was described even for MAs^V, $DMAs^V$, and $TMAs^VO$ when noncorresponding arsanes (after loss of one or more methyl groups) were identified. The mechanism of the As-C bond cleavage was studied thoroughly in a detail and it was postulated that it proceeded through the action of the second and third hydridoboron species.[18]

Based on our previous work,[18] we investigated HG activity of As-sugars in more detail and tried to clarify this phenomenon and mechanism of this action. Our next objective was to reach a maximum HG efficiency and test the feasibility of this derivatization approach (without preceding UV decomposition step) for speciation analysis by HPLC-HG-AFS.

2 Experimental section

2.1 Standard and Reagents

Deionized water (DIW; <0.2 μS cm^{-1}, Ultrapur, Watrex, USA) was used for the preparation of all solutions. A 1000 μg mL^{-1} As standard solution (Merck, Germany) was used as iAs^{V} stock standard solution. Stock solutions of 1000 μg mL^{-1} As were prepared for iAs^{III}, MAs^{V}, $DMAs^{V}$, $TMAs^{V}O$, and AsB species in DIW using following compounds: As_2O_3 (Lachema, Czech Republic); $Na_2CH_3AsO_3 \cdot 6H_2O$ (Chem. Service, USA); $(CH_3)_2As(O)OH$ (Strem Chemicals, Inc., USA); AsB (Sigma-Aldrich, USA); $(CH_3)_3AsO$ was obtained by courtesy of Dr. William Cullen (University of British Columbia, Canada). The total As content of methylated arsenic species standards was confirmed by liquid sampling graphite furnace-atomic absorption spectrometry as described previously.[19] The solution of THB was prepared fresh daily from $NaBH_4$ (Fluka, Germany) in 0.1% KOH (Lach-Ner, Czech Republic). HCl (p.a., Merck, Germany), HNO_3 (semiconductor grade, Sigma-Aldrich, Germany) and H_2SO_4 (suprapure, Merck, Germany) were used for HG.

Mobile phase for anion exchange chromatography was either 20 mmol L^{-1} phosphate buffer prepared from KH_2PO_4 (Lach-Ner, Czech Republic) with pH adjusted to 5.6 with KOH[9] or 20 mmol L^{-1} bicarbonate buffer from NH_4HCO_3 (Lachema, Czech Republic) with pH adjusted to 10.3 with aqueous ammonia (Sigma-Aldrich, Germany) mixed 9:1 with methanol (Sigma-Aldrich, Germany).[8] Solid NaOH (Lach-Ner, Czech Republic) in the form of 3 mm pearls was used as a filling of a NaOH dryer.[20]

2.2 Instruments

The in-house assembled research grade non-dispersive atomic fluorescence spectrometer was employed as the detector. The experimental set up is described

elsewhere.[19,21]Briefly, the instrument was equipped with an arsenic electrodeless discharge lamp (EDL system II, Perkin Elmer, USA) as a radiation source, an interference filter (193 nm, full width at half maximum 18.7 nm, CVI Melles Griot, USA) to isolate fluorescence radiation from an atomizer and a solar blind photomultiplier (165–320 nm, Perkin Elmer Optoelectronics, USA) as the detector. A miniature diffusion flame (MDF) was used as the atomizer. The atomizer optimum observation height (7 mm), flow rates of flame hydrogen (200 mL min^{-1}) and flame argon (600 mL min^{-1}) were optimized previously - see Ref.[21] for details.

An Agilent 7700x ICP-MS spectrometer was used as an element specific detector for comparative purposes. Measurements were carried out in helium gas mode (4.8 mL min^{-1}) in the collision cell. Arsenic was measured directly as ^{75}As. A solution of 10 ng mL^{-1} rhodium (^{103}Rh) was used as an internal standard.

An Agilent HPLC system 1200 (USA) was employed in combination with both the AFS and ICP-MS detectors. 50 µL of sample was injected by an autosampler. PRP-X100 column (250 x 4.6 mm, 10 µm particle size, Hamilton, USA) with a guard column was used as the chromatographic column with a flow rate of 1 mL min^{-1} for phosphate buffer and 0.4 mL min^{-1} for bicarbonate buffer.

A HCT-Ultra ETD II Mass Spectrometer (Bruker, USA) with electrospray ionization (ESI, capillary exit voltage was 102.3 V) in positive mode was used for MS^2 measurements. Operation conditions: drying gas N_2 12 L min^{-1}, drying gas temperature 350 °C, nebulization pressure 35 psi (241.3 kPa). MRM method was used for MS^2 measurements. Selected precursor ions were 329.0, 393.0, 409.0 and 483.0, the isolation width was 4 m/z, the collision amplitude was 0.8 V, scan 90-490 m/z.

2.3 Seaweed extracts

Dried edible seaweed samples (*Hijiki*, *Nori*, *Kombu* and *Wakame*) were purchased at a local supermarket and milled to the fine powder. A 15 mL polyethylene tube containing 0.2 g of seaweed powder and 8 mL of DIW were placed in an ultrasonic bath (Elmasonic One, Elma, Germany) at laboratory temperature for three hours. The samples were then centrifuged 5 min at 4000 rpm. 6 ml of supernatant was removed into 50 mL vessel and diluted to 25 mL and immediately frozen (–18 °C). The seaweed extracts were thawed before analysis, filtered through a syringe filter (PTFE, 25 mm, pore size 0.45 μm) and spiked with H_2O_2 (to 3% solution) to convert any extracted iAs^{III} species to iAs^{V} before HPLC-HG-AFS or HPLC-ICP-MS analysis.

2.4 Hydride generators

2.4.1 Flow injection and postcolumn mode

The hydride generator in the FI mode (see Fig. S1a of Supporting Information for the scheme) was the same as described previously.[22] Sample was injected into the flow of DIW by a six-port injection valve (Rheodyne, USA) with 0.6 mL sample loop volume. Solution of THB, acid and DIW were pumped by a peristaltic pump (Ismatec, Switzerland) at the flow rates of 1 mL min^{-1}. A PTFE reaction coils of various inner diameter (i.d.) and volume were tested - 1 mm i.d. for 0.8 mL and 1.85 mm i.d. for 3.5, 5.4 and 8.9 mL. Generated arsanes were separated from the liquid phase in the gas-liquid separator (GLS Unit I – Ref.[22]).

When explicitly stated, the solutions of THB were introduced to the generator by two channels. Solution of THB introduced by the first channel was mixed in a T-junction with the acidified sample. The reacting mixture flew to the reaction coil (3.5 mL) which was connected downstream to another T-junction where the additional solution of THB was introduced. The mixture followed to a second reaction coil (5.4 mL) connected to the GLS. This generator was

also employed in the postcolumn mode of HG when the injection valve and the channel for DIW was replaced by the outlet from the chromatography column. GLS Unit IV (Ref.[22]) was used (Fig. S1b of Supporting Information).

2.4.2 Batch generator and cryogenic trap

The batch hydride generator was described previously (Fig. S1c of Supporting Information).[18] The generator consisted of peristaltic pumps (Ismatec, Switzerland), a GLS with a forced outlet of total volume of 7 mL, a chemifold between the pumps and the NaOH dryer.[20]

HCl or H_2SO_4 was pumped by the peristaltic pump at the flow rate of 4 mL min^{-1}. A 0.6 mL of As standard was introduced into the acid channel by a six-port injection valve (Rheodyne, USA). Carrier gas (argon) merged the acid channel downstream the standard introduction point. The acid channel was equipped with an additional T-junction upstream the GLS that served for cleaning of the GLS with DIW by a syringe. Another channel was used to remove liquid waste from the GLS by the other syringe. THB was pumped by another peristaltic pump at the flow rate of 1 mL min^{-1}. The output of the gases from the GLS was connected to the NaOH dryer. The gaseous phase leaving the dryer was mixed with flame hydrogen and flame argon for the MDF atomizer. In some experiments, a cryotrap (CT) was implemented between the dryer and the point where flame gases were introduced. The carrier gas was helium in this case. The details on the CT can be found in Refs.[18,19,23]

The procedure was the same as used previously.[18] A standard was injected into the flow of acid and it was introduced to the bottom of the GLS. The total volume of liquid was 1.2 mL. Subsequently, recording of the fluorescence signal was switched on (210 s read time) and 2 mL of THB was being introduced into the GLS. After recording had been completed remaining

liquid was removed from the GLS and the GLS was cleaned with DIW. The procedure for HG-CT-AFS is described elsewhere.[18]

2.5 Data evaluation

Peak area was invariably employed as the analytical quantity. Since the AFS detector output yields response in μV units that are specific to the instrument, peak area values cannot be simply related to those yielded by different instruments. Therefore, in the batch mode, we deal with normalized peak areas related to that of 2 ng mL^{-1} iAs^{III} that was generated by 1% THB from 1 mol L^{-1} of HCl. In the FI mode, the peak areas are related to the signal of 2 ng mL^{-1} iAs^{III} generated by 1% THB from 1 mol L^{-1} HCl medium using the reaction coil of 3.5 mL. Since arsane from iAs^{III} is generated quantitatively (HG efficiency 100%) both in the batch and FI modes under these conditions,[18,22] normalized peak area also expresses HG efficiency. HG efficiencies of As-sugars in the FI and batch mode aren't corrected for the impurities of hydride active species in the 'standard' (see later) because their total content was lower than 1.5%. As species concentrations or mass are expressed always as elemental concentration or mass. All results are shown as mean ± standard deviations (SD) from three replicates. The uncertainty of percentage of arsenic species in sample were calculated from propagation of error formula (the relative SD lower than 1% are not presented). Limits of detection (LODs) for our HPLC-HG-AFS approach were calculated as SD (n=10)/sensitivity. The sensitivities of As-sugars were derived from the sensitivity of MAs^{V} multiplied by HG efficiency of individual As-sugar.

Mathlab 2012b software was used to solve a system of differential equations, OriginPro 9.0 was used for model fitting.

3 Results and discussion

3.1 Preliminary experiments

Arsenic species were extracted by DIW from dried seaweed samples using ultrasonic bath.[24] Total arsenic content and speciation was determined by liquid sampling ICP-MS and by HPLC–ICP-MS, respectively. Preliminary identification of As-sugar peaks in the chromatograms using phosphate buffer as the mobile phase (1 mL min^{-1}) was based on the elution order and retention times achieved in the other works.[8,9] The As-sugars were quantified according to the calibration curves of the nearest eluting standard species (*i.e.* As-sugar-gly on AsB, As-sugar-PO_4 on MAs^V, As-sugar-SO_3 and As-sugar-SO_4 on iAs^V). The results are summarized in Table 1. The determined column recoveries are in agreement with other works[12,25]. Since phosphate buffer is not compatible with ESI-MS, the definite identification of the individual As-sugars in *Hijiki*, *Nori*, and *Kombu* extracts was based on the retention times, determined concentrations from HPLC-ICP-MS and structure analysis obtained with HPLC–ESI-MS^2 using bicarbonate buffer as the mobile phase (0.4 mL min^{-1}). The chromatographic conditions were taken from Ref.[8] HPLC–ICP-MS chromatograms of seaweed extracts at these conditions are in Fig. S2 while the ESI-MS^2 spectra are in Fig. S3 of Supporting Information. *Wakame* extract was not examined with ESI-MS because the detected As-sugars peaks in HPLC-ICP-MS chromatogram were the same as for the other seaweed extracts. Observed fragmentation spectra were similar to the spectra published by McSheehy *et al.*[26] and by Gallagher *et al.*[27] The molecular ion $[M-H]^+$ for As-sugar-SO_4 was at m/z 409 and fragment ions at m/z 329 and 237. For As-sugar-SO_3 the molecular ion $[M-H]^+$ was at m/z 393 and fragment ions at m/z 375, 295, 237, 195, and 165. For As-sugar-PO_4 the molecular ion $[M-H]^+$ was at m/z 409 and fragment ions at m/z 465, 391, 329, and 237. For As-sugar-gly the molecular ion $[M-H]^+$ was at m/z 329 and fragment ion at m/z 237. Taking into account the determined concentrations of As-sugars in seaweed extracts, the retention times (t_r) for As-sugar-gly, As-

sugar-PO_4, As-sugar-SO_3 and As-sugar-SO_4 using phosphate buffer for HPLC-ICP-MS were assigned as 2.7, 7.4, 17.7 and 41.5 min, respectively (Table 1). One species, most probably also As-sugar species, eluting at 11.9 min remained unidentified due to its low content.

Nori extract with 114 ± 5 ng mL^{-1} As was properly diluted to have the total As content 2 ng mL^{-1}. This standard was further used as "pure" As-sugar-PO_4 "standard" for investigation of HG "activity" because the relative content of As-sugar-PO_4 determined by HPLC–ICP-MS was 94%. Moreover, 98% of As was found in the form of As-sugars (see Table 1) with negligible contribution of the classical hydride active species *i.e.* iAs^V, MAs^V and $DMAs^V$. HG in the FI mode carried out from 0.5 mol L^{-1} HCl using 1% THB solution exhibited low HG efficiency corresponding to 9 ± 1%. No matrix effect on HG was observed because the recovery of $DMAs^V$ (2 ng mL^{-1}) spiked into this standard was 100 ± 4%. HG carried out from 0.5 mol L^{-1} HNO_3 resulted in even lower HG efficiency corresponding to 1.2 ± 0.1%. This value is in pretty good agreement with the total content of classical hydride active species, iAs^V and $DMAs^V$ (1.4% ± 0.1%) in Table 1 indicating that HG from As-sugars is fully suppressed in HNO_3 medium. This observation is in line with our previous work that the ability of HG to cleave As–C is dramatically reduced in the medium of HNO_3.[18] The As-sugars do not form volatile arsanes from HNO_3 medium was stated also by Schmeisser *et al.*[16] The above experiments proved HG activity of As-sugars in HCl medium and verified the suitability of the prepared As-sugar 'standard' to systematically investigate the conditions of HG from As-sugars.

3.2 HG in batch mode

HG activity of As-sugar-PO_4 was investigated in the range from 0.1 to 4 mol L^{-1} HCl at THB concentrations of 1% and 2%, respectively (Fig. 2). The maximum HG efficiency was achieved at 1 mol L^{-1} HCl and 1% THB. The inherent property of the batch generation is that

pH of the reaction mixture increases in time with THB supply. For 1% THB solution, there is a lack of acid for full decomposition of THB at HCl concentrations below 1 mol L^{-1}. For example, for 0.25 mol L^{-1} HCl the acid is completely consumed by THB hydrolysis within 32 seconds of THB solution introduction. Since the THB solution is added over a period of 120 seconds, almost 75% amount of THB is not hydrolyzed. For 2% THB solution, the minimal concentration of HCl for complete THB hydrolysis is shifted to 2 mol L^{-1}. The observed decrease of HG efficiency at higher concentrations of HCl indicates that keeping strong acidic conditions during the whole period of HG is not ideal as well.

The interesting phenomenon observed during these experiments was the As-sugar-PO_4 signal shape (see Fig. 3). It was entirely different from the other arsenic species (see below). For 1% THB solution, the rising edge of the As-sugar-PO_4 peak was relatively steep reaching the maximum at t_{max} = 42 s but the falling edge was rather slow. At 2% THB solution, the peak maximum was reached even sooner (t_{max} = 25 s), then signal was slowly decreasing to the minimum but at about half of the peak maximum it started slowly increasing again (Fig. 3). This increase is probably due to increase of pH during the reaction. It appears that the optimum pH for cleavage of As–C is at higher values.

It should be noted that for $TMAs^{V}O$ in 6 mol L^{-1} HCl, which exhibited similar HG efficiency (around 24 ± 1%)[18] as the As-sugar-PO_4, a completely different signal shape was recorded having the form of a broad but rather symmetrical peak with its maximum at around 82 s. This difference in signal shapes clearly suggests a different mechanism of HG (see chapter 3.5 for details).

H_2SO_4 was also tested as the medium for HG of As-sugar-PO_4 with 1% THB solution in the concentration range from 0.05 to 3 mol L^{-1} (Fig. 2). The maximum HG efficiency was obtained at 1 mol L^{-1} H_2SO_4 and not at 0.5 mol L^{-1} which would correspond to the same acidity as 1 mol L^{-1} HCl. Furthermore, the HG efficiency at optimum was almost twice higher (68 ±

1%) compared to HCl medium (35 ± 1%). This is in agreement with our previous results that the cleavage of As–C bond during HG is more efficient in H_2SO_4 medium than in HCl.[18] Also the signal shape is different from that obtained with HCl (Fig. 3).

The identity of formed volatile arsanes was investigated by coupling the generator in the batch mode to the CT (HG-CT-AFS) allowing for their simple separation in the gaseous phase. It was found out that under the conditions of HG with the highest yield of arsanes (1 mol L^{-1} H_2SO_4 and 1% THB solution), 66 ± 3% was in the form of $(CH_3)_2AsH$, 32 ± 3% as CH_3AsH_2, and 3 ± 1% as AsH_3. No traces of $(CH_3)_3As$ were detected. This observation is quite in line with the statement by Regmi *et al.*[17] who reported that $(CH_3)_2AsH$ with traces of CH_3AsH_2 were the volatile products formed from As-sugar-SO_3 and As-sugar-SO_4.

3.3 HG in FI mode

HG efficiency of As-sugar-PO_4 was examined in the FI generation mode in the range from 0.25 to 3 mol L^{-1} HCl and from 0.5 to 2.5% of THB solution. The surface plot is shown in Fig. 4a. The highest HG efficiencies were observed when the molar ratio HCl/ THB was about 2. Generally, HG efficiency increased with more concentrated THB solution up to 2% but at 2.5% there was rather a slight decrease. It also decreased with the concentration of HCl which strongly suppressed the HG efficiency, especially at low THB concentration.

In the medium of H_2SO_4 (tested in the range from 0.125 to 3 mol L^{-1} H_2SO_4 and 0.5 to 2.0% THB solution) the volatile arsanes can be generated from As-sugar-PO_4 in a wider range of reagents concentrations (Fig. 4b). HG efficiency is not so impaired at higher concentrations of acid compared to HCl (Fig. 4a). This result indicates that HG is suppressed by higher concentration of Cl^- ions which may interact with hydridoboron species resulting in chloride-hydridoboron species which cannot cleave As–C bond or only with low probability. The difference in the highest HG efficiencies achieved from HCl and H_2SO_4 media was insignificant

(16 ± 0% and 19 ± 1%, respectively). The reaction time which can enhance the HG efficiency can be controlled in the FI mode by the volume of the reaction coil.[22] Three different volumes of the reaction coil were tested (0.8, 3.5, and 8.9 mL) using 1.5 mol L^{-1} H_2SO_4 and 1% THB solution (maximum HG efficiency in Fig. 4b). Reduction of the reaction coil to volume 0.8 mL caused decrease in the HG efficiency to 13 ± 1%. On the other hand, increasing the volume to 8.9 mL did not significantly increase the HG efficiency.

The HG efficiency achieved in the FI mode with H_2SO_4 was much lower (19 ± 1%) than in the batch mode (68 ± 1%). This can be explained by the previously observed phenomenon that only the first two hydrolytic products of THB hydrolysis ($[LBH_3]^n$ and $[L_2BH_2]^n$) are capable of cleaving As–C bond[18] which is a necessary condition in the case of As-sugars for the formation of volatile arsanes. Since the analyte is continuously supplied in the batch mode with the fresh solution of THB, the first two hydrolytic products of THB are present during the whole process of HG. On the other hand, in the FI mode the analyte can interact with the first two hydrolytic products only in the front part of the reaction coil. In the farther points of the reaction coil these products are consumed, converted to different hydridoboron species, less or not active in cleavage of As-C bond. This was demonstrated by no substantial effect of increased volume of the reaction coil.

There are two ways to theoretically sustain the effective concentration of first two hydrolytic product of THB in the whole length of the reaction coil: (i) use more concentrated solution of THB or (ii) introduce additional solution of THB. The former way was shown to result in decrease in the HG efficiency (Figs. 4a and 4b). Therefore, a new HG system was constructed with two channels to introduce THB solution to acidified sample. The first reaction coil was 3.5 mL while the second one (after introduction of additional THB solution) was 5.4 mL. The HG efficiency in this modified generator increased to 29 ± 3% (using 1.5 mol L^{-1} H_2SO_4 and 1% THB solution in both channels). The HG efficiencies of the other “hydride

active" As species were also investigated in this arrangement of the generator for comparison and they corresponded to 102 ± 2%, 96 ± 2%, 100 ± 2%, 93 ± 2%, and 20 ± 1% for iAs^{III}, iAs^{V}, MAs^{V}, $DMAs^{V}$, and $TMAs^{V}O$, respectively.

3.4 HPLC–HG–AFS

The optimized design of the hydride generator was connected to HPLC for postcolumn HG and the seaweed extracts were analyzed without further dilution except *Hijiki* which was twice diluted due to high content of iAs^{V}. Obtained chromatograms are shown in Fig. 5. As shown in the paragraph above, MAs^{V} is converted to hydride with 100% efficiency. Consequently, the amount of hydride generated from an As-sugar corresponds to the ratio of the peak area of the As-sugar in question the HPLC–HG–AFS chromatogram to MAs^{V} sensitivity. Since concentrations of As-sugars in the seaweed extracts are known (determined by HPLC-ICP-MS - see Tab. 1), an assessment of HG efficiency from individual As-sugars is straightforward. The HG efficiencies were 13 ± 1%, 28 ± 2%, 31 ± 3%, and 17 ± 1% for As-sugar-gly, As-sugar-PO_4, As-sugar-SO_3, and As-sugar-SO_4, respectively.

The HG efficiency of As-sugar-PO_4 determined from these measurements using HPLC correlated very well with the 29 ± 3% found in the FI mode for diluted As-sugar-PO_4 "standard". Although the achieved lower column recoveries (76% for As-sugar-PO_4, see Table 1) could evoke the presence of As species not able to elute from the column - different from those studied, this result fully supports the statement that As-sugars-PO_4 was really the dominant arsenic species (94%) in the As-sugar "standard". It clearly justifies the assumption to use diluted *Nori* extract as As-sugar "standard" for HG optimization. The HG efficiency of 33 ± 12% was found for the unknown species (retention time of 11.9 min). High uncertainty is due to its low concentration in the extract. The achieved HG efficiencies are similar to those published by Schmeisser *et al.*[16] (21–28%). Nevertheless, HG efficiencies for As-sugar-SO_3

and As-sugar-SO_4 achieved in our work are about three times higher than those published by Regmi *et al.*[17].

The achieved LODs are comparable or even better to HPLC–UV-decomposition–HG–AFS based methods (see Table 2) although the HG efficiency was far from 100%. The explanation can lie in the excellent sensitivity of our AFS instrument given by lower noise of the baseline, efficient EDL source used for fluorescence excitation and/or due to lower contamination because no other additive reagents are required for UV-decomposition (hydroxide and peroxydisulfate).

3.5 Mechanism of HG of As-sugars

Under several simplifying assumptions, the shape of the peak produced by a batch hydride generator can be expressed as:[13]

$$S(t)=A\cdot\{\exp(-k_1 t)-\exp(-k_m t)\} \quad (2)$$

, where *S(t)* is the observed AFS signal. The constant *A* includes all experimental parameters.[13] The most important assumption for the validity of eq. 2 is that concentration of THB and its hydrolysis products are constant during the signal evolution. Hydride release from the solution is thus a pseudo-first order process controlled by the analyte concentration in the reaction mixture with the rate constant k_1. Constant k_m is the first order rate constant of hydride removal from the GLS.[13,28]

Fig. 6a shows a result of the non-linear regression of the AFS signal of iAs^{III} to the function (2). To fulfill the assumption of the pseudo-first order hydride release, the curve fitting does not start at the beginning of THB solution addition but by 5 s later. There is a very good correlation between this simple model and the experiment.

However, signal shapes for As-sugar-PO_4 (Fig. 3) suggest that they cannot be described by the function (2). The obvious reason is that the hydride release from the reaction mixture cannot be considered to be the simple pseudo-first order process.

Two reaction mechanism schemes leading to the hydride release from the reaction mixture (Fig. 7) could be taken into account.

(A) As-sugars are firstly cleaved by the action of THB (and/or its intermediates) to hydride active arsenic species (*e.g.* $DMAs^V$). In the second step, it is converted to hydride which is released to gaseous phase.

(B) There are two competitive reactions between the As-sugars species and THB (and/or its intermediates). The first reaction is analogous (but with different rate constant) with that considered for derivation of eq. (2). The second reaction leads to a formation of an ABC from which a hydride is not formed but which is in an equilibrium with the As-sugar species.

In both the reaction mechanism schemes, the gaseous hydride is removed from the GLS by the first order process with the rate constant k_m identical to that in eq. (2). Taking the same assumption as to derive eq. (2) (constant concentration of THB and its hydrolysis products during the signal evolution) all reactions defined in Fig. 7 are of the first or pseudo-first order with the corresponding rate constants. Consequently, we get a system of differential equations and its solution describe the signal shape corresponding to HG of As-sugar-PO_4 (see details in Supplementary Information). The both solutions work pretty well for the signal of As-sugar-PO_4 generated from 4 mol L^{-1} HCl with the addition of 1% THB solution (see Fig. 6b. However, for 4 mol L^{-1} HCl and addition of 2% THB solution (see Fig. 6c), and for 2 mol L^{-1} H_2SO_4 and addition of 1% THB solution (Fig. 6d), there is much better correlation for mechanism (B)

Mechanism B also explains the decrease of the signal at more concentrated THB (Fig. 2) because in this proposed mechanism the reaction yield depends not only on concentration of THB but also on the ratio of hydridoboron species which are capable or incapable of cleaving

the As–C bond, this ratio can be affected by the total concentration of THB. But this ratio is probably affected also by concentration of Cl^- ions, therefore in H_2SO_4 the HG efficiency is much higher than in HCl medium and it dramatically decreases at higher concentrations of HCl in the FI mode.

Although the reaction of hydride formation is shown schematically as one step reaction in mechanism B (Fig. 7), the reality is much more complicated and the true reactions steps are unknown. They probably include the formation of ABC but this one is capable of cleaving the As–C bond results in formation of dimethylated (or even less methylated) arsenic species which are subsequently converted to the volatile arsanes.

Conclusion

This study shows that volatile arsanes can be generated from As-sugars in the batch mode with relatively high HG efficiency (68 ± 1%). However, the HG efficiency is much lower in the FI mode due to a more complex mechanism which includes formation of two kinds of analyte-borane-complex: the first kind results in formation of volatile arsanes and the second kind decomposes back to the analyte. Nevertheless, major As-sugar compounds occurring in seaweed samples can be in principle determined by HPLC–HG–AFS method without the UV decomposition step in the optimized hydride generator. Unfortunately, the lack of available standards makes this analysis currently impossible because As-sugars cannot be quantified by other species (like in HPLC–ICP-MS method).[8,9] Achieved HG efficiencies for As-sugars are similar or even better than those published up to now depending on the mode of the generator used.

Acknowledgments

This work was supported by Institute of Analytical Chemistry of the CAS, v. v. i. (project no. RVO: 68081715), by Ministry of Education, Youth and Sports of the CR (Program Kontakt II project No. LH15174), and by Charles University (project SVV)

Figures

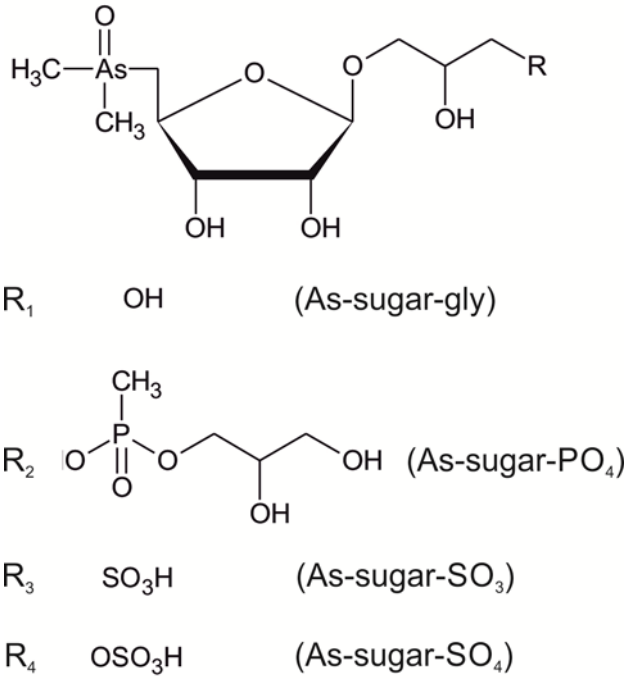

Figure 1 Structures of four major As-sugars found in marine seaweed.

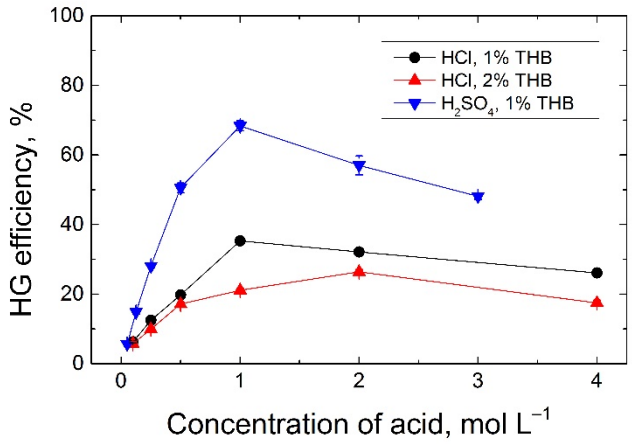

Figure 2 Dependence of HG efficiency from As-sugar-PO_4 on concentration of acid in the batch hydride generator; ● (black) – HCl, 1% THB solution; ▲(red) – HCl, 2% THB solution; ▼ (blue) – H_2SO_4, 1% THB solution.

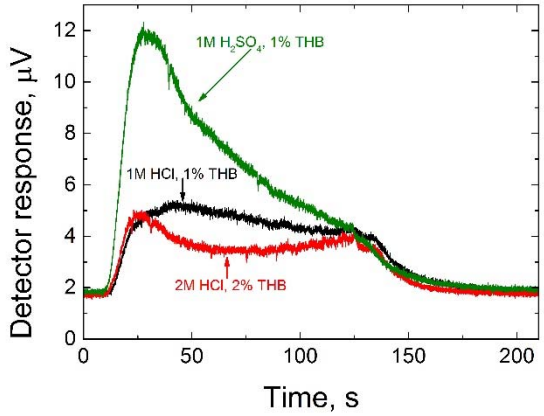

Figure 3 Signal shapes from HG of As-sugar-PO_4 in the batch hydride generator; (black) – 1 mol L^{-1} HCl, 1% THB solution; (red) – 2 mol L^{-1} HCl, 2% THB solution; (green) 1 mol L^{-1} H_2SO_4, 1% THB solution; concentration of As was 2 ng mL^{-1}. THB solution was introduced to the generator from time 4 to 124 s.

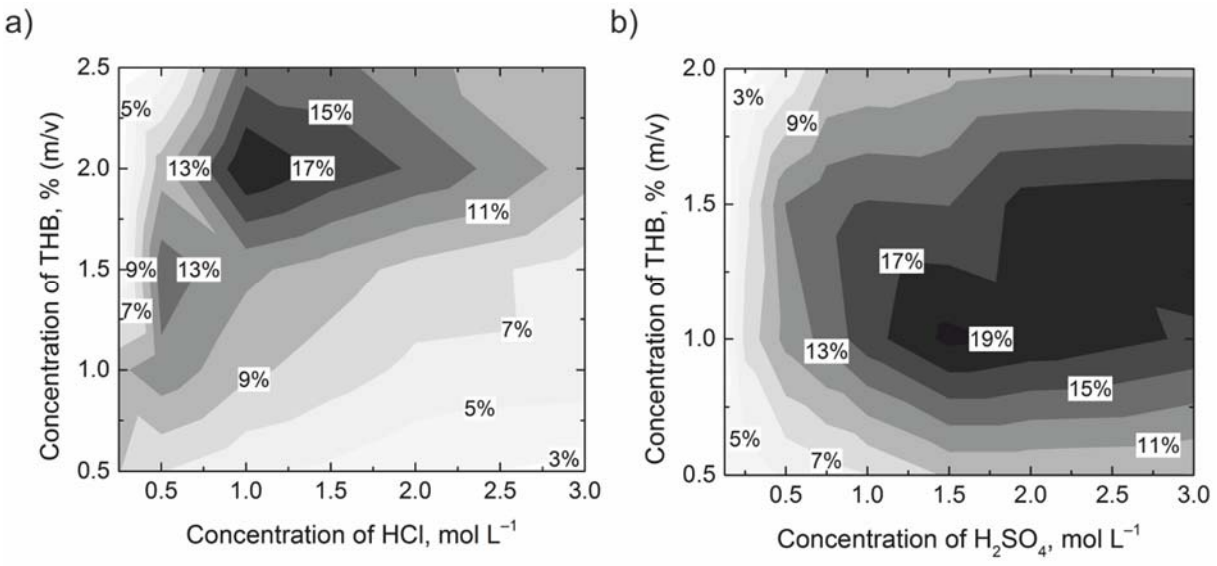

Figure 4 Dependence of HG efficiency of As-sugar-PO_4 on THB concentration and on concentration of (a) HCl and (b) H_2SO_4 in the flow injection mode; 3.5 mL volume of the reaction coil; concentration of As was 2 ng mL^{-1}.

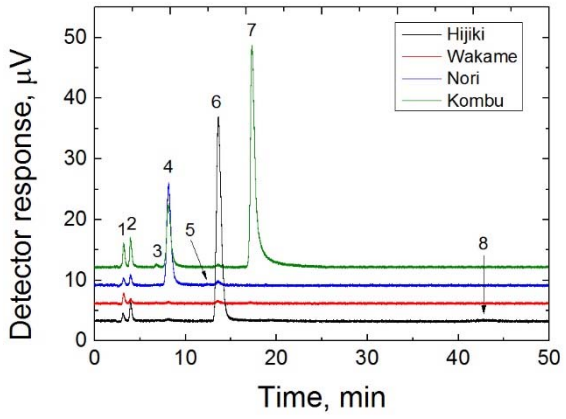

Figure 5 HPLC–HG–AFS chromatograms of four seaweed samples; HG conditions: 1.5 mol L^{-1} H_2SO_4, two inlets of 1% THB solution; 1– As-sugar-Gly, 2–$DMAs^V$, 3–MAs^V, 4–As-sugar-PO_4, 5–unknown, 6– iAs^V, 7– As-sugar-SO_3, 8– As-sugar-SO_4.

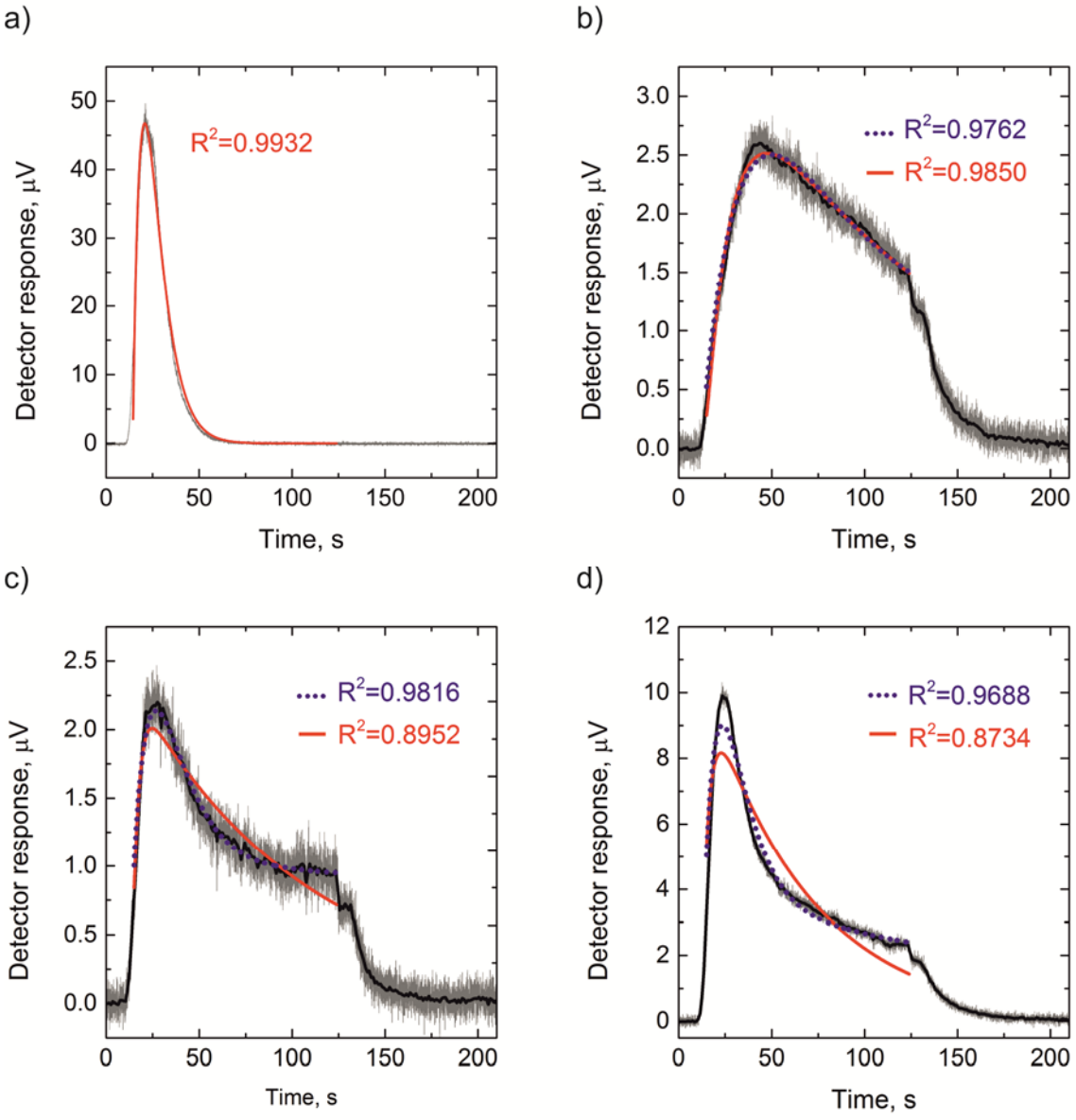

Figure 6 Signal shape (grey) of (a) iAs^{III} in 4 mol L^{-1} HCl, addition of 1% THB solution in the batch hydride generator fitted to the equation (2) (red); (b) As-sugar-PO_4 in 4 mol L^{-1} HCl, (black line represents smoothed data), addition of 1% THB solution in the batch hydride generator fitted with equations which correspond to mechanisms A (red – solid line) and B (blue – dotted line); (c) As-sugar-PO_4 in 4 mol L^{-1} (black line represents smoothed data), addition of 2% THB solution in the batch hydride generator fitted with equations which correspond to mechanisms A (red – solid line) and B (blue – dotted line); (d) As-sugar-PO_4 in 2 mol L^{-1} H_2SO_4 (black line are smoothed data), addition of 1% THB solution in the batch

hydride generator fitted with equations which correspond to mechanisms A (red – solid line) and B (blue – dotted line). Concentrations of As were 2 ng mL^{-1}.

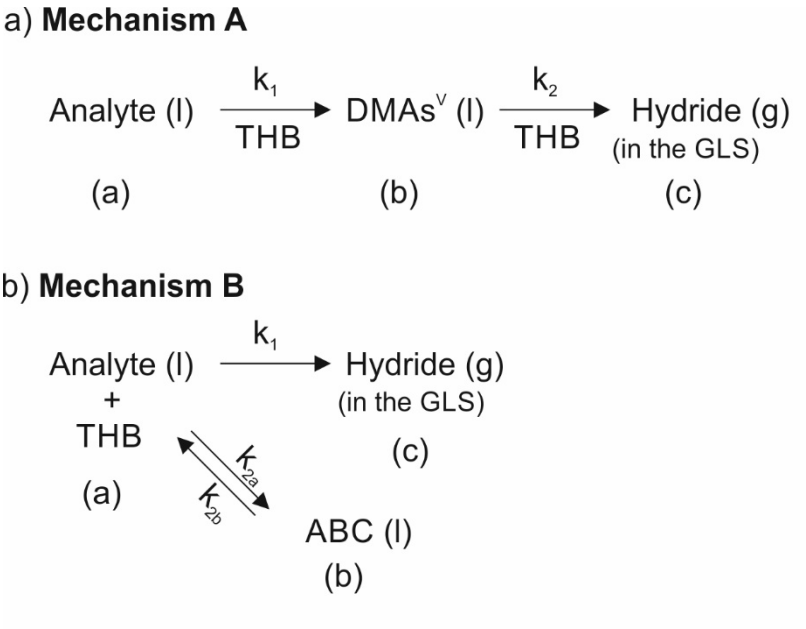

Fig. 7 Schemes of the proposed mechanisms for HG of As-sugars

Tables

Table 1 Concentration in ng mL^{-1} (mean ± SD, $n = 3$) of arsenic species in seaweed extracts determined by HPLC–ICP-MS (20 mmol L^{-1} phosphate buffer pH 5.6)

Seeweed	As-sugar-gly	$DMAs^V$	MAs^V	As-sugar-PO_4	U1	iAs^V	As-sugar-SO_3	As-sugar-SO_4	As total[d]	Column recovery[e]
Hijiki	6.27 ± 0.29	4.51 ± 0.18	<LOQ[a]	2.07 ± 0.16	ND[b]	99.3 ± 0.9	1.15 ± 0.04	9.70 ± 0.24	146 ± 5	84 ± 3%
Wakame	4.98 ± 0.16	0.41 ± 0.03	<LOD[a]	0.99 ± 0.10	ND[b]	0.26 ± 0.04	0.81 ± 0.06	ND[b]	31 ± 1	24 ± 2%
Nori	3.63 ± 0.13	0.98 ± 0.03	<LOD[a]	81.6 ± 2.5	0.42 ± 0.07	0.23 ± 0.10	<LOD	ND[b]	114 ± 5	76 ± 4%
Kombu	13.95 ± 0.25	2.76 ± 0.21	<LOD[a]	46.59 ± 0.27	ND[b]	<LOD[c]	199 ± 1	ND[b]	341 ± 8	77 ± 3%
t_r, min	2.7	4.0	6.8	7.4	11.9	13.7	17.7	41.5		

[a]LOD and LOQ for MAs^V were 0.08 and 0.031 ng mL^{-1}, respectively

[b]not detected

[c]LOD and LOQ for iAs^V were 0.07 and 0.022 ng mL^{-1}, respectively

[d]As total determined by liquid nebulization ICP-MS

[e]Column recovery = sum of As species/ As total

Table 2 Comparison of LODs of As-sugars and other arsenic species obtained with HPLC-HG-AFS (this work) with approaches based on HPLC-UV-decomposition-HG-AFS

Reference	LOD	As-sugar-gly	$DMAs^V$	As-sugar-PO_4	MAs^V	As-sugar-SO_3	iAs^V	As-sugar-SO_4
This Work	instrumental, ng mL^{-1}	0.81	0.04	0.19	0.04	0.26	0.06	0.38
	inst. absolute, pg	41	2.1	9.5	2.0	13	2.9	19
[12]	instrumental, ng mL^{-1}	0.24	0.06	0.38	0.22	0.50	0.22	0.61
	inst. absolute, pg	24	5.6	38	22	50	22	61
[10]	instrumental, ng mL^{-1}	5.0	1.6	6.6	0.9	17	1.1	33
	inst. absolute, pg	500	160	660	88	1650	110	3300
[29]	instrumental, ng mL^{-1}	0.06	0.11	0.1	0.14	0.04	0.22	0.06
	inst. absolute, pg	6	11	10	14	4	22	6

Reference List

1 K. A. Francesconi *Pure Appl. Chem.* 2010 **82**, 373.

2 V. Nischwitz and S. A. Pergantis *J. Anal. At. Spectrom.* 2006 **21**, 1277.

3 M. F. Hughes *Toxicol. Lett.* 2002 **133**, 1.

4 J. Feldmann and E. M. Krupp *Anal. Bioanal. Chem.* 2011 **399**, 1735.

5 V. Sele, J. J. Sloth, A. K. Lundebye, E. H. Larsen, M. H. G. Berntssen and H. Amlund *Food Chem.* 2012 **133**, 618.

6 B. Witt, S. Meyer, F. Ebert, K. A. Francesconi and T. Schwerdtle *Arch. Toxicol.* 2017, 1.

7 C. Niegel and F. M. Matysik *Anal. Chim. Acta* 2010 **657**, 83.

8 A. D. Madsen, W. Goessler, S. N. Pedersen and K. A. Francesconi *J. Anal. At. Spectrom.* 2000 **15**, 657.

9 G. Raber, K. A. Francesconi, K. J. Irgolic and W. Goessler *Fresenius' J. Anal. Chem.* 2000 **367**, 181.

10 R. Schaeffer, C. Soeroes, I. Ipolyi, P. Fodor and N. S. Thomaidis *Anal. Chim. Acta* 2005 **547**, 109.

11 D. Sánchez-Rodas, A. Geiszinger, J. L. Gómez-Ariza and K. A. Francesconi *Analyst* 2002 **127**, 60.

12 S. García-Salgado, M. A. Quijano and M. M. Bonilla *Anal. Chim. Acta* 2012 **714**, 38.

13 J. Dědina and D. L., Tsalev *Hydride Generation Atomic Absorption Spectrometry* John Wiley & Sons, Chichester, Inc., 1995.

14 A. D'Ulivo *Spectrochim. Acta, Part B* 2010 **65**, 360.

15 A. G. Howard *J. Anal. At. Spectrom.* 1997 **12**, 267.

16 E. Schmeisser, W. Goessler, N. Kienzl and K. A. Francesconi *Anal. Chem.* 2004 **76**, 418.

17 R. Regmi, B. F. Milne and J. Feldmann *Anal. Bioanal. Chem.* 2007 **388**, 775.

18 K. Marschner, S. Musil and J. Dědina *Anal.Chem.* 2016 **88**, 6366.

19 S. Musil, T. Matoušek, J. M. Currier, M. Stýblo and J. Dědina *Anal. Chem.* 2014 **86**, 10422.

20 P. Taurková, M. Svoboda, S. Musil and T. Matoušek *J. Anal. At. Spectrom.* 2011 **26**, 220.

21 K. Marschner, S. Musil and J. Dědina *Spectrochim. Acta, Part B* 2015 **109**, 16.

22 K. Marschner, S. Musil and J. Dědina *Anal.Chem.* 2016 **88**, 4041.

23 T. Matoušek, J. M. Currier, N. Trojánková, R. J. Saunders, M. C. Ishida, C. González-Horta, S. Musil, Z. Mester, M. Stýblo and J. Dědina *J. Anal. At. Spectrom.* 2013 **28**, 1456.

24 T. Narukawa, K. Inagaki, Y. B. Zhu, T. Kuroiwa, I. Narushima, K. Chiba and A. Hioki *Anal. Bioanal. Chem.* 2012 **402**, 1713.

25 T. Llorente-Mirandes, M. J. Ruiz-Chancho, M. Barbero, R. Rubio and J. F. López-Sánchez *J. Agric. Food Chem.* 2011 **59**, 12963.

26 S. McSheehy, M. Marcinek, H. Chassaigne and J. Szpunar *Anal. Chim. Acta* 2000 **410**, 71.

27 P. A. Gallagher, X. Wei, J. A. Shoemaker, C. A. Brockhoff and J. T. Creed *J. Anal. At. Spectrom.* 1999 **14**, 1829.

28 J. Dědina *Fresenius' Z. Anal. Chem.* 1986 **323**, 771.

29 S. Simon, H. Tran, F. Pannier and M. Potin-Gautier *J. Chromatogr. A* 2004 **1024**, 105.

Hydride Generation from Arsenosugars

Karel Marschner[1,2,*], Stanislav Musil[1], Ivan Mikšík[3], Jiří Dědina[1]

[1]Institute of Analytical Chemistry of the CAS, v. v. i., Veveří 97, 602 00 Brno, Czech Republic

[2]Charles University, Faculty of Science, Department of Analytical Chemistry, Albertov 8, 128 43 Prague, Czech Republic

[3]Institute of Physiology of the CAS, v.v.i., Vídeňská 1083, 142 20 Prague, Czech Republic

*Corresponding author; E-mail: karel.marschner@biomed.cas.cz

Hydride generators

Fig. S1 shows experimental setups of the hydride generator in the flow injection (FI), postcolumn and batch modes.

Identification of As-sugars

The *Hijiki, Nori, and Kombu* extracts and mixed arsenic species standard (iAs^V, MAs^V, and $DMAs^V$) were investigated by HPLC–ICP-MS, (HPLC column PRP-X 100, mobile phase was 20 mM ammonium bicarbonate buffer (pH 10.3) and methanol (9:1)). Chromatograms are shown in Fig. S2. The elution order of individual As-sugars were determined by HPLC–ESI-MS^2 used for identification at the same chromatographic conditions. The fragmentation spectra are shown in Fig. S3.

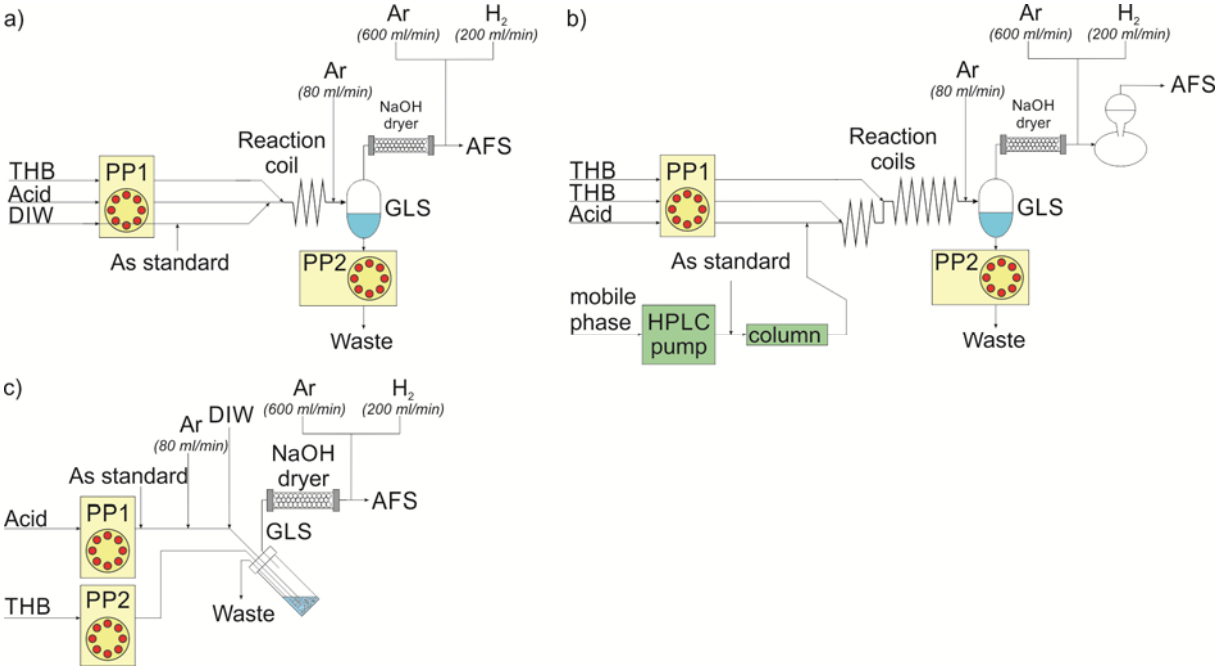

Figure S1 Scheme of the hydride generator in a) FI mode; b) postcolumn mode; c) batch mode; AFS – atomic fluorescence spectrometer, GLS – gas-liquid separator, PP1/PP2 – peristaltic pumps, THB – solution of $NaBH_4$, DIW – deionized water.

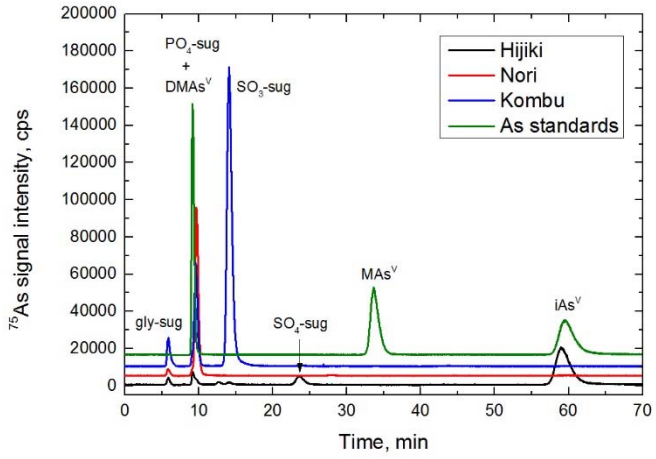

Fig. S2 HPLC–ICP-MS chromatograms of seaweed extracts and arsenic standards

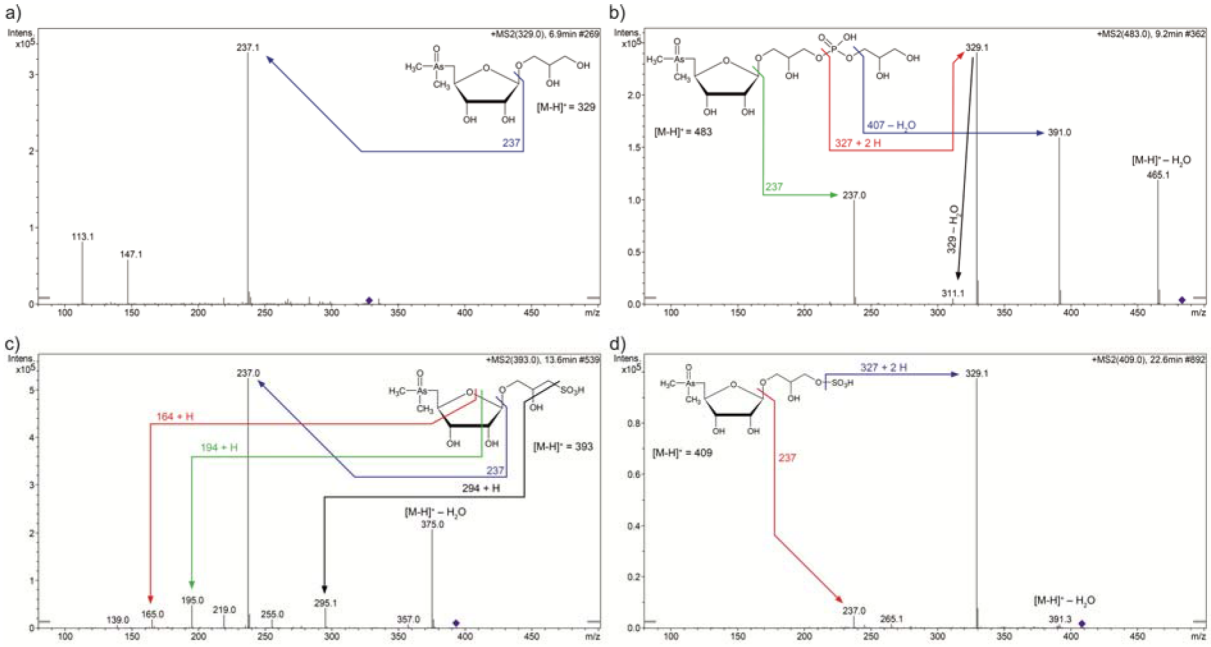

Figure S3 MS^2 fragmentation spectra of a) As-sugar-gly (at time 6.9 min); b) As-sugar-PO_4 (9.2 min); c) As-sugar-SO_3 (13.6 min); d) As-sugar-SO_4 (22.6 min)

Mechanism of HG of As-sugars

Since all reactions in schemes (Fig. 7) are of the first order (or pseudo-first order) and since the hydride removal from the GLS is also the first order process, we get the following systems of differential equations for mechanism A: $d[a]/dt = -k_1 \cdot [a]$; $d[b]/dt = k_1 \cdot [a] - k_2 \cdot [b]$; $d[c]/dt = k_2 \cdot [b] - k_m \cdot [c]$; $d[d]/dt = k_m \cdot [c]$ ($d[d]/dt$ describes hydride removal from the GLS) and for mechanism B: $d[a]/dt = -(k_1+k_{2a}) \cdot [a] + k_{2b} \cdot [b]$; $d[b]/dt = k_{2a} \cdot [a] - k_{2b} \cdot [b]$; $d[c]/dt = k_1 \cdot [a] - k_m \cdot [c]$; $d[d]/dt = k_m \cdot [c]$. The *a*, *b*, and *c* describes the arsenic form from the Fig.7. In the initial time (t = 0) no THB solution was added to the analyte in the liquid phase. Therefore, initial conditions in both cases are for t = 0; [a] = A_0, [b] = [c] = [d] = 0. Where A_0 is the initial concentration of analyte in the liquid phase. Function *c* stands for gaseous hydride concentration in the GLS and therefore describes the transient peak signal. Solution of function *c* for mechanism A is:

$$c(t) = (A_0 \cdot k_1 \cdot k_2 \cdot \exp(-k_1 \cdot t))/((k_1-k_2) \cdot (k_1-k_m)) - (A_0 \cdot k_1 \cdot k_2 \cdot \exp(-k_2 \cdot t))/((k_1-k_2) \cdot (k_2-k_m)) + (A_0 \cdot k_1 \cdot k_2 \cdot \exp(-k_m \cdot t))/((k_1-k_m) \cdot (k_2-k_m)) \quad \text{(S1)}$$

And for mechanism B is:

$$c(t) = (A_0 \cdot k_1 \cdot \exp(-(t \cdot k_1)/2) \cdot \exp(-(t \cdot k_{2a})/2) \cdot \exp(-t \cdot k_m) \cdot \exp(-(t \cdot k_{2b})/2) \cdot \exp(-(t \cdot (k_1^2 + 2 \cdot k_1 \cdot k_{2a} - 2 \cdot k_1 \cdot k_{2b} + k_{2a}^2 + 2 \cdot k_{2a} \cdot k_{2b} + k_{2b}^2)^{(1/2)})/2) \cdot (k_1 \cdot k_{2b} \cdot \exp(t \cdot k_m) - k_{2b}^2 \cdot \exp(t \cdot k_m) - k_{2a} \cdot k_{2b} \cdot \exp(t \cdot k_m) + k_{2b} \cdot \exp(t \cdot k_m) \cdot (k_1^2 + 2 \cdot k_1 \cdot k_{2a} - 2 \cdot k_1 \cdot k_{2b} + k_{2a}^2 + 2 \cdot k_{2a} \cdot k_{2b} + k_{2b}^2)^{(1/2)} + k_{2b}^2 \cdot \exp(t \cdot k_m) \cdot \exp(t \cdot (k_1^2 + 2 \cdot k_1 \cdot k_{2a} - 2 \cdot k_1 \cdot k_{2b} + k_{2a}^2 + 2 \cdot k_{2a} \cdot k_{2b} + k_{2b}^2)^{(1/2)}) + k_{2b} \cdot \exp(t \cdot k_m) \cdot \exp(t \cdot (k_1^2 + 2 \cdot k_1 \cdot k_{2a} - 2 \cdot k_1 \cdot k_{2b} + k_{2a}^2 + 2 \cdot k_{2a} \cdot k_{2b} + k_{2b}^2)^{(1/2)}) \cdot (k_1^2 + 2 \cdot k_1 \cdot k_{2a} - 2 \cdot k_1 \cdot k_{2b} + k_{2a}^2 + 2 \cdot k_{2a} \cdot k_{2b} + k_{2b}^2)^{(1/2)} - k_1 \cdot k_{2b} \cdot \exp(t \cdot k_m) \cdot \exp(t \cdot (k_1^2 + 2 \cdot k_1 \cdot k_{2a} - 2 \cdot k_1 \cdot k_{2b} + k_{2a}^2 + 2 \cdot k_{2a} \cdot k_{2b} + k_{2b}^2)^{(1/2)}) + k_{2a} \cdot k_{2b} \cdot \exp(t \cdot k_m) \cdot \exp(t \cdot (k_1^2 + 2 \cdot k_1 \cdot k_{2a} - 2 \cdot k_1 \cdot k_{2b} + k_{2a}^2 + 2 \cdot k_{2a} \cdot k_{2b} + k_{2b}^2)^{(1/2)}) - 2 \cdot k_{2b} \cdot \exp((t \cdot k_1)/2) \cdot \exp((t \cdot k_{2a})/2) \cdot \exp((t \cdot k_{2b})/2) \cdot \exp((t \cdot (k_1^2 + 2 \cdot k_1 \cdot k_{2a} - 2 \cdot k_1 \cdot k_{2b} + k_{2a}^2 + 2 \cdot k_{2a} \cdot k_{2b} + k_{2b}^2)^{(1/2)})/2) \cdot (k_1^2 + 2 \cdot k_1 \cdot k_{2a} - 2 \cdot k_1 \cdot k_{2b} + k_{2a}^2 + 2 \cdot k_{2a} \cdot k_{2b} + k_{2b}^2)^{(1/2)}))/(2 \cdot (k_1 \cdot k_m - k_1 \cdot k_{2b} - k_m^2 + k_{2a} \cdot k_m + k_{2b} \cdot k_m) \cdot (k_1^2 + 2 \cdot k_1 \cdot k_{2a} - 2 \cdot k_1 \cdot k_{2b} + k_{2a}^2 + 2 \cdot k_{2a} \cdot k_{2b} + k_{2b}^2)^{(1/2)}) - (A_0 \cdot k_1 \cdot k_m \cdot \exp(-(t \cdot k_1)/2) \cdot \exp(-(t \cdot k_{2a})/2) \cdot \exp(-t \cdot k_m) \cdot \exp(-(t \cdot k_{2b})/2) \cdot \exp(-(t \cdot (k_1^2 + 2 \cdot k_1 \cdot k_{2a} - 2 \cdot k_1 \cdot k_{2b} + k_{2a}^2 + 2 \cdot k_{2a} \cdot k_{2b} + k_{2b}^2)^{(1/2)})/2) \cdot (\exp(t \cdot k_m) \cdot (k_1^2 + 2 \cdot k_1 \cdot k_{2a} - 2 \cdot k_1 \cdot k_{2b} + k_{2a}^2 + 2 \cdot k_{2a} \cdot k_{2b} + k_{2b}^2)^{(1/2)} + k_1 \cdot \exp(t \cdot k_m) + k_{2a} \cdot \exp(t \cdot k_m) - k_{2b} \cdot \exp(t \cdot k_m) - k_1 \cdot \exp(t \cdot k_m) \cdot \exp(t \cdot (k_1^2 + 2 \cdot k_1 \cdot k_{2a} - 2 \cdot k_1 \cdot k_{2b} + k_{2a}^2 + 2 \cdot k_{2a} \cdot k_{2b} + k_{2b}^2)^{(1/2)}) - k_{2a} \cdot \exp(t \cdot k_m) \cdot \exp(t \cdot (k_1^2 + 2 \cdot k_1 \cdot k_{2a} - 2 \cdot k_1 \cdot k_{2b} + k_{2a}^2 + 2 \cdot k_{2a} \cdot k_{2b} + k_{2b}^2)^{(1/2)}) + k_{2b} \cdot \exp(t \cdot k_m) \cdot \exp(t \cdot (k_1^2 + 2 \cdot k_1 \cdot k_{2a} - 2 \cdot k_1 \cdot k_{2b} + k_{2a}^2 + 2 \cdot k_{2a} \cdot k_{2b} + k_{2b}^2)^{(1/2)}) + \exp(t \cdot k_m) \cdot \exp(t \cdot (k_1^2 + 2 \cdot k_1 \cdot k_{2a} - 2 \cdot k_1 \cdot k_{2b} + k_{2a}^2 + 2 \cdot k_{2a} \cdot k_{2b} + k_{2b}^2)^{(1/2)}) \cdot (k_1^2 + 2 \cdot k_1 \cdot k_{2a} - 2 \cdot k_1 \cdot k_{2b} + k_{2a}^2 + 2 \cdot k_{2a} \cdot k_{2b} + k_{2b}^2)^{(1/2)} - 2 \cdot \exp((t \cdot k_1)/2) \cdot \exp((t \cdot k_{2a})/2) \cdot \exp((t \cdot k_{2b})/2) \cdot \exp((t \cdot (k_1^2 + 2 \cdot k_1 \cdot k_{2a} - 2 \cdot k_1 \cdot k_{2b} + k_{2a}^2 + 2 \cdot k_{2a} \cdot k_{2b} + k_{2b}^2)^{(1/2)})/2) \cdot (k_1^2 + 2 \cdot k_1 \cdot k_{2a} - 2 \cdot k_1 \cdot k_{2b} + k_{2a}^2 + 2 \cdot k_{2a} \cdot k_{2b} + k_{2b}^2)^{(1/2)}))/(2 \cdot (k_1 \cdot k_m - k_1 \cdot k_{2b} - k_m^2 + k_{2a} \cdot k_m + k_{2b} \cdot k_m) \cdot (k_1^2 + 2 \cdot k_1 \cdot k_{2a} - 2 \cdot k_1 \cdot k_{2b} + k_{2a}^2 + 2 \cdot k_{2a} \cdot k_{2b} + k_{2b}^2)^{(1/2)}) \quad \text{(S2)}$$

The final equation has to be corrected for the sensitivity of the instrument, hydride transport efficiency, *etc*. All these effects may be corrected by constant *C*. Then the final equation is:

$$S(t) = C \cdot c(t) \tag{S3}$$

, where *c(t)* is the expression (S1) for mechanism A and (S2) for mechanism B.